Assessment of geopolymer material for the manufacture of a nuclear fuel core catcher

TD Mokgele

orcid.org/ 0000-0002-7994-5255

Dissertation submitted in fulfilment of the requirements for the degree *Masters of Science in Applied Radiation Science* at the North-West University

Supervisor: Prof V Tshivhase

Co-supervisor: Dr R Koen

Graduation: July 2019

Student number: 23702982

Declaration

I, Tsholofelo Desiree Mokgele hereby declare that this research dissertation titled "Assessment of geopolymer material for the manufacture of a nuclear fuel core catcher", is my own work executed at the North-West University. This work has not been submitted in any form in order to be awarded a degree at any other institution, nor has it been previously published. All the resources that were consulted in the preparation of this work has been cited and acknowledged.

Signature: __ TDMokgele _____ Date: _30 May 2019___

Acknowledgements

I would like to thank God primarily for granting me the opportunity and renewed strength to be able to carry out this research project.

I would like to express my sincere gratitude to Dr Renier Koen, for his valuable suggestions, support, and guidance that helped in the writing of this dissertation. I would like to extend my thanks to Prof Victor Tshivhase for always having his door open, ready to assist, support and continuous encouragement.

My sincere thanks also go to Prof Willie Meyer, Dr Thulani Dlamini, Dr Machel Mashaba, Dr Maulusi Nelwamondo and to the CARST team for their valuable insight and assistance throughout this journey.

The financial assistance of the National Research foundation (NRF) towards this research is hereby acknowledged. Opinions expressed and conclusions arrived at, are not necessarily to be attributed to the NRF. Many thanks to Necsa for their support since the start of the project and for their financial assistance in this project.

Lastly, I would like thank my family and friends for their support and continuous motivation. This research project would have not been possible without any of you, I am forever indebted.

Abstract

Nuclear accidents such as the ones that occurred at Three Mile-Island and Chernobyl, have led to the requirement for enhancements in the development of various reactor materials, in order to maintain safety in the nuclear industry. During these types of nuclear criticality events, attained residual corium materials need to be comprehensively immobilized, to restrict the potentially harmful effects. Accordingly, research is needed for the development of new core-catcher materials that are more reliable against the release of radionuclides and hazardous aerosols into the environment, in the event of a nuclear accident.

For this investigation, the applicability of geopolymer materials, produced from naturally occurring aluminosilicates through alkaline activation, was evaluated as potential candidate material for nuclear core-catching application. The aluminate species contained in the geopolymer matrices have been documented to afford an extremely robust compound lattice and accordingly is deemed a viable candidate to surpass the effectivity of standard OPC-type (Ordinary Portland Cement) compounds in the reduction of the potential release of radioactive isotopes and aerosols into the environment.

The aim of this study was to develop and structurally evaluate OPC and geopolymer matrices and to use the OPC results as baseline standard for the envisaged geopolymer species to attempt to supersede current OPC core-catching application. This was done by assessing the durability of different OPC samples in comparison with various geopolymer matrices when exposed to the ASTM standard; water absorptivity, sulphuric acid resistance and compressive strength testing protocols. From the results, geopolymeric superiority was established and subsequent recommendations were made for optimized geopolymer mixtures that are ideal for core-catching applications.

In this study the water to cement ratios (w/c ratios) for ambient cured OPC baseline pastes were varied between 0.31-0.40 and were subjected to air, water and plastic sealed curing. It was observed that increasing the w/c ratio, as well employing ambient curing conditions resulted in extremely porous samples with lower compressive strength values. However, OPC samples cured in sealed plastic bags with a 0.31 w/c ratio resulted in optimum compressive strength of (30.94 (33) MPa), a low percentage weight (% wt.) loss due to sulphuric acid digestion (83.95 (33)%) and lower sorptivity rates relative to other OPC samples.

For the second part of the investigation, various fly ash based geopolymers with either silica fume or mineral clay additives and activated with various alkaline solutions were identified for

the proposed application of the study. From the pre-screening process it was observed that plastic sealed cured fly ash based geopolymers (F-GlP) activated with 14 M NaOH/ Na_2SiO_3 solutions, displayed increased durability relative to the other fly ash/mineral clay geopolymeric mixtures. These samples were then subjected to various ASTM testing protocols to substantiate their geopolymer superiority over the OPC analogue mixtures.

It was found that, contrary to OPC samples, increasing the alkaline solution to binder ratio (AS/B ratio) in geopolymers improves the durability of the geopolymers samples. As a result, F-GlP samples with a higher AS/B ratio (0.40) resulted in an optimum compressive strength of 35.1 (30) MPa, an insignificant degree of % wt. loss when exposed to sulphuric acid (1.28 (11)%) and low sorptivity rates. Accordingly, it is therefore evident that not only did the F-GlP mixtures significantly outperform the OPC idealized baseline values, but it was also possible to identify the 0.40 AS/B ratio as a mixing formulation for the proposed application of this study.

Table of Contents

List of Figures

List of Tables

List of Abbreviations

CSH	Calcium Silicate Hydrate
HLW	High Level Waste
IAEA	International Atomic Energy Agency
ILW	Intermediate Level Waste
LLW	Low Level Waste
NESCA	South African Nuclear Energy Corporation
OPC	Ordinary Portland Cement
SEM	Scanning Electron Microscopy
XRD	X-ray diffraction

Chapter 1 Introduction

Radioactivity has a vast range of beneficial applications and has successfully been functional in; the generation of power, development of medicine, various agricultural practices and to drive the continuous growth of the entire nuclear industry (Waltar, 2003). The execution of these beneficial applications has been carried out under strict guidelines and safety protocols. This is done in order to prevent any future nuclear accidents which may be harmful to radiation workers, the general public and to the environment, as stated by the International Atomic Energy Agency (IAEA, 2006).

Unfortunately, significant amounts of hazardous radioactive waste are generated during or post the aforementioned applications, in the various areas or fields. This problem has led to the required development of various methods that have been employed in order to maintain and restrict the potentially harmful effects of the generated radioactive waste (IRSN, 2013). According to the aforementioned guidelines, these practices guarantee the protection of radiation workers and the environment against radiation in two ways, containment of radioactive waste (prevents their dispersion into the environment) or physical shielding against ionising radiation (Palomo & dela Fuente, 2003).

These safety practices and the execution thereof are also subject to the type of waste that requires containment and/or passivation. Over the last few decades radioactive wastes have been categorised and managed according to the level of residual radioactivity (IRSN, 2013). High-level wastes (HLW) have generally been controlled by means of deep geological storage, whereas intermediate level wastes (ILW) and low level wastes (LLW) are incorporated or encapsulated into nuclear waste matrices.

It should be noted that, for the sake of this investigation, newly refined waste management systems for especially HLW (such as residual corium materials acquired during a nuclear criticality incident) but also for the potential application of these improved cementitious matrices for ILW and LLW will be investigated, in order to attempt to improve overall safety within a nuclear environment. Accordingly, for this investigation, it is imperative that the HLW, ILW and LLW encapsulating matrices, are durable enough to not only immobilize the waste products within their matrices and maintain structural integrity, but also assist in the dissipation/elimination of the residual radiation from the nuclear debris to the outside

environment. These nuclear wastes matrices include cement, borosilicate glass, bitumen and geopolymers.

Currently, ordinary Portland cement (OPC) materials or binders have been used for many years to encapsulate/immobilize these waste materials, due to their low development costs and the abundant nature of the materials. However, these binders possess an excessively porous structural nature and have low thermal stability, both of which increase the chance of radioactive materials leaching out of the matrix, especially post a nuclear incident. This susceptibility makes it vulnerable to being replaced by more durable and structurally superior geopolymeric type materials (Duxson et al., 2007).

Geopolymer is a term used to describe a family of synthetic alkali aluminosilicate materials (Duxson et al., 2007). These compounds are essentially manufactured from the reaction of a solid aluminosilicate donating species and a highly concentrated aqueous alkali hydroxide (sodium or potassium hydroxide) and/or silicate solution (sodium silicate or potassium silicate) (Duxson et al., 2007) at room or slightly elevated temperatures.

This geopolymer technology has been predominantly applied in construction applications, in countries like France, Spain, Russia and Germany for many years. The development of this technology grew exponentially after the catastrophic fires that broke in France in the early 1970's, as quest for non-flammable and non-combustible materials were in demand. In the following years, this type of research led to the application of geopolymer composites in construction of structures such as fire resistant coatings, railway sleepers, pipes, pavement, and roads. Even though the use of geopolymer technology was increasing, it only started receiving great deal of attention when the levels of CO_2 emissions due to ordinary Portland cement (OPC) production became alarming. Statistically, the global emission levels of CO_2 due to the production of OPC is estimated at 7% and is still growing, whereas the development of geopolymeric compounds afford a significantly smaller carbon footprint as compared to OPC production (Nanavati et al., 2017).

Recent investigations have also noted that geopolymers are not only used as construction materials but have also found application as waste matrices and core catching materials for the immobilization of nuclear or toxic waste in order to maintain safety in the nuclear industry. It has been well documented that these geopolymeric systems are known to be more resistant to, spalling damage, acid attack, chemical leaching and chloride ingress *vs*. regular OPC cement (Davidovits, 1991). Additionally, geopolymers have; a low thermal expansion up to 800℃, low

apparent porosity, high compressive strength, improved acid resistance and are known to be stable up to 1200-1400℃ (Mikheykin, 2017). The stability of geopolymers when exposed to temperatures above 1000℃ and the fact they are resistant to thermal shock, leads to the suggestion to use this class of compounds in reactors as a core catching material for nuclear reactors.

A core-catcher is generally made from special type of OPC concrete that is designed to prevent leaking of molten core out of the entrapment vessel; it is water-cooled, and built directly under a reactor to catch the molten core material, known as "corium," in the case of a reactor meltdown. It has been noted that several advances have become prominent in the study of the development core catcher matrices, following the Three Mile Island nuclear accident in 1979 and the Chernobyl nuclear accident in the late 1980's caused by subsequent steam explosions within the reactor causing it to rupture (NEI, 2008).

The graphite-concrete sandwich concept by a physicist Leonid Bolshov (Conant, 2012), paved the way for the incorporation of neutron-absorbing metallic alloys within core catcher vessels as well as the incorporation of water-cooling systems built directly under a reactor to sustain the amount heat produced. However, it has been noted that this technology is far from perfect and significant development is still required (Conant, 2012).

It is important that the core catcher containment unit be designed in a way that it is able to provide cooling to the melted corium during a nuclear accident but also afford structural integrity when exposed to the extreme conditions that are "felt" during a nuclear incident. From the aforementioned, it would seem that the class of geopolymeric materials might serve as ideal candidates for application as a core-catcher.

1.1 Problem statement

Geopolymeric compounds have been studied for the past century and in that timeframe, only a recent minority of 20 years has been dedicated to their use in the nuclear industry, mainly for the solidification of radioactive waste. Although the positive ecological characteristics of geopolymers have been published in many papers, other geopolymer applications such as its use as construction, encapsulation or shielding materials in the nuclear industry have not been thoroughly exploited and or explicitly published, leading to continuous reliance on sub-optimal OPC concrete mixtures. As mentioned in the introduction above, the physicochemical properties of geopolymers may play an important role in potentially replacing OPC concretes in order to increase the overall safety in the nuclear industry.

It has been well documented that the structure of OPC concrete is based on hydrated calcium silicate (C_3S and C_2S) products that contribute greatly to the strength of the cement, as well as on retaining hydration water (Talaber, 1981). However, these water molecules entrapped within the cement matrix can easily evaporate at high temperatures, causing high pore pressure thus resulting in the spalling or deformation of the structure (Zhang & Guang, 2012). Moreover, the interactions of the core catcher concrete with the melted core gives rise to explosions during a core melt; this is because of the heat given off by the corium leading to concrete ablation (Allelein et al., 2005). In Figure 1.1, an illustration is noted where the effect of the molten corium on the OPC core-catcher material is shown. From this, it becomes evident that (at high temperature) as the concrete decomposes, gas bubbles are released (hydrogen, carbon monoxide and carbon dioxide) into the containment atmosphere and are generally responsible for any explosive gases that might form in the containment atmosphere (Allelein et al., 2005).

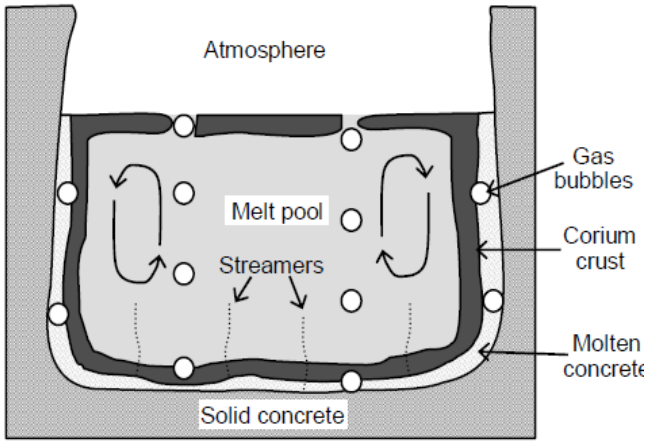

Figure 1.1: Molten core concrete interaction (Sevón, 2005).

Further literature also revealed that current core-catcher OPC mixtures contain about a 30 wt.% of moisture content which in turn affords unbounded pore water within the structural matrix that could undergo radiolysis (depending on radiation flux) resulting in additional hydrogen gas formation. If the gas pressure exceeds the tensile strength of the concrete structure, cracking will occur resulting in a release of hydrogen gases into the atmosphere, which in the presence of oxygen catches fire. This explosive nature and cracking that occurs in the reactor core during a reactor spill, can lead to catastrophic radioactive fallout. Consequently, a radioactive fallout can release radionuclides (Cs ^{137}, I ^{133}, Sr ^{90}) into the environment, which in most cases, decontamination of such radionuclides is unlikely or will take years before it can be achieved. Mounting evidence has also shown that high levels of radiation exposure can cause adverse

health effects and or immediate death in humans (IAEA, 2006). It is therefore, imperative that practical efforts are made in order to prevent and mitigate nuclear accidents (IAEA, 2006).

Many aspects regarding mechanical durability of geopolymer pastes are still unknown. Therefore, this study addresses the lack in research, around the use of geopolymer materials in potentially increasing safety and physicochemical control of nuclear accidents. The aluminate species contained in the geopolymer matrices leads to the reduction in subsequent explosions and in the release of radioactive aerosols into the environment. Therefore, particular attention should be paid on the proliferation of geopolymer type materials and their applicability in nuclear core catcher materials, over traditional core-catcher OPC mixtures seems promising.

1.2 Research aim and objectives

The aim of this study was to develop OPC and geopolymer matrices and to use OPC physicochemical results as baseline for comparison with envisaged geopolymer species to attempt to supersede current OPC core catching applications. This was done by assessing the stability of different OPC samples in comparison to various geopolymer matrices when exposed to harsh environments (acidic conditions, stress load) and make recommendations on the optimum composition of geopolymer materials that could enhance core catcher systems in nuclear reactors.

Accordingly, the objectives of this study are to:

- Identify various candidate geopolymeric type source materials, alkaline activators and additives for desired application by means of an in-depth literature review.
- Undertake preliminary synthetic protocols to obtain familiarity with sample preparation. This is an essential course of action as this may assist in;
    - Optimizing the manufacture of OPC pastes in terms of w/c ratio,
    - Determine the best curing method of OPC as baseline for geopolymer synthesis,
    - Defining the baseline physicochemical results (properties) required for geopolymer comparison.
- Postulate and test a novel pre-screening methodology to minimize the labour and exorbitant lab time required to investigate all possible candidate materials identified in the literature review section.

    - Utilize this methodology to identify at least two sets of candidate formulations for geopolymer synthesis and OPC comparison.

- Compare geopolymer materials physicochemical observations with that of OPC baseline pastes, in terms of; water absorption/penetration, sulphuric acid resistance, and compressive strength testing protocols.
- And finally, to utilize the results from these testing procedures to define an optimal formulation for use in fuel core catcher applications, according to prescribed criteria

Chapter 2 Theoretical background

From the previous section, it was noted that radiation shielding mechanisms of nuclear reactor core-catching containment areas, are known to be costly and very complex. These systems usually require two overarching types of shielding conventions; a shield to protect the walls of the reactor from radiation damage and at the same time reflect neutrons back into the core and a structurally sound biological shield to protect people and the environment from leaking radioactive materials. Therefore, this research will contribute to increased safety in the nuclear industries. The complexity of this type of development requires that each identified shielding category be optimized sequentially. Accordingly, focus for this study will mainly be placed on structural lattice optimization of these core catching materials. Subsequent investigations may be concentrated on the incorporation of neutron moderators, etc. into these matrices, to fully develop a well-rounded core-catching cementitious formulation, but this is outside the scope of the present study.

As was mentioned in Chapter 1, ordinary Portland cement (OPC) materials or binders have been used for many years to encapsulate/immobilize these corium materials, with their selection being ascribed to their low development costs and the abundance. However, these binders are known to possess an excessively porous structural nature and have low thermal stability, both of which increase the possibility of hazardous radioactive materials leaching out of the immobilization matrix. This susceptibility makes it vulnerable to being replaced by more durable and structurally superior geopolymeric type materials (Duxson et al., 2007). In the following sections, these superior geopolymeric properties will be discussed and their applicability to the envisaged application emphasized. This will then be followed by the identification of possible, source materials, alkaline activators and admixtures that may be applicable to the continuation of this study.

2.1 History of geopolymers

Several milestones took place in the developmental chemistry of alumino-silicate compounds prior to the coining of the term geopolymers. Early observations have been reported for the use of alkali activated materials that dates all the way back to the 1940's, in the work of A. Purdon (Pacheco-Torgal et al., 2008). Purdon, who was a civil engineer, investigated the reaction of blast furnace slag binders activated with an alkali solution and found that the product-hardened binders were comparable to OPC in terms of strength (Pacheco-Torgal et al., 2008).

In the late 1950's V. Glukhovsky postulated that there are three processes; destruction–coagulation; coagulation-condensation and condensation–crystallization that take place during alkali activation of alumino-silicate materials, leading to the formation of strong binder materials (Duxson et al., 2007).

As the quest for non-flammable and non-combustible materials increased post the catastrophic fires that broke in France in 1970-1973, the advancement of geopolymer technology lead to its increased application as a composite material. This encouraged the development of water-resistant ceramics for industrial application and fire-resistant chip-board in the years 1972-1978 (Davidovits, 2002).

In 1979, Joseph Davidovits created the term geopolymer after he conducted a tremendous amount of research on these inorganic aluminosilicate polymers. This work set the tone for several advances to take place in the 1980's, when Lone Star Industries and the Shell Oil Company collaborated with Davidovits with the aim of creating high strength geopolymer cements. These cementitious compounds were a combination of both geopolymer raw materials and hydraulic Portland cements which were referred to as PYRAMENT Blended Cements. High early strength attained from the PYRAMENT cement made it fit for use in industrial pavements and for repairing highway roads (Davidovits, 2002)

Geopolymer development gained more momentum in the 1990's when their favourable non-combustible nature paved the way for the use of geopolymers as thermal shields in the interior of aircrafts and other specialized automotive applications, for fire resistance enhancement (Davidovits, 2002).

Currently, various types of geopolymers such as: fly ash based, ground blast furnace slag and mineral clay geopolymers are being extensively studied as potential replacements for OPC (Al Bakri et al., 2015). Additionally, as environmental concerns arise owing to the release of CO_2 during the production of OPC has placed geopolymer material at the forefront as the new generation binder for concrete. Subsequent sections in this chapter will further discuss geopolymer chemical, physical and mechanical properties and the factors that affect the durability of the materials, such as geopolymerisation.

2.2 Geopolymer chemical properties

Geopolymers are produced from a geopolymerization process whereby solid aluminosilicate compounds and aqueous alkali activators undergo a polycondensation reaction. These alkaline activators generally consist of sodium hydroxide (NaOH) and/or potassium hydroxide (KOH).

The resultant structure is a silicon-oxo-aluminate (sialate) analogue that exhibits Si^{3+} and Al^{3+} in a IV-coordination mode, linked alternately by neighbouring oxygen atoms (Davidovits, 1991). Positive ions such as Na^{+} or K^{+} present in alkali solutions compensate for the charge imbalance around the IV-fold coordinated Si and Al-atom (Davidovits, 1991). The generalized empirical formula for poly(sialate) compounds is given by;

$$M_n\{-(SiO_2)_z - AlO_2\}_n \cdot wH_2O \qquad (1)$$

where M is a monovalent cation (Na^{+} or K^{+}), n is the degree of poly-condensation and z is 1, 2 or 3 which represents the Si to Al ratio.

According to Davidovits there are three types of poly(sialate) compounds, namely; (1) Poly(sialates), which are polymers comprised of basic Si-O-Al-O units (Si:Al = 1:1), (2) Poly(sialate-siloxido) compounds with chemical units Si-O-Al-O-Si-O (Si:Al = 2:1) and (3) Poly(sialate-disiloxido) compounds with Si-O-Al-O-Si-O-Si-O basic units (Si:Al = 3:1). The chemical structure of each of these compounds are schematically shown in Figure 2.1.

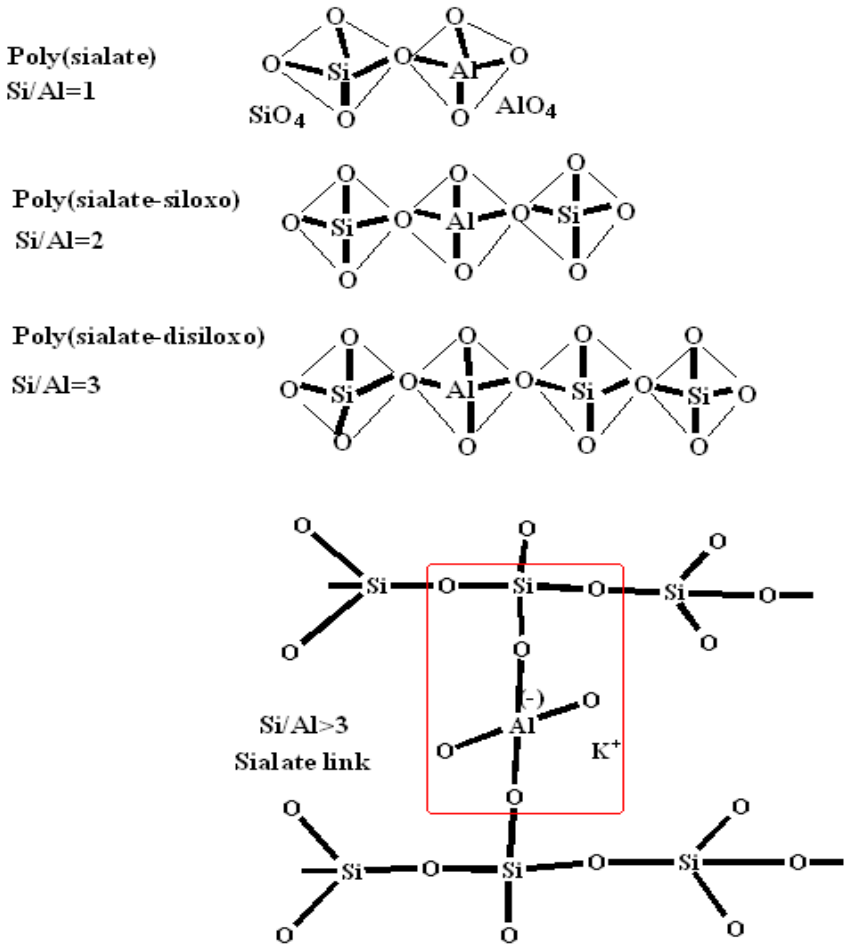

Figure 2.1: Three types of Poly(sialate) classified according to the Si:Al atomic ratio (Davidovits, 1991).

2.3 Geopolymerization process

The intricate structure of these compounds is responsible for the superior chemical and thermal stability that geopolymer based materials as opposed to standard OPC based materials (Mane & Jadhav, 2012). Even though the mechanism of geopolymerization has been intensely researched it is still not yet fully understood (Yao et al., 2009). Various mechanistic processes have been postulated but in general it was noted that geopolymerization can be reasonably explained by the following discussions and equations (Giannopoulou & Panias, 2007);

1. Dissolution of Si and Al from the alumino-silicate materials in an alkaline aqueous solution (NaOH and KOH).

The concentration of alkaline solutions plays an important role in dissolution of raw materials and in the catalysing reactions. The higher the concentration of the alkaline solution the more effective it will be in breaking the polysialate bonds and releasing the Si and Al ions. In addition, water molecules present in the alkaline solution are taken up in this stage and this leads to the formation of reactive silicate and aluminate monomers contained in a disordered geopolymerization gel binder.

$$\left(SiO_{2,}Al_2O_3\right) + 2NaOH + 5H_2O \rightarrow Si(OH)_4 + 2Al(OH)_4^- + 2Na^+$$

2. The product monomers of silicate and aluminate polymerize to form various oligomers This process gives rise to polymeric chain and ring structure consisting of Si-O-Al-O bonds. These structures are cross-linked via a condensation reaction.

$$Si(OH)_4 + Si(OH)_4 \leftrightarrow (OH)_3Si - O - Si(OH)_3 + H_2O$$

$$Si(OH)_4 + Al(OH)_4^- \leftrightarrow (OH)_3Si - O - Al^{(-)}(OH)_3 + H_2O$$

3. Finally, there is evident growth of crystalline structures that forms an interlinked network of the oligomers to form the 3D aluminosilicate framework. This is referred to as the poly-condensation stage (Giannopoulou & Panias, 2007).

This framework is amorphous owing to the fact that fast reactions between alkali metals and raw material do not allow sufficient time for the growth of a well-structured network to be formed. The final product of geopolymerization is an amorphous, semi-crystalline cementitious material (Petermann et al., 2010). Figure 2.2 illustrates the simplified geopolymerization process of the described stages above.

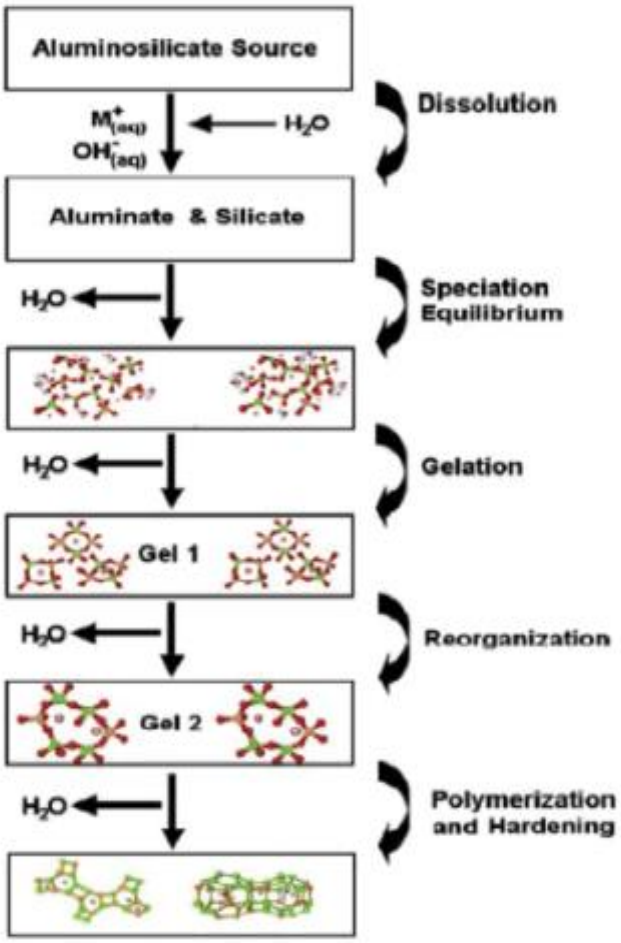

Figure 2.2: Schematic representation of the dissolution, gelation and polycondensation stages that take place in the geopolymerization process (Petermann et al., 2010).

Geopolymers display varying physicochemical properties depending on the types of raw materials used to produce them. Natural minerals such as kaolinite or natural pozzolan that are rich in Si and Al are widely used as raw materials in producing geopolymer cements. Although geopolymers are considered to have superior structural properties, like any other binders, there are certain factors that influence their superiority, e.g. the source materials used, the types of alkaline solutions, curing temperature, the Si/Al ratio and additives used.

2.3.1 Source materials used for geopolymerization

Various solid starting compounds known as source materials are used for different geopolymers for desired outcomes. For geopolymerization to occur, the source material should preferably consist of a Si- and Al-rich mixture in an amorphous form. Fly ash, ground blast furnace and mineral clays (Metakaolin, Bentonite) are rich in Si and Al, and as such they are the most common source materials used for the production of geopolymers. Source materials are often replaced by small percentages of additives in geopolymers and as well as being used as admixtures in OPC to improve the properties of cementitious materials. These chemical or mineral ingredients play an important role in increasing the compressive strength, attaining preferred plasticity, slowing down or fast tracking the setting time and inducing entrained air voids for better freeze thaw resistance (Haji-Esmaelii, 2012). In this study, fly ash class F was used as the starting material due to its high Si dissolution rate (Xu & Van Deventer, 2003) and was supplemented with portions of silica fume, bentonite mineral clay, attapulgite source materials. This was done so as to analyze the influence of mineral additives to the fly ash geopolymers and to identify geopolymers that display enhanced physical, chemical and mechanical properties.

2.3.1.1 Fly ash

Fly ash is one of the most abundant industrial wastes world-wide. This alumino-silicate source material has been noted to be responsible for the increased strength in geopolymers and its mechanical properties under various conditions (Hardjito & Rangan, 2005). Fly ash is generally a light type of ash-like material that results from the combustion of coal during electricity production, which remains in flue gas until it is removed by filter baghouses, before release of flue gas into the atmosphere. It is then marketed to cement companies which use the fly ash to improve the durability of cement, which also reduces the amount of ash that is deposited in landfills that may contaminate underground water (ACAA, 2003).

Xu & Van Deventer (2003) investigated and reported the effect of source materials on geopolymer properties. They found that fly ash generally has a higher Si ion dissolution rate and a Si/Al content ratio that is desirable for higher compressive strength in the manufacturing of geopolymers. Andini et al. (2008) also reported that coal fly ash can be used as a base material for geopolymers and the durability thereof can be influenced by different factors such as the curing temperature or curing time.

According to literature, the type of fly ash used also plays a role in the physical characteristics of subsequent geopolymers. Fly ash class F, is known for its high Si and Al content versus class C type fly ash, which has lower Si and Al content and higher calcium content (> 10%) (Temuujin et al., 2009). The class C type fly ash is believed to lower the mechanical strength of produced geopolymers due to the interference of the calcium ions during the geopolymerization process (Li et al., 2011). On the other hand, the presence of calcium ions gives rise to a secondary C-S-H gel, which alongside the geopolymer alumino-silicate gel gives higher compressive strength (Diaz et al., 2010). Additionally, according to Indu & Elangovan (2016) class C fly ash needs to be incorporated in bulk to be effective and is less resistant to sulphate attack as compared to class F fly ash.

Fly ash can be incorporated in Portland cement as an admixture where it undergoes pozzolanic activation during cement hydration. This reaction mechanism begins during cement hydration with water, releasing calcium hydroxide $Ca(OH)_2$, which then reacts with the available fly ash thus producing secondary C-S-H cement products (Mallisa & Turuallo, 2017). The produced secondary C-S-H thus yields added compressive strength to hardened cement mortar or concrete.

2.3.1.2 Silica fume

Silica fume has also been widely used as an additive in geopolymer production and as an admixture in OPC concrete. During the production of silica or silica alloys, raw materials such as quartz, coal and woodchips are mixed together in an electric arc furnace and are heated to about 2000℃. The smoke that results from the furnace is filtered and its residue collected as silica fume, otherwise known as micro-silica (Siddique & Khan, 2011).

Silica fume has very notable physical properties which improve the durability and impermeability of concrete when used as admixture. This pozzalon material also has high SiO_2 content, which has been established to be advantageous in the production of geopolymers. The high Si content in silica fume promotes the formation of alternating Si-O-Al- amorphous 3D polymeric chains, yielding a stronger geopolymer sample. Additionally, silica fume consists of very small spherical particles that are about 150 nm in diameter, capable of filling in little voids in concrete or cement pastes, thus reducing the number of pores, making the concrete very dense or highly impermeable.

According to Memon et al. (2013) the addition of about 5-10 wt.% silica fume to a low-calcium fly ash based geopolymer leads to increase of the compressive strength of the geopolymer

sample of about 6.9% versus the unmodified sample. Another study by Okoye, Durgaprasad and Singh (2016) confirmed that the presence of silica fume in fly ash based geopolymers lead to a more acid resistant geopolymer as compared to OPC samples, when immersed in H_2SO_4 (2%) solution. The impermeability of fly ash-silica fume based geopolymers was deemed to be partly responsible for the resistance against acid attack, as opposed to porous OPC samples (Khater, 2013).

Alternately, another study has indicated that a higher additional content of silica fume in geopolymer pastes does not always lead to improved performances (Ramezanianpour & Moeini, 2018). As stated above, the finer particles act as filler in concrete structures increasing density, but in some instances, the finer particles are more readily accessed or taken up by the alkaline reaction solutions very promptly, leaving the larger particles with less alkaline liquid to react with. The workability of the paste with the addition of silica fume will thus be reduced (Wong & Razak, 2005), resulting in a paste that is less coherent and resulting in cracks forming more readily. To counteract this, it is suggested that the water to cement (w/c) ratio should be increased, but this in turn leads to increased pore formation during the curing of geopolymer pastes.

2.3.1.3 Mineral clays

In general, it has been documented that the basic building blocks in the formation of most mineral clays are silica tetrahedron units and aluminum/magnesium octahedron units which essentially join to form layers of sheets. The different manner in which the silica tetrahedron sheets and the octahedron sheets are arranged, gives rise to the different range of mineral clays (Schulze, 2005). The most common types of clay mineral groups are; kaolinite, montmorillonite/smectitte and the illite groups. Within these groups are the Si-Al moeities that form the basic building blocks for mineral clays and are essential for geopolymerization.

Metakaolin

Metakaolin (kaolinite mineral clay) is a source material that has most readily been used for geopolymer synthesis, owing to its high chemical reactivity (Dinakar, 2011). Other, less readility used examples of mineral clay source materials includes the usage of bentonite (monomorillonite group) and attapulgite (illite group) as additives in geopolymer concrete.

Several studies have been centered on the usage of metakaolin as source mineral clay for the production of geopolymer cements. This mineral clay originates from the de-hydroxylation of

kaolinite ($Al_2Si_2O_5(OH)_4$) to the chemical structure $Al_2Si_2O_7$ known as metakaolin, through heating kaolinite at about 700℃ for several hours.

Although metakaolin will not form part of this study (it is expensive to produce), a brief review on its applicability will be discussed. As mentioned, metakaolin is a source material that has most readily been used for geopolymer synthesis, owing to its high chemical reactivity (Dinakar, 2011). This highlights the fact that these natural Si-Al mineral clays are deemed crucial as potential source materials and additives for the synthesis of geopolymers pastes or mortars (Xu & Van Deventer, 2000).

Various publications also substantiate the affectivity of metakaolin as geopolymer source material. Autef et al. (2013) reported the application of metakaolin as geopolymer synthon by dissolving it in KOH and amorphous silica in water. It was noted that this aforementioned reaction occurs rapidly, resulting in strengthened material consisting of a geopolymer network, mica layers, a Si-rich phase and an Al-rich phase. Chen et al. (2016) studied the properties of alkali activated metakaolin based geopolymers and found that the metakaolin activated with NaOH and Na_2SiO_3, cured at 60℃ for 168 hours, resulted in the optimum compression strength of 52.26 MPa. Conversely, the compressive strength was 37.4 MPa for metakaolin based geopolymers cured at 20℃ for 168 hours, corroborating the importance of heat curing on the strength development of geopolymers.

According to Duan et al. (2015), fly ash/metakaolin geopolymers showed a compressive strength loss of 10.4% after 28 days of exposure to 2% sulphuric acid and 2% hydrochloric acid, relative to a compressive strength loss of 34.4% for OPC after 28-days of exposure to the acid mixture. The study also revealed a reduced mass loss of 3.34% for geopolymer samples exposed to 1000℃, as opposed to OPC samples which experienced great spalling at 600℃, such that further readings on the mass loss could not be obtained. Furthermore, lower water absorption in the fly ash/metakaolin geopolymers was reported relative to OPC samples (Duan, et al., 2015).

Bentonite

Bentonite ash (volcanic ash) is formed by the fallout from volcanic activity. After a substantial volcanic event, the resulting bentonite ash undergoes chemical and structural modification in the presence of water, leading to the formation of a white sticky clay called bentonite.

Bentonite forms part of the montmorillonite group of clay materials. This mineral clay mainly consists of 2-silica tetrahedral moeities with 1 alumina octahedron sheet positioned in-between the silica sheets. A schematic representation thereof is presented in Figure 2.3.

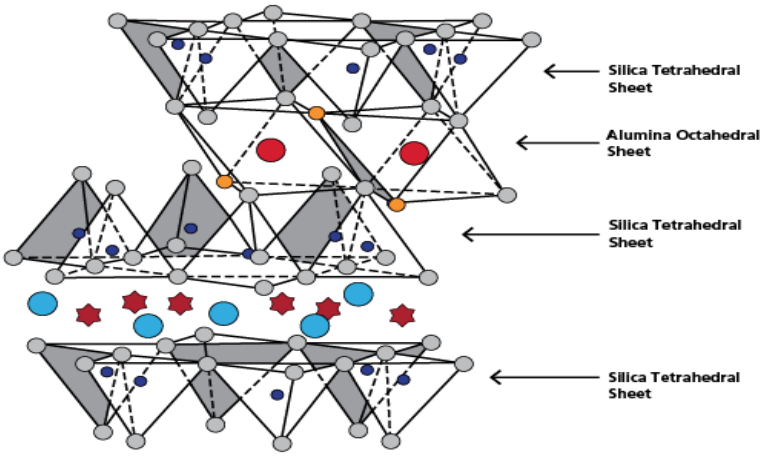

Figure 2.3: A basic montmorillonite schematic representing an alumina octahedral sheet sandwiched between 2 silica tetrahedral sheets (Schulze, 2005).

Bentonite may also contain different types of cations in its interlayer, giving rise to the different variants of the clay, namely; the sodium, calcium and nitrogen derivatives. The sodium bentonite analogue displays significant dimensional swelling due to its single water layer, whereas calcium bentonite clay is known as a non-swelling class of compound with its double water layer (Kutlić et al., 2012). The expandable nature of the bentonite clay plays an important role in preventing leaching of waste during waste encapsulation processes by serving as a sealant for the waste containers (Krupskaya et al., 2017).

A study by Srinivasan & Sivakumar (2012) showed that higher compressive strengths were obtained for geopolymer samples containing a combination of bentonite (40%) and fly ash (30%). It was also noted that the optimum compressive strength of fly ash/bentonite based geopolymers was obtained from higher temperature curing in an oven, as opposed to room temperature curing leading to superior performance *vs.* the combination of bentonite/OPC cement (Srinivasan & Sivakumar, 2012). Conversely, Hu, Zhu, & Long (2009) also studied the use of bentonite as a mineral additive to CaOH and NaOH activated fly ash based geopolymers. It was concluded from the study that, addition of bentonite simply acted as a filler material to make the geopolymer more compact but showed no improvement in the mechanical strength and acid resistance of the material relative to using zeolite as an additive (Hu et al., 2009). The lower compressive strength could have resulted from the use of NaOH with no additional alkali

silicate as an activator, which stems from a study that reported that the type of alkaline liquid is a significant factor affecting the mechanical strength of a geopolymeric cement (Palomo et al., 1999).

Attapulgite

The chemistry of attapulgite has not been fully understood or thoroughly documented. Attapulgite is believed to form at the surface of the earth and has a needle-like structure, consisting of two outer silica tetrahedral layers and an octahedral interlayer. In 1970, Carroll proposed that attapulgite mineral clay has a chemical form presented follows (Carroll, 1970);

$$[Si_8Mg_5O_{20}(OH)_2(OH_2)_4.4H_2O]$$

The use of attapulgite as an additive for the production of fly ash geopolymers has also not been thoroughly studied or documented, however Salman (2016) manufactured alkali activated bricks from attapulgite mineral clay. In this study attapulgite mineral clay was used as the source mineral and was hydrated with various concentrations of NaOH. Different burning temperatures were applied to the produced alkali activated bricks to increase the stability of bricks and to study the effect of the burning temperatures on the bricks.

It was concluded that attapulgite bricks burnt at 500℃ yielded in higher compressive strengths as opposed to bricks burnt at 350, 400, 450, 550, 600 and 650℃. Additionally attapulgite bricks made from 4M NaOH and burnt at 500℃ resulted in the optimum compressive strength of 13.9 MPa as opposed to 6 M and 8 M NaOH activated bricks which resulted in 13.3 MPa and 13.5 MPa respectively (Salman, 2016).

2.3.2 Alkaline solutions for source material activation

For gelation or geopolymerization to occur, there be should an alkaline solution present in the reaction mixture. The most important aspects regarding alkaline solutions for hydrating the solid material in geopolymers are; the type of alkaline solution and/or the combination of alkaline solutions, the concentration of alkaline hydroxides and the ratio of soluble silicates to alkaline hydroxides.

The following section gives a brief review on the various combinations of soluble silicates to alkaline hydroxide, the type of alkaline hydroxide concentrations and the ratio of soluble silicate to the alkaline solution. The studies indicate how alkaline solutions influence the physical and mechanical properties of geopolymers.

2.3.2.1 NaOH and Na_2SiO_3

The first step of geopolymerization requires the breakdown of Si-O-Si and Al-O covalent bonds present in the solid source material. The role of NaOH or an alkali metal hydroxide in the geopolymerization process, is to activate the Si and Al ions present in the source material by breaking down and liberating these Si and Al ions (Ryu et al., 2013).

Additionally, it should be noted that by increasing the concentration of NaOH improves the solubility of Si and Al ions in the source material thus resulting in higher compressive strengths of fly ash/slag based geopolymers (Puertas et al., 2000). A study by Memon et al. (2013) also confirmed that the compressive strength of fly ash based geopolymers improved sequentially as the concentration of NaOH was raised from 8 M - 12 M. The study also presented a change in the behavioural trend where a decrease in the compressive strength was noted when the concentration of NaOH reached 14 M (Memon et al., 2013). This change in trend was substantiated by the fact that higher NaOH concentrations leads to excess OH^- ions in the alkaline solution. An excess OH^- ions leads to the formation of a white precipitate and thus interferes with successive geopolymerization processes (Memon et al., 2013). Accordingly, it becomes imperative that an idealized set of alkaline concentration conditions be defined for optimal geopolymerization.

As mentioned in previous sections, a combination of NaOH and Na_2SiO_3 as hydration liquid mixture in the production of fly ash/slag geopolymers materials, results in higher compressive strengths as opposed to other alkaline combinations (Phoo-ngernkham et al., 2015). The high Si content in Na_2SiO_3 is important for enhancing Si-Al oligomer formation via the poly-condensation reaction. The combination of these Si-Al oligomers promotes the formation of aluminosilicate hardened structure, giving rise to fly ash based geopolymers with substantially improved compressive strengths (Thokchom et al., 2009). Using a Na_2SiO_3/NaOH ratio that manufactures geopolymers with enhanced strength is therefore important.

Once again, literature sources substantiate the aforementioned postulations. A higher compressive strength of 11.9 MPa was obtained for palm oil boiler ash based geopolymers manufactured from a 14 M NaOH and a Na_2SiO_3/NaOH ratio of 1.5 and 2.5 after 7 days of curing (Yahya et al., 2015). On the other hand, when palm oil boiler ash based geopolymers were synthesized from 0.5, 1 and 3.0 Na_2SiO_3/NaOH ratio, the compressive strength was below 2 MPa, 5 MPa and roughly 10.8 MPa respectively (Yahya et al., 2015).

Another study (Mustafa Al Bakri et al., 2012) concluded that fly ash based geopolymers (activated by Na_2SiO_3/NaOH solutions), afforded a maximum compressive strength of 94.50 MPa after 7 days of curing. In this study it was noted that the optimal compressive strength of the fly ash based geopolymer was obtained from a 12 M NaOH and a 2.5 Na_2SiO_3/NaOH ratio mixture. This was relative to 6 M, 8 M, 10 M, 12 M and 14 M concentration of NaOH and 0.5, 1.0, 1.5, 2.0, and 3.0 of Na_2SiO_3/NaOH ratios.

2.3.2.2 KOH and Na_2SiO_3

As mentioned in the previous section, a mixture of NaOH and Na_2SiO_3 as an alkaline activator has been the most readily utilized combination of alkali metal hydroxides and other soluble silicate mixtures for geopolymer synthesis. Owing to the scarcity of use of KOH and Na_2SiO_3 as activators for geopolymerization processes, a study by Okoye et al. (2015) was conducted and it confirmed that KOH (14 M) combined with Na_2SiO_3 resulted in a reduced compressive strength as compared to the combination of NaOH (14 M) and Na_2SiO_3 (Okoye et al., 2015). In contrast, Satpute et al. (2016) also reported that the combination of KOH (8 M and 10 M) with Na_2SiO_3 concentrations resulted in the highest compressive strength when the geopolymer was cured at 80℃ and 90℃ for 24 hours, as compared to other alkaline combinations. Accordingly, it seems that the KOH and Na_2SiO_3 combination would be deemed useful in geopolymer synthesis, however it does afford a lower geopolymer compressive strength with KOH concentrations > 12 M at 90℃, owing to the interference of increased hydroxide ions in the KOH solution.

2.3.2.3 NaOH and K_2SiO_3

The combination of NaOH and K_2SiO_3 displayed a similar trend to that noted for the combination KOH and Na_2SiO_3, in terms of compressive strength. At 8 M NaOH concentration, this combination resulted in a compressive strength of 18.9 MPa at an 80℃ curing temperature. When the concentration was increased to 10 M the compressive strength of geopolymer also increased to 33.15 MPa at 90℃, whereas between 12 M - 14 M the combination showed a decrease in compressive strength (Satpute et al., 2016).

2.3.2.4 KOH and K_2SiO_3

KOH and K_2SiO_3 is a common combination for alkali activation of geopolymers but is applied less readily than the NaOH and Na_2SiO_3 mixture, due to lack of chemical availability and cost affectivity. It has also been observed that a majority of research has confirmed that the NaOH

and Na_2SiO_3 combination gives higher compressive strength relative to that observed for KOH and K_2SiO_3 (Tippayasam et al., 2016).

The KOH and K_2SiO_3 combination however, performs better with regards to compressive strength when heat cured as opposed to curing in ambient temperature for certain K_2SiO_3/KOH ratios. According to Hosan et al., (2016) the compressive strength of geopolymers containing a combination of KOH and K_2SiO_3 (3:1 mass ratio), resulted higher in higher compressive strengths, lower micro-cracking and were stable at all elevated temperatures, relative to NaOH and Na_2SiO_3 based geopolymers. Tippayasam et al. (2016) conducted a study on the activation of geopolymers with K_2SiO_3 and KOH, where the compressive strength of KOH (10 M) and K_2SiO based geopolymers (1.5:1 mass ratio) was found to be 34.75 MPa, cured at 40℃ for 28 days.

2.3.2.5 $Ca(OH)_2$

Various studies have been conducted on the effect of calcium hydroxide when either added as an alkaline solution or present in the solid form as source material in the production of geopolymers. It was found that the presence of $Ca(OH)_2$ somewhat increased the compressive strength of hardened ambient cured geopolymers (Temuujin et al., 2009). During the hydration of standard geopolymers, an amorphous aluminosilicate is the resulting hydration product, but in the presence of $Ca(OH)_2$ portions of C-S-H bridges are detected in the sample during SEM analysis. It is believed that this combination of the C-S-H portions and geopolymeric products results in improved mechanical strength in geopolymer samples. This is attained from the C-S-H bridging the gaps between the different hydrated phases and voids found in the geopolymer binders (Yip et al., 2005).

However, the incorporation or presence of $Ca(OH)_2$ could lead to increased carbonation processes in cementitious materials and as a result it is not always advantageous (reduced longevity) in reinforced steel cementitious materials (Yip et al., 2005). The famous example of when carbonation occurs is noted when $Ca(OH)_2$ is produced during cement hydration in OPC cement production and reacts with atmospheric CO_2, forming a precipitate know as calcium carbonate ($CaCO_3$). In slag based geopolymers the high calcium oxide content is responsible for the accelerated rates of carbonation. In addition, class F fly ash based geopolymers activated with Na_2SiO_3 displayed the formation of sodium bicarbonates when high thermal curing conditions were induced in a study conducted by (Criado et al., 2005).

Bernal et al. (2012) confirms that increased carbonation process in slag based geopolymers leads to the modification of calcium and sodium carbonates to sodium bicarbonates. These available bicarbonates are responsible for reducing the pH in pore solutions (Bernal et al., 2012), thus leading to the corrosion in steel reinforced cements (Johannesson & and Utgenannt, 2001).

2.4 Physical properties of geopolymers

The longevity of a concrete material plays a major role in construction applications. Concrete is widely used as a building material, and as such, it must be durable in potentially aggressive environments. Concrete durability is largely influenced by the flow or movement of fluid or gases through the material due to capillary suction and the effect this has on the material structure.

Capillary suction or pressure occurs when film water (water that forms at the surface of fresh concrete) evaporates more rapidly than the transport rate of water molecules within the concrete to the surface (Schmidt & Slowik, 2013). As more water is lost at the surface of the concrete, the then solid particles are exposed to the surface and water between solid particles form a meniscus creating capillary pressure. The more water evaporates the closer the solid particles, the smaller the distance between the solid particles thus initiating greater pressure. Fine voids present in concrete are therefore the driving force of capillary pressure and increased intake of water and mineral ions by concrete.

The deterioration in concrete results from excess water uptake, or the ingress of chloride or sulphates into the concrete, therefore, the reduction in movement of such ions is essential for concrete to reach high potential performance. Some of these properties will be discussed in the following sections which can affect the longevity of cementitious materials.

2.4.1 Pores and porosity

The presence of pores can be very detrimental to the strength of cementitious materials. These pores tend to weaken the internal structure of cement and make it susceptible to the ingression of water, sulphates or acids (Fernando & Said, 2011).

There are various ways in which different types of pores are created. The different types of pores include; (1) capillary pores; ranging from 10 μm to 10 nm in size, (2) gel pores which are smaller, ranging from 10 nm to 0.5 nm, and (3) air voids.

During cement hydration, hydration products such as the gel phase and un-hydrated cement portions are formed. Larger pores are capillary pores and are known as the unfilled spaces in cement not containing hydration products. The areas that do contain hydration products (such as C-S-H) afford even finer pores, known as gel pores (Jennings et al., 2008). Moreover, air trapped in concrete can result in further empty space or air voids. Air voids can be entrapped or entrained, where the former arises from air that is trapped during improper mixing in cement. The latter is air that is deliberately incorporated by using air entrainment agents, for the purpose of releasing certain pressures in the cement or concrete (Darraugh, 2009).

Unfortunately, it is very hard to completely eliminate the gel pores or air voids but several methods have been employed to minimize their occurrence when making cementitious or concrete matrices. The water to cement (w/c) ratio, which basically refers to the weight of added water to cement or source material, can be reduced to minimize pore formation. As has been mentioned, pore formation occurs when there is an excess of water added during cement hydration, allowing more empty spaces or voids to form when the hydration water evaporates during cement curing (Jennings et al., 2002). Accordingly, it is important that the w/c ratio is kept at a minimum, to reduce the amount of empty spaces or voids post evaporation.

In general, the occurrence of pores in cementitious materials affects the density or compactness of the structure, thus resulting in reduced compressive strength. However, in some cases, fewer pores in the cementitious structure do not necessarily result in improved compressive strength. This was observed in the study by Ramezanianpour & Moeini (2018) that as mentioned previously, even though silica fume was added to make the geopolymer structure more compact and less porous, it did not necessarily increase its compressive strength but instead led to incomplete geopolymerization.

Additionally, air entrainment in cement is sometimes important in freeze-thaw cycles and these types of agents are largely used to create tiny air bubbles in concrete. The water molecules (occupied within the concrete) increase in volume in cold weather and as they expand these molecules induce pressure or tension that is too much for cement concrete to maintain. This tends to lead to cracking as the concrete attempts relieve the pressure. The tiny air bubbles created by air entrainment agents, creates added space that will accommodate the expansion of water molecules in cold conditions (Shang & Yi, 2013). Accordingly, it would definitely be deemed advantageous to study the nature of porosity or permeability cause by compound synthesis of any cementitious structure to investigate the overall properties of concrete.

2.4.2 Water sorptivity tests

Water absorptivity testing has been noted as the optimal approach to ascertain how porous or permeable the cementitious material is. Permeability of a cementitoius material has to do to with the ability of fluid transport into the material under pressure. Different types of water absorptivity methods are explained below, which have been used to determine the rate at which the volume of water is absorbed per unit area.

2.4.2.1 Initial Surface Absorption Test (ISAT)

The British Standard BS Part 208:1996 describes the Initial Surface Absorption Test **(**ISAT). In this method, a cap with a defined area is clamped to the surface of the concrete material to be tested. The cap unit is connected to two tubes; one being an inlet connected to a water reservoir and the other an outlet connected to a calibrated capillary tube as shown in Figure 2.4. The former is used to supply water to the test surface of concrete and the latter is connected to the capillary tube that measures the rate of absorption.

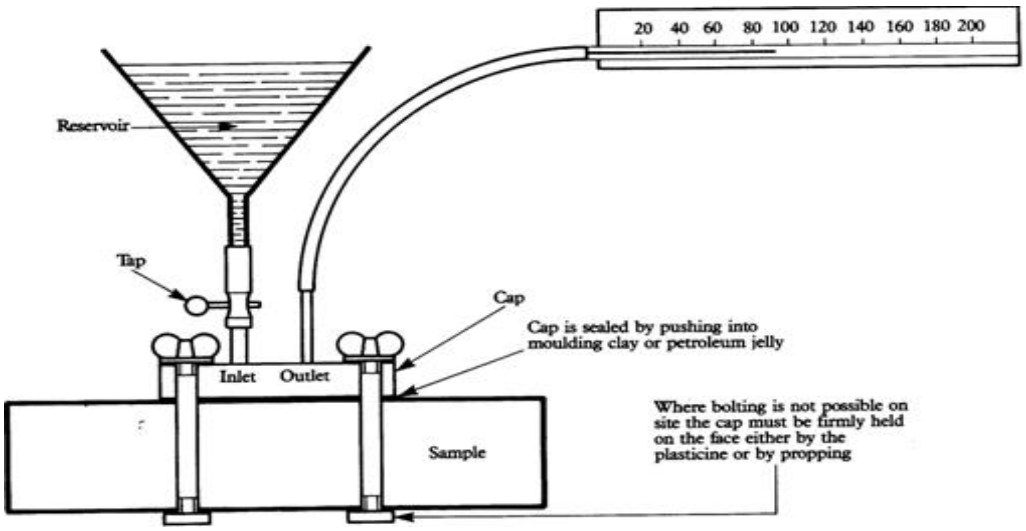

Figure 2.4: ISAT setup showing the flow of water to the surface of concrete and how the rate of water absorption is measured (Claisse, 1997).

The concept of the ISAT is based on the high initial water absorption rate through capillary action, which is experienced by dry concrete or specimens. The water absorption rate then decreases readily as capillary pores get filled with ingress water or moisture. This data is then incorporated into a mathematical equation derived by Levitt (1969), which expresses the movement of liquid itinerant through a single capillary tube as follows;

$$ISA = \frac{F}{\theta} = at^{-n}$$

Where, ISA is the initial surface absorption ($m^3/m^2/s$), F is the flow rate (m^3/s) , θ is the area under cap (m^2), a, n are regression parameters and t is the absorption time(s) (Levitt, 1969).

2.4.2.2 Covercrete Absorption Test (CAT)

The covercrete absorption test (CAT) method was developed by Dhir et al. (1987) to assess absorption characteristics of a hole drilled in concrete with 13 mm diameter and 50 mm depth. The test setup, like the ISAT method, uses a cap with an inlet attached to it that supplies water to the concrete test cavity and an outlet attached to the capillary tube. In the CAT method however, the water inlet tube is located inside the drilled hole, where it feeds the cavity with water. The drilled hole method is deemed to be a more advantageous setup, as the absorption process is less likely affected by local surface attacks (Patel, 2009).

2.4.2.3 Other sorptitivity test methods

As has been mentioned, when a cementitous material or concrete comes into contact with water, the rate at which the unidirectional flow of water through unsaturated concrete, by capillary suction is referred to as sorptivity. The acceptance of sorptivity as standard method for obtaining applicable information about the porosity or strength of concrete comes from earlier work undertaken by Levitt (1969) and Hall (1989). Hall's (1989) investigations led to the development of both automated and manual (ASTM C 1585-04 Standard test) systems for the measurement of sorptivity in mortar and concrete.

Sabir et al. (1998) conducted an automated study where the test specimen immersed in water is directly linked to balance, that automatically records the change of mass and sends the data to a PC installed with a written software (Sabir et al., 1998)**.**

The ASTM Standard C1585-04 method is a simple laboratory test method used to determine the sorptivity of cement concretes manually. In this method, samples with dimensions of; 100 $\pm$ 6 mm in diameter and a height of 50 $\pm$ 3 mm, are cured for 28 days after which specific conditioning of the material is required prior to testing. For conditioning, the ASTM C1585-04 standard specifies that the samples be placed in an environmental chamber, or alternately samples be placed in a desiccator, within an oven (at 50℃) for 3 days at an 80 $\pm$ 3% relative humidity. After removal from the oven, the samples should be sealed in a plastic container for 15 days before testing for water absorptivity. After sample conditioning, the samples should be

sealed with protective coating on the sides of concrete, to allow water to flow in one plane and are weighed before immersing in water. The specimens are then immersed in a tray containing water, ensuring that the water level above the concrete is maintained at a few mm. This will allow the ingress of water into the unsaturated concrete in one direction. The gain in weight of the concrete is recorded against the start time. A typical water sorptivity setup is presented in Figure 2.5 below;

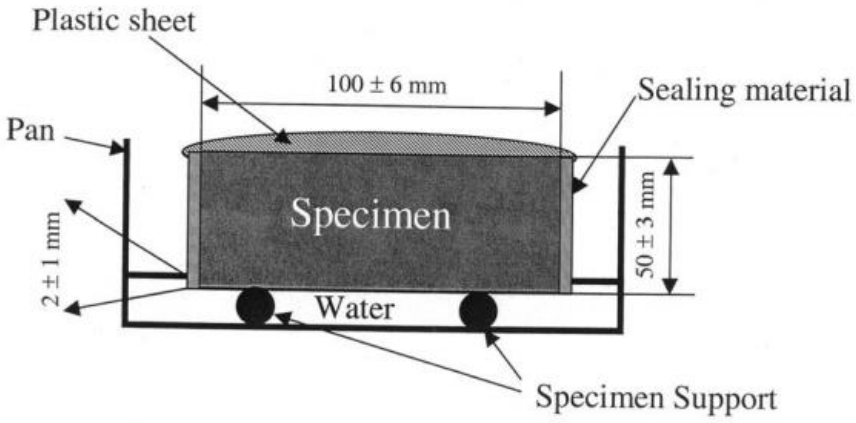

Figure 2.5: Schematic of a typical water sorptivity test as described in the ASTM C1585-04.

Sorptivity is then determined using the following equation;

$$\mathbf{I} = \frac{\Delta \mathrm{M}}{\mathrm{a/d}} \qquad (1)$$

where I is absorption, ΔM is change in mass of sample (g), a is exposed area of sample (mm^2) and d is density of water (g/mm^3). Sorptivity (unit required) is given by the slope of best fit line of absorption versus square root of time curve (ASTM Standard C1585).

2.5 Mechanical properties of geopolymers

2.5.1 Dimensional change

There are a few factors that contribute to the change in volume of hardened cement pastes and these changes often lead to micro-cracking. Micro-cracking can pose great deal of problems in construction when concrete structures are weakend and are unable to carry their intended design load.

The increase (swelling) and decrease (shrinkage) in volume of cement pastes are as result of both environmental and mechanical stresses to which the samples are exposed. In high relative humidity conditions, the air is moist which can lead to the uptake of water vapor by the cement

samples and eventually cause the sample to swell. Conversely, at low relative humidity, the air is dry, which could induce loss of water from the concrete sample, leading to shrinkage (Vijayakumar, 2013). The various types of shrinkage will be discussed in more detail in the following sections.

2.5.2 Types of shrinkage

The shrinkage of any material has been readily associated with the decrease in volume of that material, but not every type of shrinkage directly plays a role in the overall reduction of volume. Therefore, the term shrinkage has been further classified to try and explain the events and causes from which the different types of shrinkage occur. The types of shrinkage are thus divided into; (a) plastic shrinkage, (b) chemical shrinkage, (c) autogenous shrinkage, (d) drying shrinkage and (e) carbonation.

(a) Plastic shrinkage

This type of shrinkage can be seen through the formation of cracks. The cracks are seen on the surface of the paste when the cement is still in the plastic state just before it hardens. The less water evaporates from the cement the less the plastic shrinkage.

(b) Chemical shrinkage

Chemical shrinkage is simply described as the decrease in volume of products formed relative to the reacting material (liquids and solids). When the hydrating liquid is added to the un-hydrated cement, the volume of water will become smaller as it gets used up by the cement for hydration. In a similar manner the volume of the starting or un-hydrated cement tends to be larger in a solid state, as the reacting liquid hydrates, the product hydrated cement (in the plastic state) will shrink in volume (Šahinagić-Isović et al., 2012).

(c) Autogenous shrinkage

This type of shrinkage is visible and can be measured by noting the change in length of the material. Autogenous shrinkage occurs when no water is lost to the environment, but rather when water from pores is taken up by un-hydrated cement for further hydration (self-desiccation). Factors such as excess water in cement will not give rise to autogenous shrinkage, however, when the w/c ratio is low, this type of shrinkage will manifest as more pore water will be taken up to for the hydration of un-hydrated cement (Vijayakumar, 2013).

(d) Drying shrinkage

Cement pastes tend to lose water at low relative humidity, thus affording shrinkage of the compound, and will gain water vapor in high relative humidity and swell. Drying shrinkage occurs when water contained in the gel pores is lost.

Certain measures can be put in place to minimize the drying shrinkage of cement specimens. When there is a lower water content within the specimen, there is ultimately less water to be lost from the capillaries and thus resulting in reduced shrinkage. This can be achieved by incorporating reinforcement and/or more aggregates to the cement pastes (Khairallah, 2009). Additionally, larger and or coarse aggregates are more effective in reducing drying shrinkage in concrete samples; this is because these aggregates tend to occupy more space in concrete materials, leaving less room for cement paste which is where water tends to evaporate. The cement specimens can also be sealed in an enclosed environment to avoid evaporation of water.

Some notable studies relating to the extent of drying shrikage within geopolymeric material has been undertaken in the past. A study by Deb et al. (2013), concluded that, slag blended fly ash geopolymer concrete, cured at room temperature, has a drying shrinkage that is comparable to that of OPC concrete with similar compressive strength. This can be seen with the 180-days drying shrinkage of the geopolymer concrete mixtures varying between 482 and 722 micro-strain, whereby the shrinkage of the OPC concrete mixture at 180 days was 564 micro-strain.

Conversely, according to a study by Vijayakumar (2013), the class F fly ash/slag based geopolymers proved to have higher drying shrinkage relative to OPC cement pastes. This was believed to be because the microstructure in cement paste may have been thoroughly settled and structured as compared to that of the geopolymers, in their investigation. Moreover, it was also noted that finer pores in geopolymer matrices tend to experience higher tensile stresses making it prone to higher drying shrinkage. A recently published paper by Deb et al. (2015) also reported that geopolymer concrete undergoes higher drying shrinkage than OPC concrete during first 30 days, due to the higher powder content.

Researchers have reported that geopolymer systems have several factors which can affect the drying shrinkage. For instance, a higher SiO_2/Na_2O ratio increases the degree of polymerization thus forming a denser network gel structure, instead of a chain like polymer structure. This type of network structure is better equipped to trap interlayer molecules thus preventing water loss, and in turn drying shrinkage (Vijayakumar, 2013).

(e) Carbonation shrinkage

As has been mentioned in previous sections, carbonation occurs when the evolved $Ca(OH)_2$ formed during cement hydration, reacts with CO_2 in the atmosphere to form calcium carbonate ($CaCO_3$) (Chang & Chen, 2006). During $CaCO_3$ formation, shrinkage takes place due to the dissolution of $Ca(OH)_2$ crystals. The resultant $CaCO_3$ gives may subsequentely cause corrosion of the steel or metal in reinforced concrete. The $CaCO_3$ lowers the pH in the concrete thus affecting the protective oxide layer of the steel (Khairallah, 2009). When this layer is affected, it can no longer prevent metal corrosion and in turn weakens the cement specimen and cause cracking.

Khan et al. (2016) reported a recent study on the carbonation of low-calcium fly ash and blended slag (90%/10%) geopolymer concrete, wherein the pH profiles of the alkalinity of the pore solution was investigated and the identification of carbonation products using XRD was reported. The pH was measured after the geopolymer concrete had been exposed to natural carbonation and 1% and 3% accelerated carbonation.

This investigation revealed the presence of natron ($Na_2CO_3.10H_2O$) in the geopolymer pore solution as a carbonaceous product after 6 weeks of natural carbonation (as well as in a 1 & 3% accelerated carbonation examples). Another product; nahcolite ($NaHCO_3$) was observed as the rates carbonation processes were increased. The pH values for the carbonated geopolymer concrete ranged between 10.5 to 11.0 which is more hospitable for steel reinforced types of concretes (Khan et al., 2016) as compared to pH values observed in high-calcium cements.

2.6 Durability of geopolymers

As mentioned in the previous sections, in order for concrete or any cementitious material to thrive in intense conditions, it has to durable. Durability defines the overall performance of concrete and thus its imperative to optimize factors such as, penetrability, compressive strength and especially acid resistance. Highly impermeable pore structure matrices for OPC and geopolymers can be obtained by modifying the w/c ratio, optimizing pore size distribution, limiting dimensional changes and improving resistance to acid ingress**.**

2.6.1 Acid resistance of geopolymers for nuclear application

During a nuclear incident, boron carbide B_4C, which is a material that is mixed with stainless steel for the production of control rods, could possibly be oxidized. The oxidation reaction of B_4C results from the interaction of B_4C with water (that is used as a moderator or a coolant) in the reactor. This reaction leads to the release of CO_2 gases, boric acids and boron oxide

(Steinbrück, 2005). It is therefore imperative that the core catcher must be able to withstand acidic conditions in the case of a molten corium spill.

As indicated by many tests, geopolymer concrete displays an improved ability to resist acidic chemical damage. This property can be ascribed to the lack of dependency on lime in the cementitious mixture that makes it less prone to acid attack, as compared to OPC which is easily degraded in acid. Although boric acid resistance will not be tested in this study, another commonly used acid, sulphuric acid, will be reviewed. Research on the sulphuric acid resistance of fly ash based geopolymer matrices is relevant to this study in obtaining recommendations for optimum geopolymer materials that could enhance containment structures of the reactor core.

Some examples noted from literature highlight the effectiveness of geopolymer matrices against acid damage, with selected cases summarised in the following section. In a recently published paper Shankar & Khadiranaikar (2012) tested fly ash based geopolymer concrete durability in a 10% sulphuric acid solution and compared their results to values obtained for standard OPC cement mixtures. During this investigation, a significant loss of mass (20%) of the OPC concrete (after 45 days of immersion in sulphuric acid) was noted. In contrast, the geopolymers performed better, losing only about 3% of its mass after 45 days (Shankar & Khadiranaikar, 2012). Another study by Bakharev (2005) tested for sulphuric acid and acetic acid resistance on low fly ash content geopolymers relative to OPC. The study concluded that although the fly ash based geopolymers experienced direct sulphuric acid attack on the aluminosilicate structure causing it to de-aluminate, it still performed significantly better than OPC. In addition, Song et al. (2005) reported a 3% mass loss for fly ash based geopolymers after immersion in 10% sulphuric acid and were also noted to be structurally intact as opposed to the 41% mass loss noted for Portland cement.

It is important to emphasize that all of the aforementioned studies noted the high calcium content within OPC as the root-cause for the decalcification process of the material in acidic conditions. Once the calcium layer deteriorates, the interior of OPC is exposed and will interact with the acid solution resulting in subsequent damage (Shankar & Khadiranaikar, 2012).

2.7 Curing methods

The method of curing influences the eventual properties of geopolymers, particularly with relation to the compressive strength of the concrete material. In order to understand the effect

of various curing methods on geopolymer durability, some previous investigations relating to different curing processes, are reviewed in the following section.

2.7.1 Effect of temperature

Davidovits (1994) investigated the effect of curing temperature on various geopolymer properties. In this study it was observed that kaolinitic (granulated iron blast furnace slag geopolymers) generally hardens rapidly at 20℃ and exhibit a compressive strength of about 20 MPa in just 4 hours. The compressive strength then increases to about 70 - 100 MPa in 28 days (Davidovits, 1994). Interestingly, it was noted that at low curing temperatures, the rate of dissolution of the source materials was found to be slow and when the temperature is increased this was counteracted. In general, increased dissolution would be deemed advantageous but elevated temperature curing may also lead to intense dehydration of the geopolymer material thus affording increased porosity or induce cracking (Muniz-Villarreal et al., 2011). Additionally, high temperature curing, as well as air curing methods has a tendency of evaporating pore water in concrete samples and as such give rise to higher water absorption rates and mineral ions absorption during testing.

With these considerations in mind, it was still noted that high temperature curing, has been readily employed to achieve optimum compressive strength in fly ash based geopolymers. Adam & Horianto (2014) reported that the highest compressive strength of 33.10 MPa was obtained for fly ash geopolymers samples cured at 120℃ for 20 hours. These fly ash based geopolymers displayed superior durability as compared to fly ash based geopolymers that were cured in air (15.0 MPa) for 20 hours, at 80℃ the samples resulted in 19.40 MPa compressive strength, at 100℃ the strength was 21.90 MPa and heat cured OPC samples with a 27 MPa compressive strength (Adam & Horianto, 2014). Al Bakri et al. (2011) also investigated the effect of curing temperature on the physical and chemical properties on fly ash based geopolymers. The study also concluded that an increase in curing temperature above ambient improved the overall compressive strength of the geopolymer, but it was conversely noted that the compressive strength decreased as the temperature was increased beyond 60℃. This was ascribed to high water loss within the geopolymer leading to poor alkaline activation of the source material thus impairing its mechanical properties (Al Bakria et al., 2011).

2.7.2 Effect of water content and humidity

Several studies have shown that moist curing (water curing or sealing) of concrete results in the reduction of movement of detrimental mineral ions or water molecules through the final

concrete material. A study by Castro et al. (2011) investigated the conditioning of concrete samples for water absorption and found that samples conditioned at 50% relative humidity, had higher water absorption rates relative to samples conditioned at 80% relative humidity.

Bozkurt & Yazicioglu (2010) studied the absorption of water in OPC concrete samples under different curing conditions (water, sealed curing and curing in air). It was found in their study that of the three methods, the water curing method with added silica fume showed lower water sorptivity values and increased compressive strength as compared to the other samples. This suggests that when OPC cements are cured in water or exposed to higher relative humidity, more water is retained in a concrete material leading to water saturation of pores, thus less pore space is available for further uptake of water. Ultimately, the water absorption rate is reduced. The saturated pores also prevent the uptake of detrimental mineral ions which can cause cement deterioration. It should also be noted that the added silica fume gives the cementitious material a more compact structure by acting as aggregates thus increasing the strength of the sample. A study by Lee et al. (2016) reported an increased compressive strength in fly ash based geopolymers, sealed in plastic containers for curing, relative to unsealed ambient geopolymers. The average compressive strength of sealed-cured geopolymers was measured to be 50 MPa after 1 day of curing and further increased to 120 - 135 MPa after 7 days of curing (Lee, et al., 2016). On the other hand, the average compressive strength for unsealed ambient fly ash geopolymers was reported to range between 60 - 90 MPa after 28 days of curing. From literature it has been documented that during the geopolymerization process, water present in the alkaline solution is taken up in the dissolution stage and is given off during the polycondensation stage (Steins et al., 2012). When the geopolymers are contained in a sealed environment the water molecules remain in the pores of the geopolymer structure. The water molecules will continue to interact with the source material forming a denser geopolymer network yielding in increased compressive strength (Lee et al., 2016).

2.8 Geopolymers with neutron absorbers

Not only do geopolymers afford enhanced physicochemical properties but owing to the internal microstructure of its compositional matrix, the structure can be modified to incorporate neutron absorbers which are ideal for the proposed application of these cements. In the following sections a brief discussing of the effect of moderator incorporation within OPC *vs.* geopolymers matrices will be discussed. Synthesis and testing of these modified compounds is beyond the scope of this study but it is important to note the applicability of geopolymer materials as housing for improved neutron moderators for long-term investigations.

2.9 Mechanical effects of moderator addition

A nuclear reactor always has to be in a critical state to avoid nuclear accidents. The use of neutron moderators and absorbers are important for maintaining safety during criticality. Most reactors use water as a moderator, that slows down high energy neutrons of about 1-2 MeV into thermal energy neutrons to an average energy of about 0.04 eV. These thermal neutrons are ideal for sustaining a fission chain reaction within a reactor. Furthermore, elements such as B, H, graphite or Cd may be incorporated into the core catcher's cementitious material within in the reactor, for the purpose of absorbing neutrons if required (Donne et al., 1976).

To substantiate the practical workability of this, a study by Taveri et al. (2017) was undertaken where borosilicate glass was added as an additive to fly ash based geopolymers and the effect thereof, as it relates to workability of the afforded cementitious compound as a potential neutron moderating material, investigated. From this investigation it was noted that FTIR spectrum indicated a boron oxide band in the fly ash based geopolymer indicating that boron formed part of the poly-condensed hardened structure of the geopolymer. This confirmed that the boron does not prevent or hinder with the hydration process of geopolymerization, which is ideal for its practical applicability (Taveri et al., 2017). A study by Nazari et al. (2014) suggested that the additional B-O bonds present in a borosilicate based geopolymer are due to the substitution of of Al-O bonds that were initiallly present in the source material with these bonds. The B-O bond is said to be responsible for the improved compressive strength of 64 MPa (versus 25 MPa noted for the unmodified sample) attained by the borosilictae geopolymer (Nazari et al., 2014).

On the other hand, a study by Palomo and Fuente (2003) on the determination of the effect of boron addition in solidification of OPC and fly ash based geopolymers systems revealed contradictory observations. The results of the study indicated that OPC incorporated with boron from boric acid hydration had a negative effect on the mechanical strength of the concrete. This was deemed to stem from the fact that the boron compounds prevent proper hydration of cement grains (Palomo & dela Fuente, 2003). Boron compounds in various concentrations can lead to formation of compounds such as CBH_4 which precipitates and inhibits the formation hydration product (C-S-H) which gives cement its strength. This mechanism also retards the setting time of OPC matrices and the addition of these types of moderators is detrimental to the durability of OPC cementitious materials (Davraz, 2015).

2.9.1 Moderator leachability

Palomo and dela Fuente (2003) also tested OPC and alkali activated fly ash based materials for the leachability of boron compounds from within the concrete lattice. Both OPC and alkali activated fly ash based material were hydrated with 6% lime and boric acid with the addition of NaOH to the latter cement. The OPC samples revealed an excess of 40% boron leaching as opposed to less than 20% boron leaching for the fly ash based materials. This increased extent of leaching indicates that OPC is not strong enough to resist leaching of boron, and again highlights the fact that OPC type matrices are not ideal for immobilising boron and are deemed impractical candidates for neutron moderation applications (Palomo & dela Fuente, 2003).

2.10 Geopolymers with radiation resistant components

There are three primary protective measures, which have been adopted when working around a radioactive source. These include the limitation of exposure time, ensuring safe working distance from the source as well as adequate radiation shielding. It is important that less time should be spent around a radioactive source and a safe distance must be kept at all times in order to minimize possible radioactive dose effects (Mettler et al., 1997). Shielding against radiation is one of the most effective ways of reducing radiation exposure, however due to the fact that materials differ in their ability to absorb radiation, finding a suitable material can become tricky especially when considering gamma radiation.

Gamma rays have no charge, a mass that is negligible, higher energy and a shorter wavelength making it a very penetrative radioactive particle as compared to alpha and beta particles. Traditionally, OPC, has been used as one of the materials in reactor shielding to attenuate both neutron and gamma rays but because the mechanical inadequacies of OPC industries are looking at geopolymer concrete as an alternative.

Additionally, some researchers have attempted to replace traditional fillers of concrete such as sand or crushed rocks with materials that exhibit larger gravity namely magnetite, hematite, barite and colemanite (Azeez et al., 2013), as well as metal particulates to concrete to enhance its density. A denser concrete means a tightly packed molecular structure which acts a cushion to prevent radioactive particles from changing direction due to the impact of striking something. This method has been adopted widely by nuclear stations and generation plants in order to make their walls and roofs radioactive proof. This approach can also be extended to geopolymeric type materials with some literature examples noted in the following sections. Once again it should be noted that the synthesis and testing of these modified compounds is

beyond the scope of this study but it is important to note the effectivity of geopolymer materials for these types of applications.

2.10.1 Geopolymers with barite content

Barite is a natural element that exists as an ore of barium. It receives its name from the Greek word "barys" which means "heavy" this can be seen from the high specific gravity of 4.5 it exhibits. Furthermore, barite is one the natural minerals with the physical ability to dissipate x-ray and gamma-ray emissions. Azeez et al. (2013) conducted a study on the effects barite when added to both OPC and fly ash based geopolymers, which revealed that the addition of powdered barite to both concrete materials increased the attenuation performance. However, the compressive strength of geopolymer concrete is decreased although not as much as observed for OPC concrete.

2.10.2 Geopolymers with heavy metals

Heavy metals are significant components in many industrial and residual wastes streams and limiting their release into the ecosystem is of great importance. Examples of these heavy metals include; Pb, Ni, Fe, Mn, Cu, Zn, Cd, As, Cd, Co and Cr. Untreated toxic wastes tend to make their way to fresh ground water posing a significant threat to human health (van Jaarsveld & van Deventer, 1996). For the past few years, landfilling was one of the most widely used methods for the processing of radioactive waste but because of costly and labour intensive maintenance considerations, other methods had to be considered. Accordingly, it is envisaged that the heavy metals (Pb or W) possibly be immobilized within geopolymer matrices.

An example of this was noted in the work of Zhang et al. (2016), where Pb (II) and Cd (II) were effectively immobilized within fly ash-based geopolymers. The study involved manufacturing geopolymer concrete from red mud and fly ash class F as raw materials.

This 'modified' concrete was immersed in sulphuric acid (of pH = 3.0) as well in deionised water (of pH = 7.0) for 120 days, with the amounts of leached heavy metals in the acid and water remaining under the US EPA limits (Zhang, et al., 2016). From this it can be confirmed that the heavy metals were adequately encapsulated in the red mud class F fly ash. There was a slight variance in durability and strength of the red mud class F fly ash geopolymers which were comparable to that of OPC; however, this was believed to be due to dissolution of gels in the structure, as indicated in Figure 2.6.

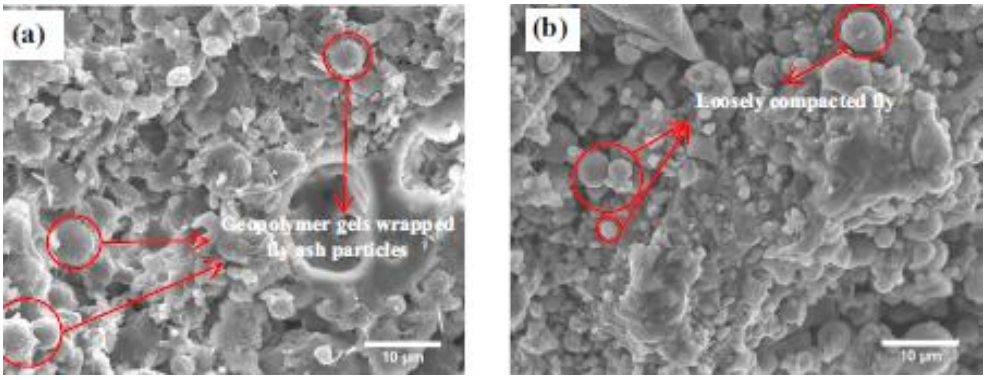

Figure 2.6: SEM image illustrating the red mud class F fly ash cementious material before and after being immersed in sulphuric acid (Zhang, et al., 2016).

Chapter 3 Definition of OPC characteristics as a baseline model in physicochemical investigations

3.1 Introduction

This Chapter describes the applied synthetic methods, the material testing protocols, as well as the physicochemical results observed during the preparation of OPC samples. Focal points include; mix designs, curing methods, sample conditioning, as well as, water absorptivity, sulphuric acid resistance and compressive strength testing of these compounds. All of these aforementioned experimental factors are indicative of the durability of the synthesized compounds and it was deemed imperative that these parameters be thoroughly defined and optimized for idealized application purposes.

3.2 OPC baseline model

As was noted in the introductory section of this study, it is imperative to improve upon the physicochemical characteristics of the current cementitious (OPC) mixtures used as core-catcher material. Although the use of OPC is established and entrenched within the nuclear industry, due to its relative abundance and cost-effectivity, various failings limit its use as an optimal candidate.

As has been mentioned, the structure of OPC type concretes is based on hydrated calcium silicate (C_3S and C_2S) products that could make it very susceptible to acid/sulphate attack. It has also been well documented that these compounds may also retain residual pore hydration water with the macrostructure (an artefact from curing process), that may be lost at temperatures above 300 - 500℃ or when exposed to high irradiation doses (> 1010 Gy) resulting in structural deformation (Fillmor, 2004). Moreover, the interactions of a core catcher cement concrete with the melted core may give rise to internal explosions during a core melt, owing to the heat given off by the corium, leading to concrete ablation (Allelein et al., 2005). As the concrete decomposes, various gasses (H_2, CO and CO_2) may be released into the containment atmosphere and be responsible for an increased explosion risk.

Although, the failings of OPC have been noted in the previous section, it would still be deemed advantageous to investigate the various properties that influence compound durability, as this gives us hands-on experience with these types of material investigations. In addition to this, as OPC type compounds are the current standard material used for core catching applications. Accordingly, it would be useful to investigate and optimize these structures in such a way to

obtain the various specifications that would serve as a baseline for comparison with envisaged geopolymer species to attempt to supersede.

3.2.1 Preliminary testing of OPC

Preliminary testing was conducted in this study to gain familiarity with the manufacturing of OPC type cementitious samples. The preliminary layout entailed the manufacturing of OPC pastes with a selected constant w/c ratio of 0.33. This w/c ratio was selected based on a study by Shamsai et al. (2012) who concluded that a 0.33 w/c resulted in the highest observed compressive strength for OPC mixtures.

During preliminary testing, it was witnessed that, although the workability of fresh OPC paste was found to be easy to mix, however, entrapped air-voids were still observed during moulding of the fresh paste. An ambient unsealed curing method was also maintained for the OPC pastes, which were then tested without any form of sample conditioning for water absorptivity and sulphuric acid resistance testing.

3.2.2 Preliminary results

It was detected that the OPC samples afforded excessive initial sorptivity values and a nonsensical percentage weight gain after exposure to sulphuric acid, relative to results noted in literature (see comparison in Table 3.1 and Figure 3.1). This observation led to the suggestion that the samples may have experienced excessive pore water evaporation during the curing process, thus yielding high water absorptivity values and percentage weight gain during sulphuric acid testing owing to a "dry" lattice structure.

Table 3.1: A comparative tabulation of the sorptivity rates of an unconditioned OPC sample versus the results observed for a conditioned sample by Patel (2009).

Unconditioned OPC sorptivity (mm/√s)		**Sorptivity results (mm/√s)**	
Initial sorptivity	**Secondary sorptivity**	**Initial sorptivity**	**Secondary sorptivity**
0.1755	0.0011	0.00453	0.00375

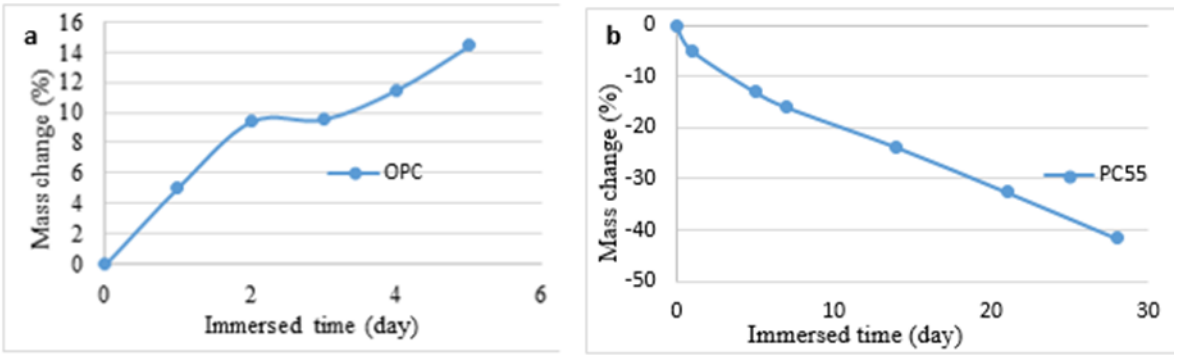

Figure 3.1: (a) An illustration of the %wt. gain noted for an unconditioned OPC-test specimen immersed in 10% sulphuric acid for 5 days (this study) and (b) A comparative illustration of the mass changed observed for an appropriately conditioned OPC sample obtained from a study by Song et al. (2005).

From literature, the ASTM C 1585-04 (ASTM, 2004) and the ASTM C267 standard test (ASTM, 2001) for chemical resistance of mortars and polymer concrete both require samples to be conditioned prior to testing. This sample conditioning method as per the ASTMC 1585-04 involves the placing of cured samples in an environmental chamber at a specific temperature and an 80% relative humidity for 3 days, then further placing the samples in plastic containers for 15 days, to allow for distribution of moisture throughout the sample (ASTM, 2004).

The initial testing showed that not conditioning the samples according to specified parameters prior to testing might negatively affect the results obtained. Although, this may seem obvious, the systematics and reasoning behind this initial approach will become evident in Chapter 4, when considering the pre-screening the various geopolymeric samples.

3.2.3 Post preliminary work considerations

In view of these initial experiments and by also conducting an in-depth literature review on similar types of comparative investigations, the following selected additional parameters/assumptions were put in place to modify further OPC studies in order to investigate the various physicochemical effects of the afforded cementitious compounds;

- The w/c ratio for OPC samples were varied (from 0.31- 0.40) in order to select the optimal w/c ratio for this study.
    - In similar studies conducted by Shamsai et al., (2012) and (Diyora et al., 2015) these w/c ratios were found to be the most effective for OPC-type sample durability.

- Three potential curing methods (water, non-ambient plastic bag sealed and unsealed ambient curing) for OPC cements were identified from literature and in an attempt to further investigate the anomaly observed in Section 3.2.2, the effectiveness of each were investigated. From the obtained results, one baseline curing method was selected for the optimization of geopolymer pastes in Chapter 4.
- Pre-conditioning of OPC samples were implemented prior to water absorptivity, compressive strength and sulphuric acid testing as per the ASTM C1585-04 standard (ASTM, 2004) and ASTM C267 standard (ASTM, 2001) to ensure that all samples are standardized.
    - As mentioned, this type of conditioning includes the application of an environmental chamber maintained at a specific temperature and relative humidity and subsequently curing these samples plastic containers that are five times the size of the sample.

It should be noted that various other parameters may possibly influence the obtained results from these types of experiments, including curing time and temperature but due to time constraints and the limited scope of this study, it was deemed surplus to requirements to investigate all of these types of effects. Accordingly, other variables were kept as fixed as possible in the general synthetic procedure to limit complexity. Additional preliminary preparations and added objectives post preliminary testing for geopolymer samples will be discussed further in Chapter 4.

3.3 Experimental procedure for OPC

OPC, type CEM 1-52.5 N, was used in this experimental study. The OPC was supplied by Chamberlains hardware store, with a detailed chemical specification sheet of OPC illustrated in Table 3.2, with distilled water used for OPC hydration**.**

Table 3.2: A tabulated summary of the main constituents of OPC (CEM 1-52.5N) composition.

Constituent	**Weight percentage (%)**
SiO_2	20 - 25
Al_2O_3	5 - 6
Fe_2O_3	2 - 3
CaO	60 - 65
MgO	1 - 2
Na_2O	0.2 – 0.3
K_2O	0.4 – 0.5
Free Lime as CaO	0.5 – 1.0
C_3A	5 - 10

3.4 Methods

3.4.1 Mixing procedure

OPC (CEM 1-42.5 N) was used to prepare four types of sample mixtures with different (w/c) ratios. The naming convention and mix proportions for the various w/c ratios are shown in Table 3.3. During OPC sample preparation, OPC and distilled water were mixed thoroughly in plastic containers for 2 minutes to attain a homogenous mixture, according to ratios noted in Table 3.3

Table 3.3: The composition of various OPC mixtures that were cured in air, water and sealed plastic.

Mix I.D	**OPM1**	**OPM2**	**OPM3**	**OPM4**
OPC (CEM 1) (g)	325	300	275	250
Water (g)	100	100	100	100
w/c (g/g)	0.31	0.33	0.36	0.40

The cement paste was placed into a 50 mm × 50 mm cylindrical plastic mold in sections to allow the mixture to be frequently (35 times) tapped to remove entrapped air. The fresh paste was allowed to set for 24 hours before being demolded, and as shown in Figure 3.2. For this

investigation, a total of 27 OPC samples were prepared according to the varying w/c ratios stated in Table 3.3.

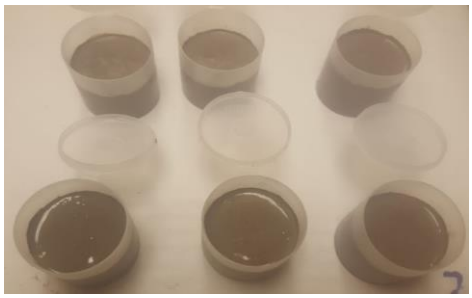

Figure 3.2: OPC samples in molds left to cure for 24 hours.

3.4.2 Curing of OPC samples

From the 27 prepared samples, (a) 9 samples were cured in water, (b) 9 in an ambient environment (air) and (c) 9 were sealed in plastic bags (controlled environment). From each set of the method (a) - (c), 3 samples of each were tested for water absorptivity, 3 for sulphuric acid resistance and the last 3 for compressive strength.

For the air curing procedure, the samples were placed on bench tops, unsealed as shown in Figure 3.3a and were allowed to cure at room temperature until the day of testing. Figure 3.3b illustrates the sealed curing method where the OPC samples were placed in plastic bags and sealed, to avoid excessive moisture loss from samples. The water curing method entailed completely submerging the OPC samples in a tray filled with distilled water as seen in Figure 3.3c. The tray containing OPC samples was loosely covered with plastic to avoid water evaporation and entry of contaminants from the air during curing.

Test samples for water sorptivity and sulphuric acid resistnace had an extended curing period of 40 days, while waiting for the oven to be delivered for sample conditioning. It should be noted that the samples used for compressive strength, were only cured for a period of 28 days.

The samples were named according to the X_1-$XXXX_2$-X_3 system where X_1 is the curing method (W denotes water curing, A represents air curing, and P is the sealed curing method); $XXXX_2$ is the composition of mixtures for various OPC (see Table 3.3) and X_3 is the sample number (1, 2 or 3). An example would be **W-OPM1-2**, where **W** is for samples cured in water, **OPM1** refers to OPC mixture **1** and **2** denotes the sample number.

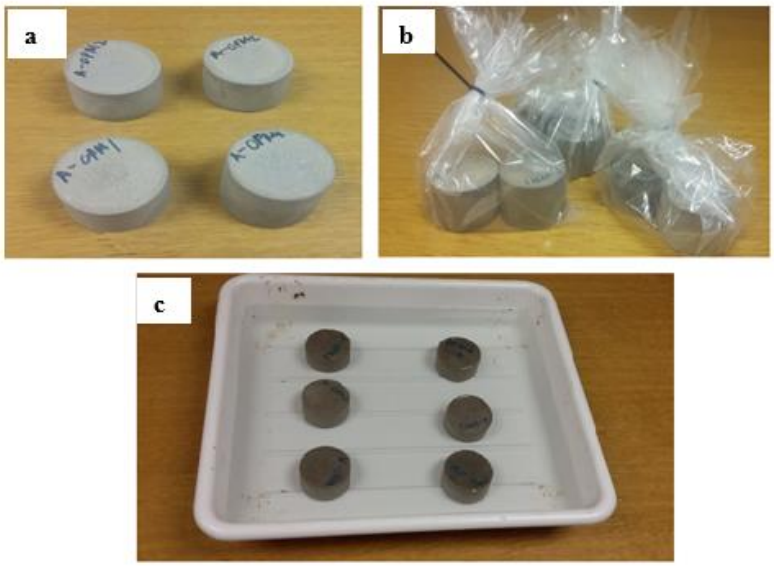

Figure 3.3: OPC samples cured in air (a), plastic (b) and water (c).

3.4.3 Sample conditioning

Sample conditioning as according to ASTM C1585-04 (ASTM, 2004) was incorporated in this study after preliminary studies were conducted on water absorptivity testing and sulphuric acid testing in Section 3.2.1. An environmental chamber for sample conditioning of OPC was created using an oven maintained at 50℃ and a desiccator. The desiccator contained a saturated KBr salt solution for maintaining the relative humidity constant at 80%. A KBr solution was prepared by dissolving 80 g of KBr in 100 ml distilled water. The analyte OPC samples were placed on a plate inside the desiccator, as seen in Figure 3.4a and the same desiccator was placed inside the oven for 3 days, as illustrated in Figure 3.4b. These conditioned OPC samples were removed and placed in plastic containers for 15 days at ambient temperature, illustrated in Figure 3.5. The samples were removed from the plastic containers and were tested for water absorptivity, sulphuric acid resistance and compressive strength.

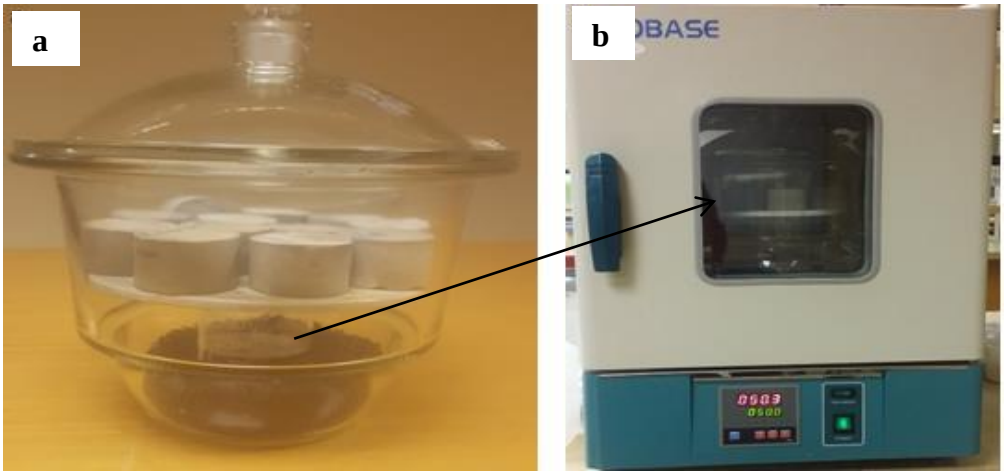

Figure 3.4: Sample conditioning illustration: (a) OPC samples inside desiccator (b) desiccator with samples inside the oven.

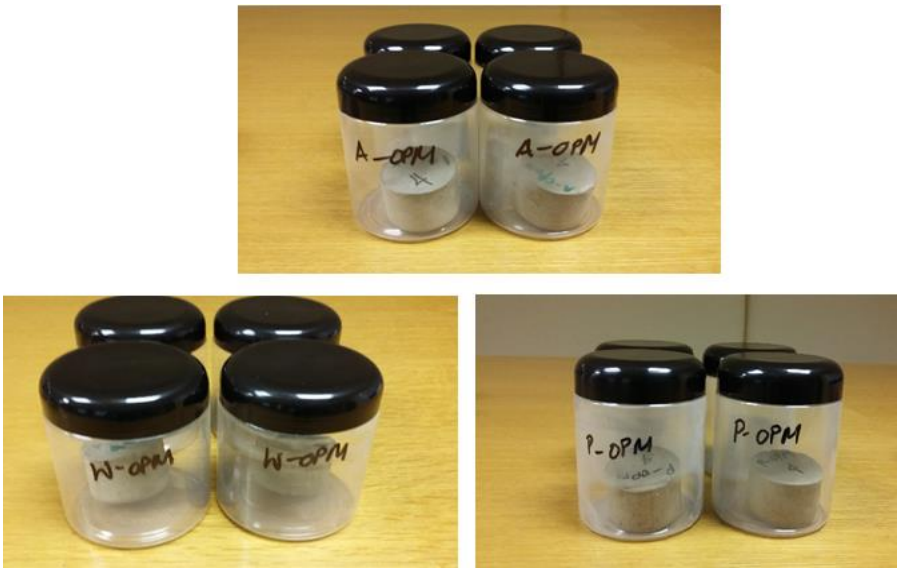

Figure 3.5: Conditioned OPC samples, placed in storage containers.

3.4.4 Sorptivity testing of various OPC samples (ASTM C 1589-04)

The ASTM C 1589 standard method (ASTM, 2001), is an inexpensive laboratory test and was employed in this study to determine the rate of water absorption for OPC samples. The standard method requires a cylindrical mould with a 100 mm diameter and a length of 50 mm. However, for this study, cylindrical moulds with a diameter of 50 mm and a length of 50 mm were used to prepare OPC samples, owing to the lack of availability of the aforementioned ASTM standard moulds.

3.4.4.1Test procedure for water sorptivity of OPC samples

For this investigation, various parameters such as initial mass (g), sample diameter (mm) and sample thickness are required to obtain the essential absorptivity information. Sample diameter (mm) was obtained by taking the average of four separate readings on a specific sample. Sample thickness (mm) was also obtained by taking the average of four readings to the nearest 0.01 mm. Petroleum jelly was used to waterproof the sides of the samples. The mass of the sealed sample was measured and recorded as the initial mass (g) to the nearest 0.001g for the water absorptivity investigation. All relevant diameters, surface areas and masses are recorded in Table 3.4.

Table 3.4: A summary of the average diameters, calculated surface area and initial masses recorded for OPC samples prior to water sorptivity testing.

Sample I.D	**Avg. diameter (mm)**	**Surface area (mm^2)**	**Initial mass (g)**
W-OPM1-1	49.84	1951.73	101.77
W-OPM1-2	48.51	1929.87	136.08
W-OPM1-3	49.96	1960.86	127.98
A-OPM1-1	49.40	1917.43	117.82
A-OPM1-2	49.50	1925.20	114.69
A-OPM1-3	49.26	1906.54	116.50
P-OPM1-1	49.40	1917.43	110.49
P-OPM1-2	49.83	1950.95	122.64
P-OPM1-3	49.52	1926.72	110.56
W-OPM2-1	49.50	1925.20	119.97
W-OPM2-2	49.40	1917.43	121.71
W-OPM2-3	49.50	1925.20	118.98
A-OPM2-1	49.51	1925.97	116.48
A-OPM2-2	49.30	1909.67	114.79
A-OPM2-3	49.63	1935.29	115.76
P-OPM2-1	49.31	1910.45	130.44
P-OPM2-2	49.46	1922.09	120.36
P-OPM2-3	48.96	1883.39	120.49
W-OPM3-1	49.30	1909.67	112.43
W-OPM3-2	49.75	1944.38	116.17
W-OPM3-3	49.50	1925.20	113.14
A-OPM3-1	49.43	1920.53	101.77
A-OPM3-2	49.36	1914.32	102.86
A-OPM3-3	49.52	1926.72	101.75

P-OPM3-1	49.41	1918.20	101.77
P-OPM3-2	49.41	1917.89	115.46
P-OPM3-3	49.00	1886.47	115.62
W-OPM4-1	49.40	1917.43	114.26
W-OPM4-2	49.41	1918.20	113.20
W-OPM4-3	49.50	1925.20	113.62
A-OPM4-1	49.18	1900.39	93.01
A-OPM4-2	49.23	1903.48	95.95
A-OPM4-3	49.44	1920.50	95.24
P-OPM4-1	49.58	1931.42	111.59
P-OPM4-2	49.51	1925.97	114.49
P-OPM4-3	49.50	1925.20	112.34

Figure 3.6 illustrates the water sorptivity test set up where a support device was placed inside a tray, half filled with distilled water. The samples were placed on the support device ensuring that the samples were submerged (3mm) in the water. Once the samples were immersed in water, the stopwatch was started, and the change in mass recorded with time. The change in mass against time, of the OPC sample was recorded at 1 min, 5 min, 10 min, 20 min, 30 min, 60 min, every hour for 6 hours and finally once a day for 8 days.

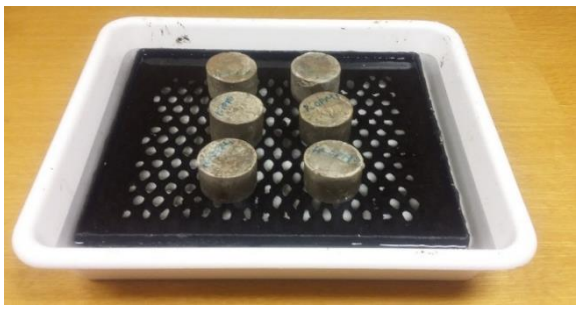

Figure 3.6: An illustration of the water absorptivity test set up for OPC samples.

The absorptivity of the samples was determined using equation (1) in this experiment.

$$I = \frac{\Delta M}{a/d}, \qquad (1)$$

Where, I is absorption (mm), ΔM is change in mass of sample (g), a is exposed area of sample (mm^2) and d is density of water (g/mm^3). Sorptivity is given by the slope of best-fit line of absorption versus square root of time curve.

3.4.5 Sulphuric acid resistance testing of OPC samples

For durability testing, the ASTM C267-01 standard test method (ASTM, 2001) for chemical resistance of mortars and polymer concrete was used as guideline for testing sulphuric acid resistance of OPC samples. In order to test this resistance, the change in mass was recorded for each sample, after immersion in a 10% sulphuric acid (H_2SO_4) solution for 20 days. The 10% H_2SO_4 solution was selected based on a similar investigation conducted by Izzat et al. (2013). In this study it was stated that a higher concentration of acid may more readily afford early effects of acid exposure observations, versus observations noted for lower acid concentrations.

For this investigation, the OPC samples as described in Table 3.3, with the specifications listed in Table 3.2 and conditioned as shown in Figure 3.4 and 3.5 were immersed in plastic containers containing 10% H_2SO_4 solution. After every 2 days of immersion in acid, the samples were removed from the containers, rinsed with distilled water, dried with a paper towel and weighed to record the mass in order to calculate the change in mass. During sample immersion, the H_2SO_4 solution was replaced every 3 days to ensure that the pH of the solution remains constant in accordance to the ASTM C267.

The percentage weight change was calculated using equation (2), according to ASTM C267 (ASTM, 2001);

$$\%\ \text{weight change} = \left[{}^{(w-c)}/_{c}\right] \times 100 \qquad (2)$$

where c is conditioned weight of specimen (g), and

w is weight of specimen after immersion (g).

3.4.6 Compressive strength test of OPC-type compounds

For this test series, standard 50 mm × 50 mm cylindrical OPC samples were made with the same varying w/c ratios illustrated in Table 3.3

After 28 days of curing, the thicknesses and diameters of the OPC samples for each set of mixtures were measured using a Vernier caliper. A 10t bench press with pressure gauge as shown in Figure 3.7 was employed on the hardened cementitious materials until the samples were destroyed.

Figure 3.7: A 10 tonne bench press used to compress OPC samples.

The maximum load (kg) at which the sample was completely destroyed was recorded. Equation (3) was used to calculate the compressive strength (Nadirshah, 1959);

$$\text{Compressive strength} = \frac{\text{force (kg)}}{\text{Area (cm}^2\text{)}} \quad (3)$$

The optimal recorded compressive strength for OPC will be compared to the compressive strengths of fly ash and fly ash/silica fume based geopolymers in Chapter 4.

3.5 Results and discussion

The various physicochemical results from the OPC samples that were prepared earlier in this Chapter will be critically analyzed in the following section. The data collected comprises of four kinds of mixtures of OPC samples, where the w/c ratio of mixture OPM 1, OPM2, OPM3 and OPM4 is 0.31, 0.33, 0.36 and 0.40 respectively as described in Section 3.3. For each set of mixture, three types of curing methods were tested; water, ambient (air) and samples sealed in plastic bags. Triplicates of each of the OPM samples were prepared for the various curing methods to substantiate reproducibility of observations.

3.5.1 General considerations for water sorptivity calculations

Figures 3.8 and 3.9, show typical plots of water absorbed by the samples for 8 days of aqueous immersion. These typical schemes were plotted for each sample and used to analyze their physicochemical behavioral trends by calculating the initial sorptivity (mm/s$^{1/2}$) and secondary sorptivity (mm/s$^{1/2}$). The sorptivity values were then calculated from the slope of absorption versus the square root of time as illustrated in Figures 3.8 and 3.9.

There are generally two noticeable near-linear slopes that can be observed in Figures 3.8 and 3.9. The first part of the curve is presented as the initial absorptivity (1 minute to 6 hours of immersion) of the sample and the second part is denoted as the secondary absorptivity (for days 1-8 of immersion) (ASTM, 2004).

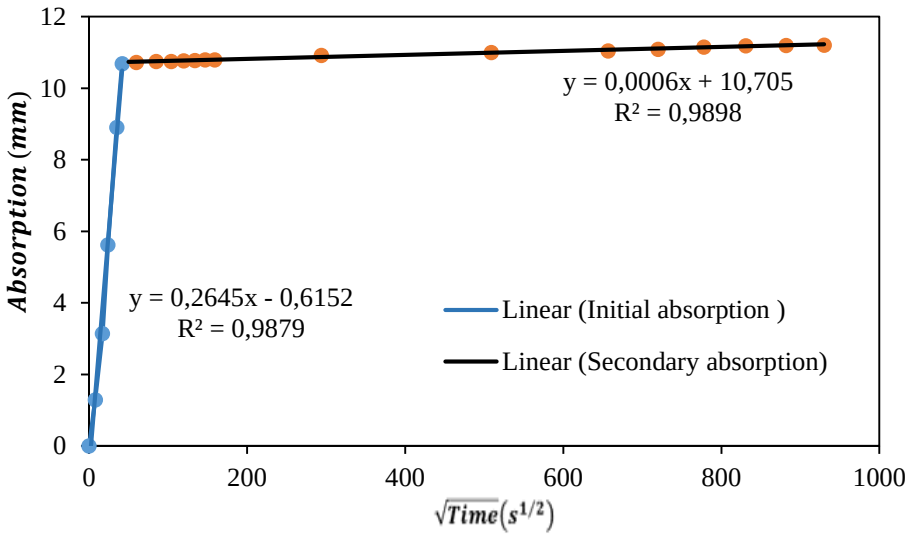

Figure 3.8: An example of the initial and secondary absorptivity definitions for an air cured sample (A-OPM4-1).

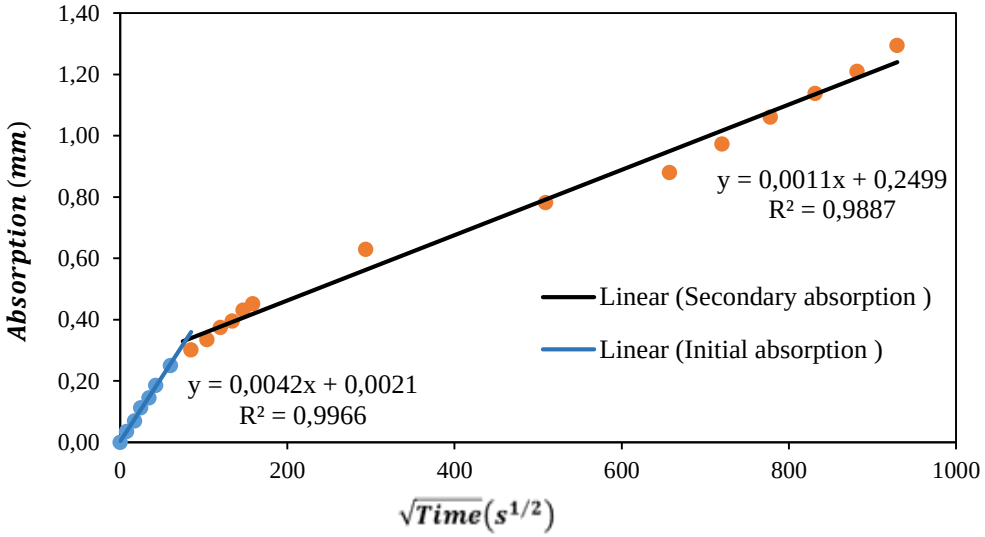

Figure 3.9: An example of the initial and secondary absorptivity definitions for a plastic cured sample (P-OPM3-2).

The calculated slopes of the initial and secondary regressions versus the square root of time (s) are referred to as the initial sorptivity (mm/s$^{1/2}$) and secondary sorptivity (mm/s$^{1/2}$), respectively (ASTM, 2004). From the data reported in Table 3.5 it becomes evident that greater rates of absorption are observed in the initial part of the experiment than noted for the secondary sorptivity. This is because in the secondary part of the experiment, the sample's capillary pores are known to be approaching saturation or are generally fully saturated, therefore not much additional water is thus being taken up by the matrix.

Table 3.5: A summary of the average water sorptivity rates with errors in parenthesis, for the various OPC type samples.

w/c Ratio	**Air cured sorptivity $(mm/\sqrt{s})$**		**Water cured sorptivity $(mm/\sqrt{s})$**		**Plastic sealed cured sorptivity $(mm/\sqrt{s})$**	
	Initial	Secondary	Initial	Secondary	Initial	Secondary
0.31	0.0889 (8)	0.0007 (4)	0.0035 (6)	0.0008 (6)	0.0122 (10)	0.0020 (10)
0.33	0.1174 (9)	0.0006 (4)	0.0035 (6)	0.0090 (6)	0.0049 (8)	0.0016 (9)
0.36	0.1942 (9)	0.0005 (3)	0.0064 (5)	0.0016 (6)	0.0055 (8)	0.0012 (8)
0.40	0.2229 (8)	0.0006 (4)	0.0011 (6)	0.0006 (5)	0.0059 (8)	0.0031 (9)

3.5.1.1 The influence of curing methods on water sorptivity

Figures 3.10 to 3.13 present the water absorption plots for the four OPC mixtures, where each set of mixture shows the effect of curing methods and w/c ratio on the averaged (from triplicate samples) water absorptivity of each mixture. In this section, emphasis will be placed on determining the effect of various curing methods on the water sorptivity rates of the aforementioned samples.

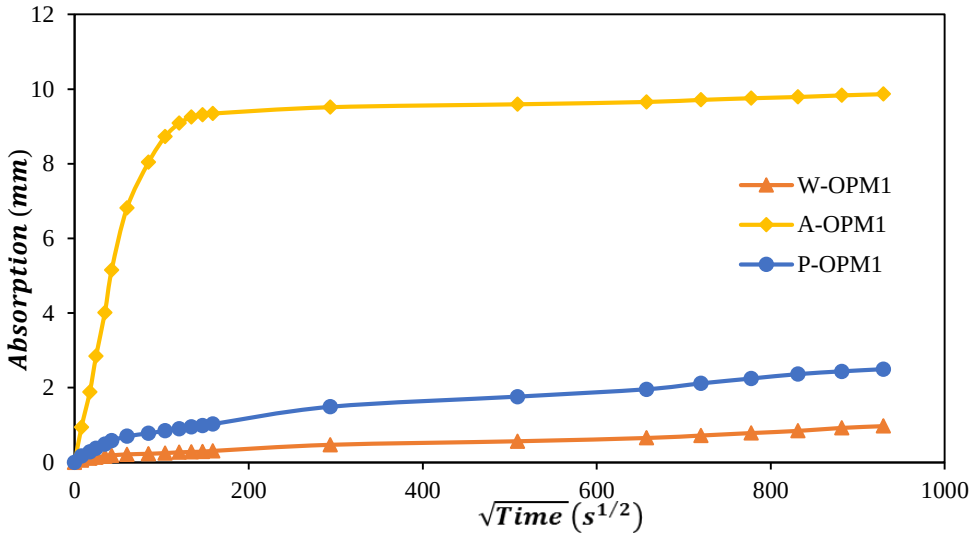

Figure 3.10: Averaged effect of curing methods on water absorption of mixture 1 (w/c = 0.31) samples.

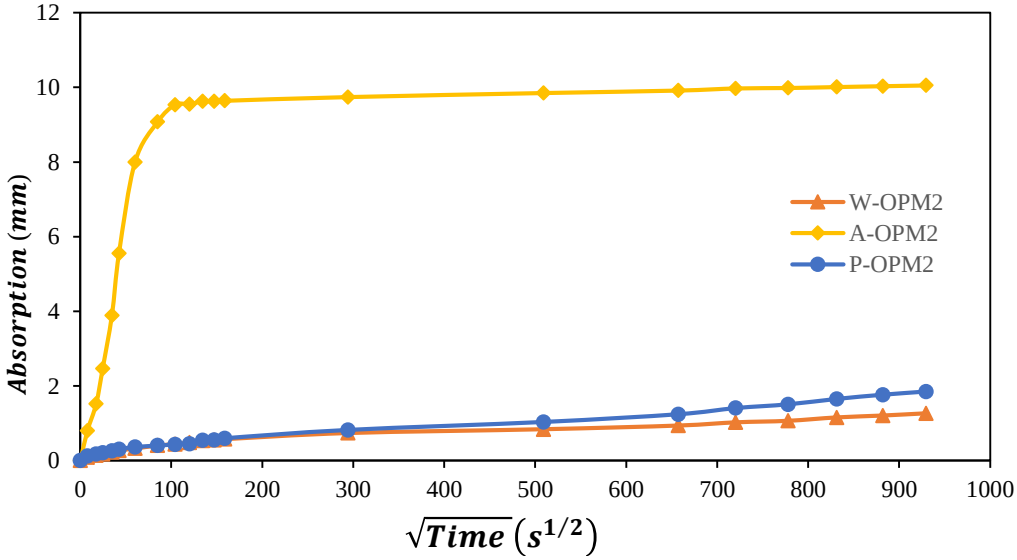

Figure 3.11: Averaged effect of curing methods on water absorption of mixture 2 (w/c = 0.33) samples.

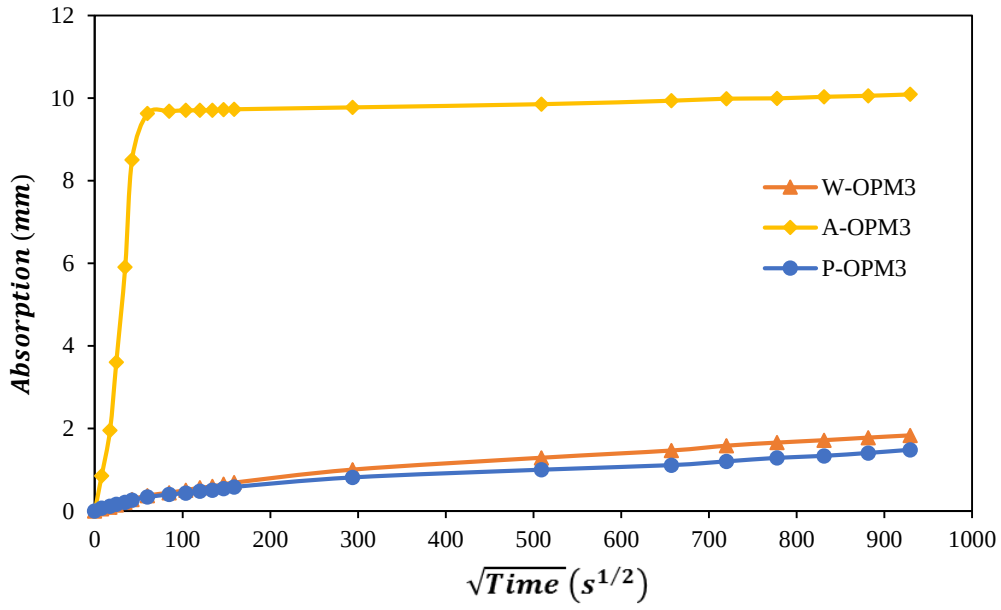

Figure 3.12: Averaged effect of curing methods on water absorption of mixture 3 (w/c = 0.36) samples.

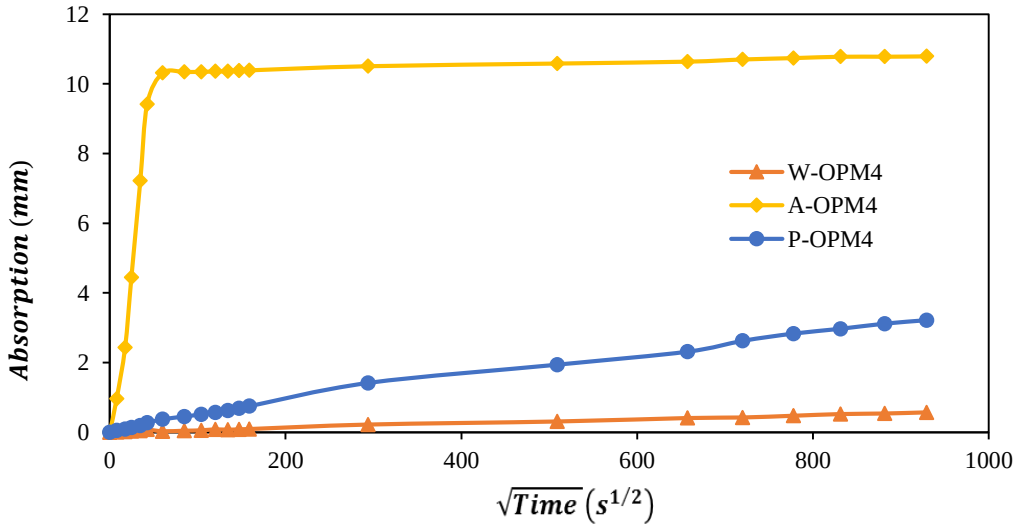

Figure 3.13: Averaged effect of curing methods on water absorption of mixture 4 (w/c = 0.40) samples.

From initial observations it is obvious that all samples cured in air (A-OPM) display a higher rate of initial water absorptivity relative to the samples that were cured in water (W-OPM) and sealed plastic containers (P-OPM) (Figures 3.10 to 3.13). To amplify the regressions observed in Figures 3.10-3.13, the effect of various curing methods on sorptivity was analyzed. This was done by averaging the initial sorptivity, for all four samples that were cured in water with the

w/c to ratio of 0.31, 0.33, 0.36, and 0.40, as well as all samples that cured in air and plastic with the w/c ratio from 0.31 to 0.40, as shown in Figure 3.14.

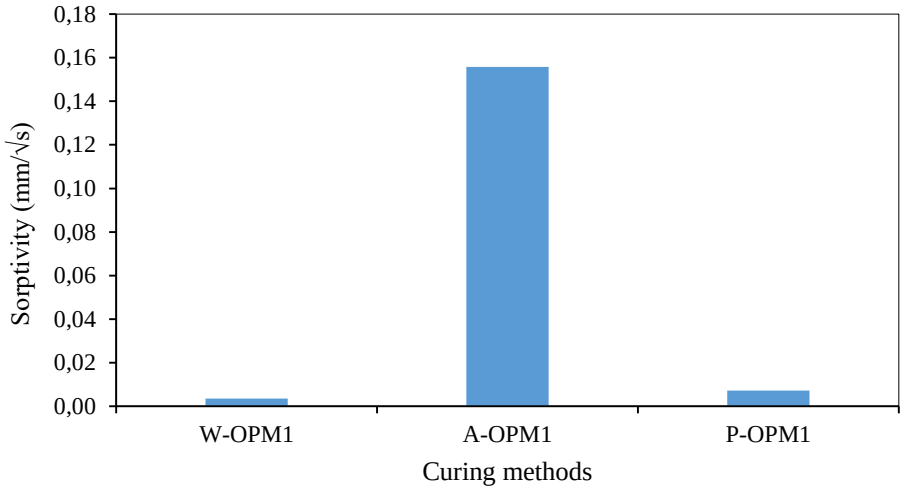

Figure 3.14: An amplification of the effect of curing conditions on water sorptivity.

Figure 3.14 verifies that air cured samples (A-OPM) have an average rate of sorptivity (for the four samples) that is more than 15 times greater than that observed for the water (W-OPM) and plastic (P-OPM) cured samples, with samples cured in water displaying the lowest sorptivity rates. As mentioned in Section 3.2.2, this leads to the suggestion that the A-OPM samples undergo excessive pore water evaporation during the curing process, affording a significant amount of air voids within the cementitious structure making the structure more susceptible to water ingress.

Figure 3.14 also highlights that the W-OPM samples have slightly lower water sorptivity rates, as compared to the P-OPM samples. According to the discussion in the previous section, this observation is to be expected, as in this case, minimal evaporation of water from the cementitious mixture (W-OPM) can occur during curing and remains saturated with moisture affording less “dry” interstitial pores. Therefore, it is evident that tailoring the moisture content by using an idealized curing method is crucial to the processes that allows for the formation of the interlinking bridges that give OPC its solid structural properties (Nahata et al., 2014).

The abovementioned postulation is supported by a literature citation by Tasdemir (2003). In this study, it was implicitly noted that the sorptivity coefficient of OPC samples is sensitive to the curing condition. It also goes further and explains the importance of water retention and sample conditioning in a concrete mixture. Similar to the observations made in this study it was noted that moist concrete or cement paste affords fewer interstitial empty pores confirmed

by structural analysis. Thus, during water absorptivity testing, less water can be taken up by the sample as there will not be enough space to accommodate incoming water uptake. This is ideal as lower sorptivity rates, indicates the resistivity of destructive ions into the sample such as chloride and nitrate or seawater, which tend to disintegrate the microstructure of cementitious material.

Thus far, we have only considered a very broad qualitative analytical overview of these sorptivity rates, however, to substantiate and accurately compare observations; a detailed investigation of the effect of w/c ratio on soprtivity is required.

3.5.1.2 The effect of w/c ratio on water sorptivity

Optimization of water content in the cementitious mixture is imperative to ensure an idealized and durable structure. Excessive water content may lead increased formation of structural pores during curing and sample conditioning, whereas a moisture shortage may lead to an incomplete structural formation and in turn afford a weakened structure. From the average initial sorptivity rates noted in Table 3.5 for all curing methods, Figure 3.15 was obtained, where the effect of w/c ratio on water sorptivity becomes quite apparent. As mentioned previously the w/c ratio was calculated based on the mass of water added divided by the mass of cement used.

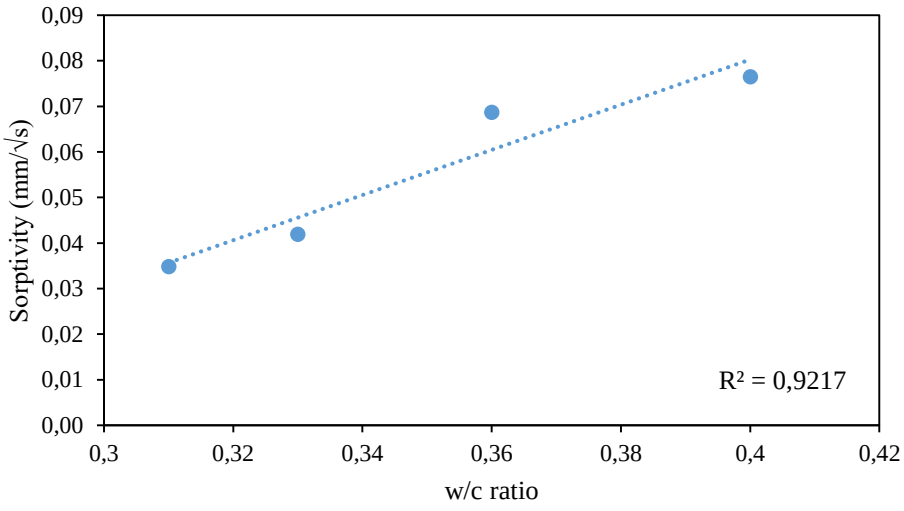

Figure 3.15: The effect w/c ratio of on the average initial sorptivity rates of OPC pastes.

Figure 3.15 shows an increasing linear relationship between the w/c ratio and initial sorptivity of OPC samples, where samples with a 0.31 w/c ratio has the lowest averaged initial sorptivity and samples with a 0.40 w/c ratio affording the highest initial sorptivity. This observation suggests that most samples at the 0.31 - 0.33 w/c ratios afford fewer interstitially connected

pores. The sorptivity begins to increase quite clearly beyond the 0.33 w/c ratio. This increase in sorptivity is not surprising, as increased water content (eg. w/c ratio = 0.40) may afford a proliferation in pore cavities within the cementitious structure during curing and conditioning, owing to increased dilution effects and incomplete cementitious cross-linking reactions. In other words, the higher the water content (w/c ratio = 0.36 and 0.40), the slower the initial structural formation is during curing. Seeing as these samples were cured in a mostly open environment, the water within these pores (which may induce the secondary structural stabilization) readily evaporates leaving an open, easy accessible structure. This makes the structure susceptible to the ingress of water during sorptivity testing, as is observed in this investigation.

However, it is also important to note that the presence of moisture within the cementitious mixture is also the life-blood of the interlinking reactions required for the formation of these structures. So having moisture entrapped within the structure may afford secondary interlinking effects and could still be advantageous with respect to the sample durability and structural integrity under the correct curing conditions. Accordingly, it would not be wise to eliminate the high moisture content samples off hand, and it would be deemed useful to corroborate the obtained sorptivity results with additional testing methods, such as, compressive strength and acid resistance testing to afford a clearer picture of optimized moisture content parameters.

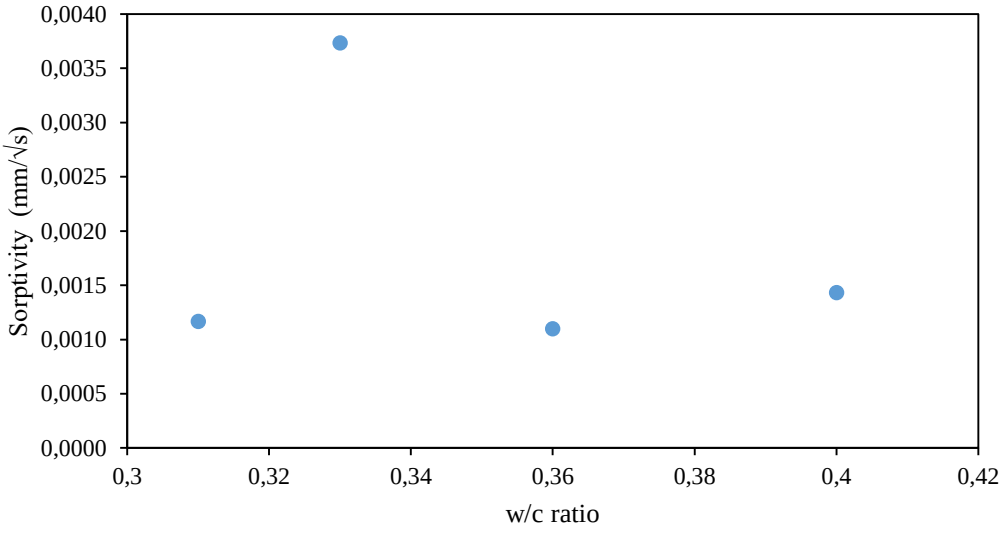

Figure 3.16: The effect of the w/c ratio on average secondary sorptivity rates of OPC pastes.

Similarly, Figure 3.16 was obtained from all the secondary sorptivity rates, noted in Table 3.5 for all curing methods with a 0.31, 0.33, 0.36 and 0.40 w/c ratio. It can be noted that most of

the OPC samples with a w/c ratio of 0.33 takes longer time to fully saturate, as such they continue to take up water, resulting in higher overall secondary values. This could possibly be ascribed to experimental error as the other mixtures displayed similar sorptivity values. It can also be seen that faster saturation is observed for samples with a 0.31, 0.36 and 0.40 w/c ratio, resulting in lower secondary sorptivity values as most of their capillary pores are almost filled up with moisture. From these initial observations, there is no obvious direct relationship between the w/c ratio and secondary sorptivity rates of OPC samples and can thus be safely said that initial sorptivity rates better indicate the effect of w/c ratio on capillary pores more clearly. It is for this reason that the focus of this study will be limited to initial sorptivity observations for comparative purposes.

When considering the curing methods individually the degree of linearity of the initial sorptivity versus w/c ratio is higher with samples that were cured in air, as noted in Table 3.5. For water curing and plastic sealed curing the picture is less clear and conclusive deductions with respect to the effect of moisture content cannot be drawn without additional testing protocols. Here it is important to idealize the balance between water content and the selected curing method. Increased water content does not essentially necessitate a more effective cementitious assembly, as it relates to water sorptivity, as dilution effects may overwhelm the secondary structure formation, leaving the structure hamstrung. However, conversely, some mixture may require longer periods of exposure to high moisture content to allow for the formation of secondary stabilization bridging reactions.

From the results documented, all the water cured and plastic sealed cured samples have similar initial sorptivity rates. Assuming some experimental error observed for the 0.40 w/c ratio particularly in water cured samples, the 0.33 w/c ratio gives the most promising results with regards water sorptivity when considering both curing methods. It is important to note that although curing method and w/c ratio are important parameters to investigate when considering water sorptivity, these results need also be compared with acid resistance and compressive strength testing to identify the optimal mixing conditions.

3.5.2 Sulphuric immersion tests of OPC samples

As mentioned in section 3.3.3 of this chapter, the performances for 4 various w/c ratio mixes of OPC samples, cured in air, water and plastic containers when exposed to 10% sulphuric acid, were evaluated.

3.5.2.1 OPC samples in a 10% sulphuric acid solution for 20 days

The sulphuric acid resistance tests were based on the ASTM C267 method (ASTM, 2001), where the samples were immersed in 10% sulphuric acid for 20 days, post sample conditioning. In this section, the change in appearance of OPC samples will be discussed, as well as how the various mixtures respond to the percentage weight change after being exposed or immersed in sulphuric acid.

(a) Visual observations

As can be seen from Figure 3.16, the various OPC samples undergo semi-rapid degradation after being immersed in acid, even after short periods of time (the figure illustrates a visual representation of this structural degradation after just 2 days sulphuric acid exposure). This observation led to the conclusion that the 10% acid solution is sufficient for to evaluate the semi-rapid digestion of cementitious paste from the hardened sample and is accordingly deemed ideal for this study and corroborates the observations made by Izzat et al. (2013). During the digestion process, cementitious paste from the surface, sides and underneath the samples is systematically eroded due to the acid solution attack.

Figure 3.16: OPC samples immersed in 10% sulphuric acid (a) immediately after acid addition and (b) after 2 days.

The destructive interaction effect between the cementitious sample and sulphuric acid is noticeable by the visible loose cement particles floating around in the sulphuric acid solution. This residue can be attributed to the reaction between the sulphuric acid and the resultant $Ca(OH)_2$ from cement hydration, present in cement. The interaction of the sulphate ions (SO_4^{2-}

) in sulphuric acid and the calcium in cement leads to the formation of gypsum ($CaSO_4.2H_2O$). Subsequently, $CaSO_4.2H_2O$ reacts with available calcium aluminate to form ettringite ($3CaO.Al_2O_3.3CaSO_4.32H_2O$) which is responsible for cement expansion (Barbhuiya & Kumala, 2017). Cement expansion creates pressure and tensile stress within the cement which leads to cracking, whereas the attacked cement losses strength, softens and scales off (Izzat et al., 2013).

After 20 days of immersion in acid, the samples changed from a grey color to a slightly brownish color. Furthermore, it was observed that the samples that were cured in sealed plastic underwent the greatest degree of chemical shrinkage (were the smallest in size) after 20 days of immersion in acid, as compared to water and air cured samples. Although samples cured in air did not lose as much mass during acid testing, it can be observed in Figure 3.17 that these samples indicate more visible signs of rough surface erosion relative to samples cured in water and plastic. After 20 days of immersion in acid, the samples changed from a grey color to a slightly brownish color. Furthermore, it was observed that the samples that were cured in plastic had undergone the greatest degree of erosion (were the smallest in size) after 20 days of immersion in acid, as compared to water and air cured samples. Although samples cured in air did not lose as much mass during acid testing, it can be observed in Figure 3.17 that these samples indicate more visible signs of rough surface erosion relative to samples cured in water and plastic.

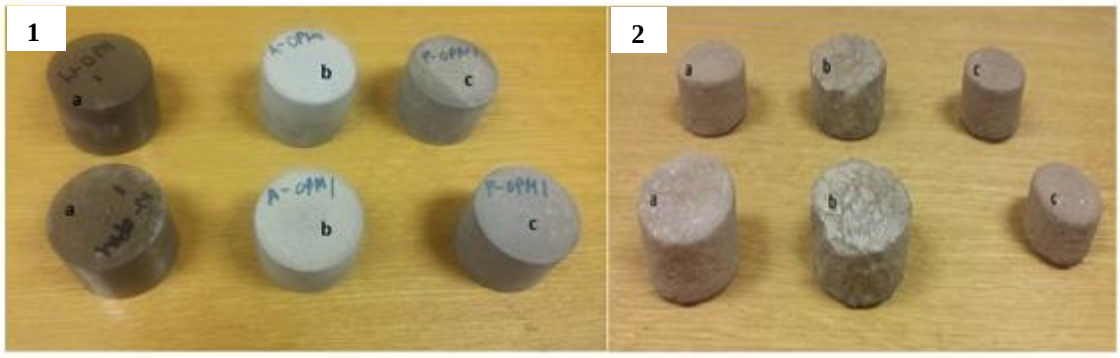

Figure 3.17: OPC samples (1) before and (2) after 20 days of immersion in 10% sulphuric acid, where (a) was water cured, (b) air cured and (c) sealed cured in plastic bags.

(b) Gravimetric observations

The averaged change in mass over time of for each mixture OPC samples with varying w/c ratios and different curing methods, under immersion of 10% sulphuric acid, is presented in Figures 3.18 - 3.21.

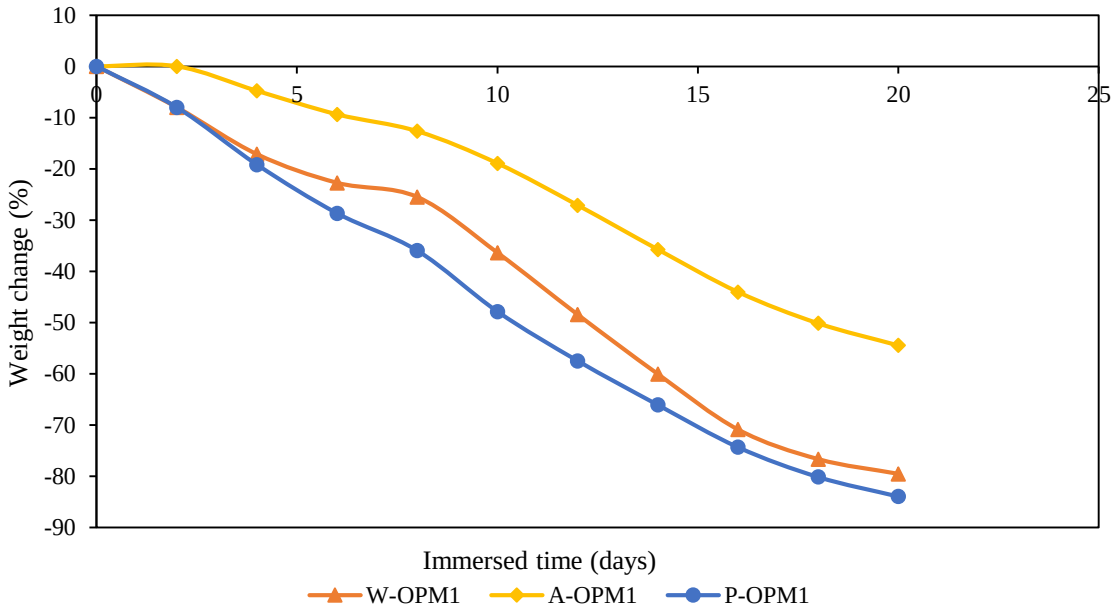

Figure 3.18: Averaged percentage weight change in OPM1 (w/c = 0.31) samples immersed in 10% sulphuric acid.

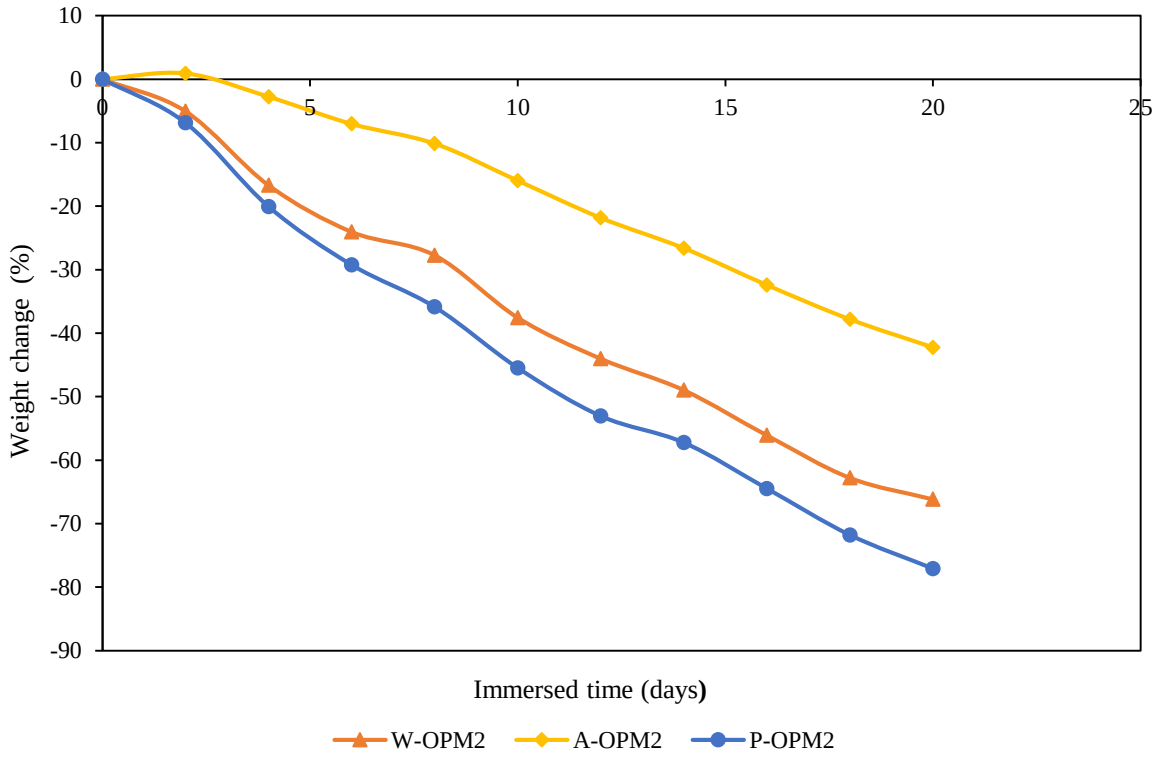

Figure 3.19: Averaged percentage weight change in OPM2 (w/c = 0.33) samples immersed in 10% sulphuric acid.

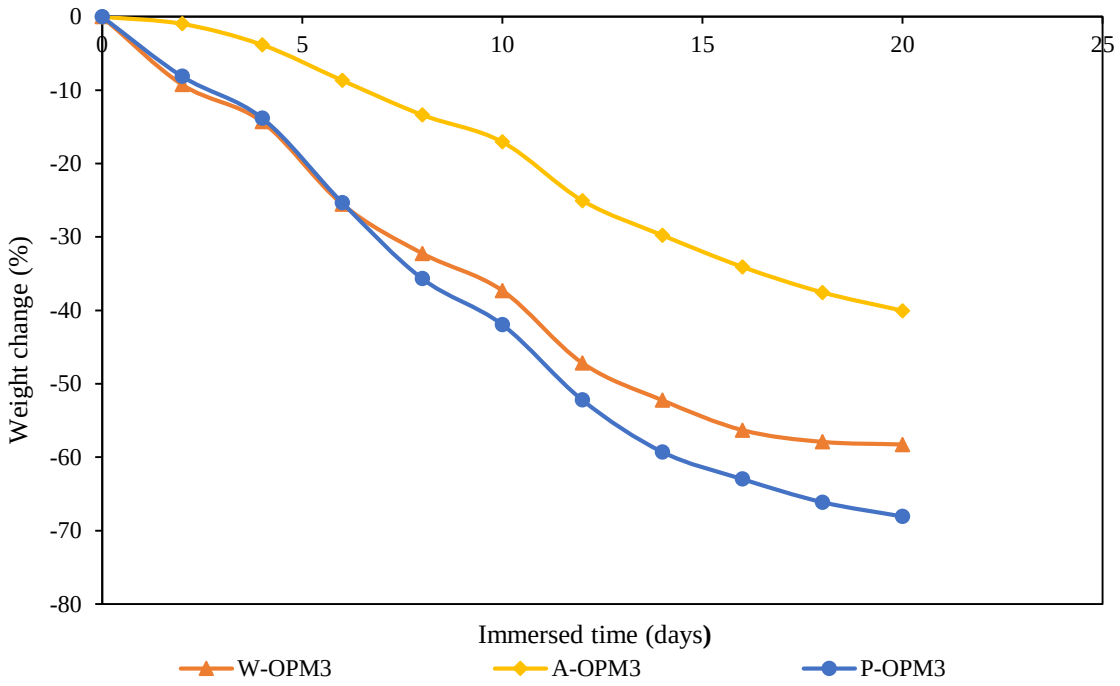

Figure 3.20: Averaged percentage weight change in OPM3 (w/c = 0.36) samples immersed in 10% sulphuric acid.

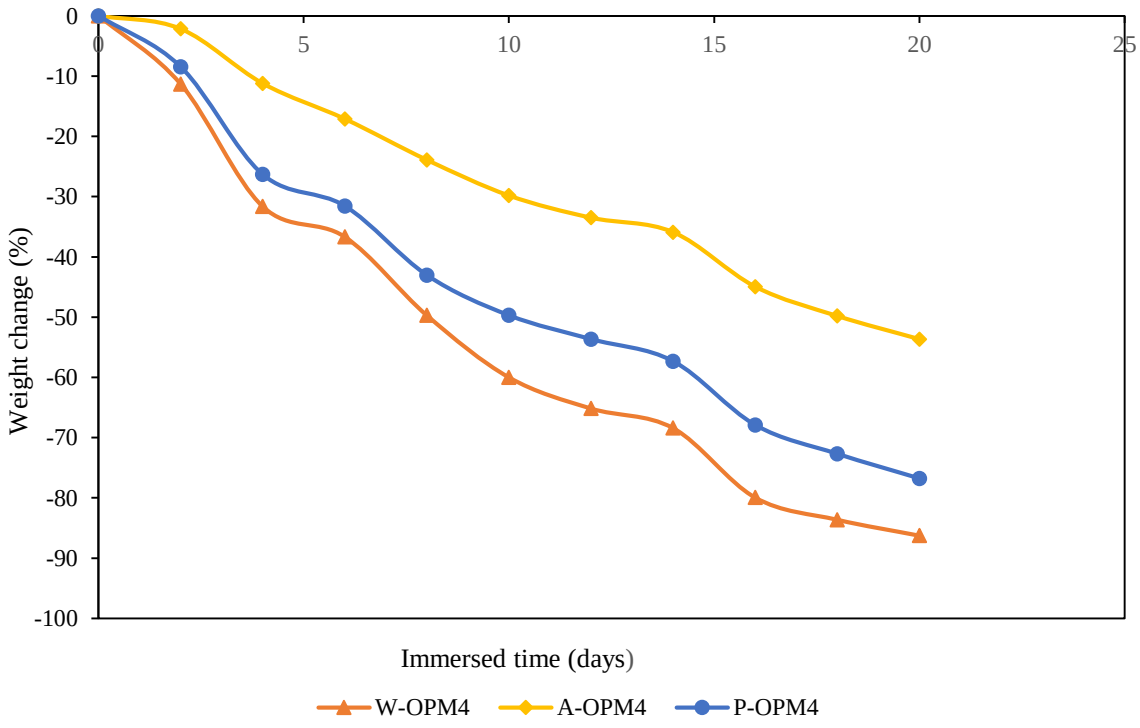

Figure 3.21: Averaged percentage weight change in OPM4 (w/c = 0.40) samples immersed in 10% sulphuric acid.

When comparing Figures 3.18-3.21, in general, the OPM4 samples (with the highest w/c ratio) experienced the most pronounced degree of percentage weight loss value (maximum of 86%) as seen in Figure 3.21 for samples cured in water (W-OPM).

As mentioned in the water absorptivity discussion, samples with a higher w/c ratio tend to have a more porous structure, owing to dilution effects. This porous nature could be an ingression pathway for sulphur ions into the sample. Once these ions are taken up by the cement sample they will react with the structural cementitious products (e.g. $CaOH_2$), breaking the structural stabilization bonds through the formation of ettringite (Izzat et al., 2013).

Figures 3.18 - 3.21 also indicate that out of all three curing methods, the samples cured in air A-OPM mixes resulted in the lowest observed percentage weight loss. These weight loss values range from 40% - 54% weight loss, relative to water and plastic cured samples with percentage weight losses between 58 - 80% and 68 - 86% respectively. Once again, it should be noted that this observation may be very deceptive, as the porous nature of the air cured samples may preferentially favor the initial ingress of the watery acid solution (more mass) over the rate of potential structural damage caused by acid digestion. Conversely, the W-OPM and P-OPM samples showed to have the highest degree of overall mass loss but a lower rate initial ingress of water may contribute to this.

From the aforementioned, it can be seen that the effect of curing does play a pivotal role in sulphuric acid resistance. It has been mentioned in a study by Rostami (2012) that samples that undergo air curing as opposed to moist curing, often have lower $Ca(OH)_2$ content available on the surface. This reduced $Ca(OH)_2$ content is possibly due to carbonation reactions in air cured samples, where CO_2 reacts with $Ca(OH)_2$ and other CSH hydration products forming $CaCO_3$ (Rostami, 2012). Therefore, air cured samples in this study, are less susceptible to sulphuric acid attack. Moreover, lower w/c ratios (0.33 - 0.36) have ideal microstructures for resisting sulphuric acid attack.

From the aforementioned results, it initially becomes difficult to suggest an idealized curing method. For example, the lower degree of percentage weight loss for the ambient cured samples may be very misleading when considering a high initial rate of aqueous acid uptake by the “dry” and porous structure, which is not ideal for envisaged purposes. However, an interesting postulation can be made when considering the acid digestion testing in its entirety.

From the visual observations, illustrated in Figure 3.17, water curing leads to a more robust structure because its surface volume remains larger than for the samples exposed to plastic

sealed curing, however this is very misleading. From the results observed for the percentage weight loss due to acid digestion, water and plastic sealed curing have comparable rates of percentage weight loss, but as mentioned in the previous section, the volume of the water-cured samples was more resistant to the digestion process. This leads to the conclusion that the water cured samples undergo more "internal" structural damage as compared to the "external" and/or superficial decomposition observed for the plastic cured samples. From a structural standpoint, it is obvious that a candidate material needs to be structurally more robust with regard to internal structural integrity as this strength affords the required durability for its envisaged use as core catching cementitious material. Accordingly, and judging from the results at hand, it leads to the conclusion that the dilution effects hampered the formation of the secondary stabilization links within the water-cured lattice and afforded a more susceptible internal cement structure.

However, for this postulation to be confirmed these results need to be corroborated with compressive strength information to emphasize the fact that even though the water cured samples may undergo a similar degree of percentage weight loss as compared to plastic sealed cured samples, the structural degradation effect is substantially more noteworthy in the water cured samples.

3.5.3 Compressive strength results for OPC

The quality of any cementitious material in any structural application is of primary importance. In this study, the compressive strength testing was conducted as a useful indicative property of the cementitious material, especially in resisting external stresses that exist in core catching applications. As mentioned previously, it is crucial that the concrete used in core catcher systems are able to withstand and entrap, not only the melted corium, but also contain as much of the residual heat and radiation flux from the corium material as possible, in case of a nuclear reactor accident.

This testing protocol is deemed the most pivotal test of this study, according to required application, and accordingly it would have been ideal for the strength testing to be conducted prior to sulphuric acid and sorptivity tests. This would have been useful in order to study how the mechanical durability was affected by varying sample mixing (w/c) ratios and testing the acid digestion effects and water sorptivity rates of these optimized candidate (strongest) materials. However, this part of the investigation could only be conducted towards the end of the study and w/c ratios had to be pre-emptively selected according to an extensive literature

comparison. The reason for this back-to-front approach was due to the lack of available equipment at the beginning of the study. The compressive strength results are reported in the following section for samples cured in water, air and in plastic containers, with the various w/c ratios noted in Table 3.6.

Table 3.6: Compressive strength results for OPC samples cured in water, air and sealed in plastic with varying w/c ratios.

	Compressive strength (MPa)		
w/c ratio	**Water**	**Air**	**Plastic**
0.31	19.98 (45)	20.24 (51)	30.94 (33)
0.33	11.95 (48)	8.13 (75)	23.89 (36)
0.36	22.02 (60)	8.09 (75)	9.01 (66)
0.40	11.21 (54)	12.99 (54)	22.44 (30)

Table 3.6 and Figure 3.22 illustrate the average compressive strength for all OPC samples with w/c ratios of 0.31, 0.33, 0.36 and 0.40 that were cured in water, air and plastic. As can be seen from Figure 3.22, the highest compressive strength was noted for the 0.31 w/c ratio for samples cured in a plastic sealed controlled environment. This compressive strength then starts to gradually decline to the 0.36 w/c ratio and increases again (at 0.40). Decrease in the compressive strengths of plastic sealed cured samples between 0.31 - 0.33 w/c ratios may be attributed to dilution effects or excessive water affording increased interstitial pore formation thus resulting in poor structural formation. This observation is in near correlation with the increasing sorptivity rates and increasing percentage losses due to acid attack attained by the plastic cured samples, at the 0.33-0.36 w/c ratios. From this, it can be confirmed that the sample had increased pore formation at these ratios, due to excess water added to cement thus compromising the internal strength of the samples.

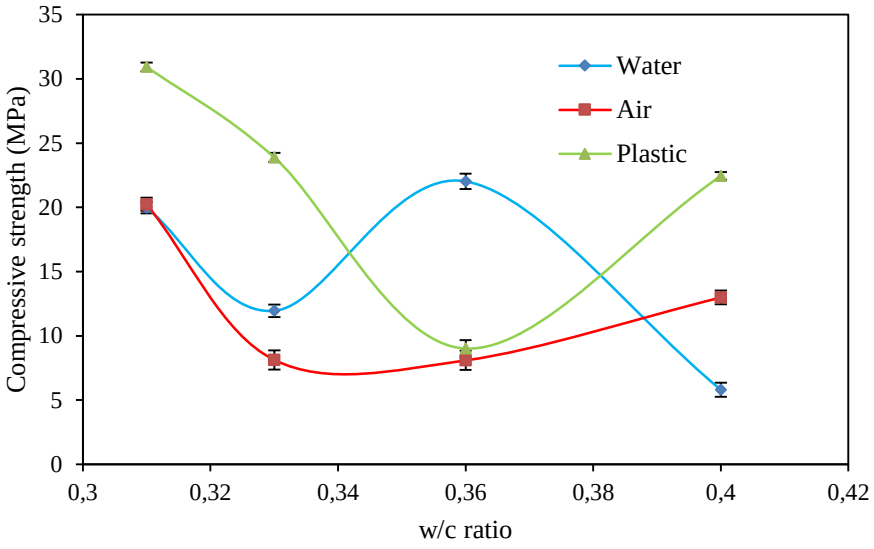

Figure 3.22: The effect of w/c ratio on the compressive strength of OPC samples cured in water, air and sealed in plastic.

It can also be observed that, the highest compressive strength for samples cured in air, was attained at the 0.31 w/c ratio while lowest value was obtained at the 0.33 w/c ratio. The compressive strength then shows a steady increase shortly after the 0.33 w/c ratio. On the other hand, samples cured in water reported the highest compressive strength at the 0.36 .31 (displays a similar value) w/c ratio and the lowest compressive strength at the 0.40 w/c ratio.

These results are in slight contrast with observations made by Shamsai et al. (2012) and Kim et al. (2014). During their studies it was found that, in general, as the w/c ratio is increases, the degree of matrix porosity is also increased, having an adverse effect on sample durability and strength. However, in this case it can be observed that the results obtained for samples cured in air and water are not completely indicative of these postulations with the results or trends found by the aforementioned authors, with an increase in compressive strength noted at a w/c ratio of 0.40. As mentioned, this increase is an unexpected observation and could possibly be attributed to the fact that the increased dilution effects allow more time (slows down the kinetic processes) for the secondary linkage formation to be constructed more coherently, forming a more intrinsic and structured matrix, as compared to the 0.36 samples.

3.5.3.1 Effect of curing methods on the compressive strength

As mentioned previously (Section 3.5.1.1), the curing method plays an important role in the overall compressive strength of cementitious samples. The averaged compressive strength for all OPC samples cured in water with w/c ratios between of 0.31 - 0.40, in air as well in plastic

sealed containers (controlled environments), with of 0.31, 0.33, 0.36 and 0.40 w/c ratios, are presented in Figure 4.23.

Figure 3.23 shows a higher average compressive strength of 21.57 MPa was attained for all samples sealed in plastic containment units (P-OPM). This compressive strength is nearly comparable to the average compressive strength of 16.29 MPa for samples cured in water (W-OPM). It can also be seen that Figure 3.23 displays the lowest average compressive strength of 12.36 MPa belonging to samples cured in air (A-OPM).

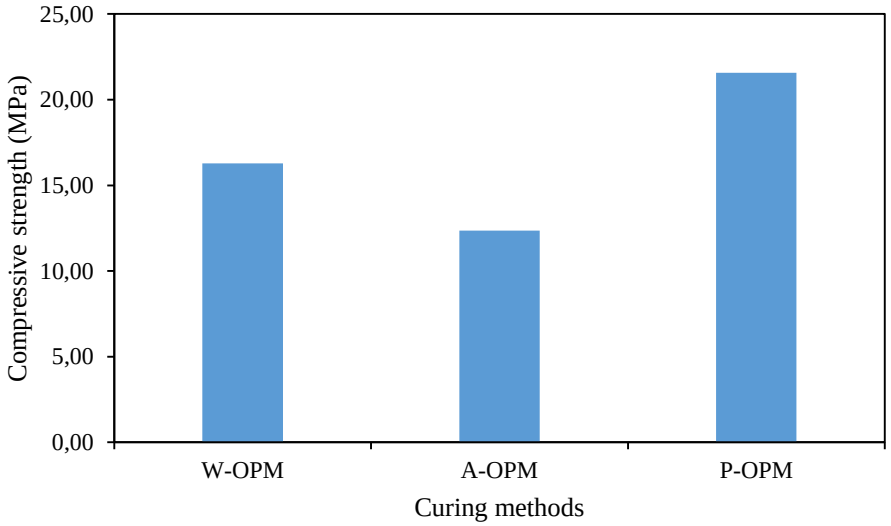

Figure 3.23: An amplified illustration of the effect of water, air and plastic curing of OPC pastes, on the compressive strength.

It is evident from the results, that a balanced moisturous environment is important during curing to facilitate optimized cement hydration products (reducing porosity) for improved mechanical characteristics. This is because moisture curing facilitates structure linkage in cement, in turn affording stronger cementitious product. Conversely, air cured samples experienced increased evaporation leading to incomplete cement matrix formation. As for the investigation at hand and the water sorptivity results discussed earlier in this section, air curing is not ideal for structural optimizations, due to weak mechanical formation from increased porosity and was accordingly be disregarded for the optimization geopolymer testing protocols.

It is evident from Figure 3.22 that the 0.31 w/c ratio of OPC samples usually resulted in the premier compressive strength values for all samples cured in water, plastic and ambient conditions. Thus, it can be preliminarily postulated that this ratio could be deemed the optimal w/c ratio for structural durability optimization of OPC samples in this study. Additionally, it

was noted that water-curing resulted in the lowest sorptivity rates, with acid digestion rates and average compressive strengths comparable to those of samples sealed in plastic sealed containment units and was thus considered the optimal curing method, for OPC samples for this study. It should be noted that results from the compressive strength testing could not completely confirm the postulation that samples that were cured in water more readily affords greater internal structural degradation (during acid digestion) as compared to the plastic sealed cured candidates and may require additional testing approaches to confirm (see Figure 3.17).

Therefore, water curing processes are important in OPC sample preparation, and this is because OPC matrices rely directly on water for the formation of hydration products and ultimately for strength gain. It is difficult to make the same analogy for geopolymer samples as they indirectly depend on water for strength development, due to the loss of water during the geopolymerization process. According to a study by Al-Shathr and Al-Attar (2016), water curing in metakaolin-based geopolymeric investigations, afforded a reduced average compressive strength of 14.87 MPa. This was opposed to non-ambient cured samples, which resulted in an average compressive strength of 29.97 MPa. Accordingly, it seems that although the preliminary testing of OPC is required to obtain the baseline parameters for comparative purposes of this study, it does not necessarily correlate that the ideal OPC synthetic methodologies will afford the optimized geopolymeric products. From this, it can be suggested although water-curing conditions may be idealized for OPC samples; however, different observations may be made for the geopolymeric samples.

Based on the comparable compressive strength and sorptivity results for water and plastic sealed curing, the latter method was chosen as the optimum curing technique for further geopolymer studies in the subsequent chapter. The decision was not made haphazardly, as similar geopolymer investigations required controlled curing environments. Similar studies by Al-Shathr & Al-Attar (2016), Haji-Esmaelii (2012), Thokchom et al. (2009) and Okoye et al. (2016) all substantiate the controlled non-ambient curing methodology.

Chapter 4 Methodology of investigation of geopolymer properties

4.1 Introduction

In the previous Chapter, emphasis was placed on investigating the effects of the mix designs, curing methods, sample conditioning on the various physicochemical properties of OPC type cementitious samples. These properties were subject to evaluation by various material characterisation testing procedures to define an optimal formulation for the required use, as defined in Chapter 1. In this Chapter, a similar systematic approach to the material investigation was undertaken on geopolymer (fly ash) type cementitious compounds. It was also noted in Chapter 3 that the specifications of the optimal formulations would serve as a baseline for comparison with envisaged geopolymer species to attempt to supersede.

4.1.1 Fly ash type geopolymeric compounds

As was noted in Chapter 2, geopolymers are produced from a geopolymerization process whereby solid aluminosilicate compounds and aqueous alkali activators undergo a polycondensation reaction. These alkaline activators generally consist of sodium hydroxide (NaOH) and/or potassium hydroxide (KOH). The resultant structure is a silicon-oxo-aluminate (sialate) analogue that exhibits Si^{3+} and Al^{3+} in a IV-coordination mode, linked alternately by neighbouring oxygen atoms (Davidovits, 1991). Positive ions such as Na^{+} or K^{+} present in alkali solutions compensate for the charge imbalance around the IV-fold coordinated Si and Al-atom (Davidovits, 1991). This intricate structure is responsible for the superior chemical and thermal stability that geopolymer materials boast as opposed to standard OPC based materials (Mane & Jadhav, 2012). Subsequently, it would be deemed advantageous to initially identify idealized geopolymeric type candidate material formulations and subject these compounds to a similar physicochemical testing as was undertaken for OPC samples. This identification and selection process of various candidate source materials, alkali activators and admixtures was discussed in Chapter 2 and their applicability to core-catching usage was tested in this Chapter.

Fly ash is one of the most abundant industrial wastes world-wide. This alumino-silicate source material has been noted to be responsible for inducing increased strength in geopolymeric compounds and its improved mechanical properties under various conditions (Hardjito & Rangan, 2005). Xu & van Deventer (2003) investigated and reported the effect of source materials on geopolymer properties. They found that fly ash generally has a higher Si-ion dissolution rate and a Si/Al content ratio that is desirable for higher compressive strength and

durability in the manufacturing of geopolymers. These noted properties are deemed crucial for application of the cementitious material in core-catching structures and as such it was decided to limit the focus of this investigation around fly ash type and fly ash/silica fume based geopolymeric admixtures, as time constraints would not allow for expanded research. Other identified additive candidates may also include various Si/Al (high content) clay samples which may improve the durability of the structures.

The selected fly ash type material to be used in this study is industrially known as Super-Pozz, which has been noted to be; "a unique, ultra-fine and highly reactive pozzolan, which can supply all round benefits to various cementitious systems." Super-Pozz is an extremely fine, light powder composed primarily of amorphous variants of silicates and aluminates. From its chemical analysis, Super-Pozz will meet the Class F fly ash requirement of BS 3892, but physically the product is unique with regard to its particle size distribution. The D_{99} value is 25 microns, the particle size below which 99% of the particles are to be found. The chemical composition of Super-Pozz is noted in Table 4.1.

Table 4.1: A tabulation of composition of the Super-Pozz type fly ash, which will serve as preliminary source material additive in the synthesized geopolymeric samples.

Chemical Analysis	Mass %
SiO_2	53.5
Al_2O_3	34.3
CaO	4.4
Fe_2O_3	3.6
K_2O	0.8
MgO	1.0
Actual Carbon Content	< 0.3
LOI @ 950 °C	< 1.0

4.2 Preliminary screening of various geopolymeric samples

When considering the project at hand, the investigations of various formulations of compounds with a high Si and Al content are required and as specified, these candidates are to be screened as potential substitutes for OPC for the envisaged core-catching application. It was also deemed a crucial point of focus that Al/Si rich additives as well as differing alkaline solutions needed

to be considered during preparation to obtain an optimal formulation. A brief overview of well-known potential geopolymeric source material candidates and admixtures was given in Chapter 2, noting that these geopolymeric sources afford differing structural outcomes, while also highlighting that these mixtures can be tailored/modified to afford optimized properties.

As has been noted, for geopolymerization to occur, the source material should preferably consist of a Si and Al rich mixture in an amorphous form. Fly ash, ground blast furnace and mineral clays (Metakaolin, Bentonite) are rich in Si and Al, and as such they are the most common source materials used for the production of geopolymers. Source materials are often replaced by small percentages of additives in geopolymers and as well as being used as admixtures in OPC to improve the properties of cementitious materials. These chemical or mineral ingredients play an important role in increasing the compressive strength, attaining preferred plasticity, slowing down or fast tracking the setting time and inducing entrained air voids for better freeze thaw resistance (Haji-Esmaelii, 2012).

From the literature review, numerous potential idealized candidate source materials, additives and alkali-solutions (for alkali activation processes) were identified and subsequently sourced, subject to availability and cost-effectiveness. A summary of the envisaged mixtures is noted in Table 4.2. The composition of the mineral clays and the specifications for the alkaline solution used in this study, was added as Appendix A.

4.2.1 Problem statement

When considering all the listed candidate formulations noted in Table 4.2, it becomes quite apparent that a significant amount of preparatory work is required to mix, optimize and cure each sample (according to prescribed ASTM methods) before being exposed to the various sorptivity, compressive strength and acid resistance testing protocols (ASTM, 2004). Accordingly, a novel pre-screening testing procedure is required to identify the most promising candidate mixtures as promptly as possible and thus limiting the amount of extra lab and equipment hours (running costs) expended on less than ideal candidate mixtures. It should also be noted that this methodology was necessitated due to the lack of the immediate availability of required testing equipment. Importantly, it should be emphasized that this pre-screening need not necessarily be an accredited method but should be envisaged rather a time-saving protocol to ensure a timeous completion of this study.

Table 4.2: A summary of the mixing strategies incorporated for the various fly ash type geopolymer samples.

Mixture no.	Fly ash	Alkaline Activators			Si Additives						Mineral clays				
	Super -Pozz	14 M NaOH	14 M KOH	5 M $Ca(OH)_2$	Na-silicate			Silica fume	Na_2SiO_3	K_2SiO_3	Bentonite				Attapulgite
					1M	2M	4M				Ca	N	MD	MX80	
1	✓	✓	×	×	×	✓	×	×	×	×	×	×	×	×	×
2	✓	×	✓	×	×	✓	×	×	×	×	×	×	×	×	×
3	✓	×	×	×	×	✓	×	×	×	×	×	×	×	×	×
4	✓	×	✓	×	×	✓	×	✓	×	×	×	×	×	×	×
5	✓	✓	×	×	×	✓	×	✓	×	×	×	×	×	×	×
6	✓	×	×	✓	×	×	✓	×	×	×	×	×	×	×	×
7	✓	×	×	✓	×	×	✓	✓	×	×	×	×	×	×	×
8	✓	×	×	✓	×	×	✓	×	×	×	✓	×	×	×	×
9	✓	×	×	✓	×	×	✓	×	×	×	×	✓	×	×	×
10	✓	×	×	✓	×	×	✓	×	×	×	×	×	✓	×	×
11	✓	×	×	✓	×	×	✓	×	×	×	×	×	×	×	✓
12	✓	×	×	✓	×	×	✓	×	×	×	×	×	×	×	×
13	✓	×	×	✓	×	×	✓	×	×	×	×	×	×	✓	×
14	✓	✓	×	×	✓	×	×	×	×	×	×	×	×	×	×
15	✓	×	✓	×	✓	×	×	×	×	×	×	×	×	×	×
16	✓	✓	×	×	✓	×	×	✓	×	×	×	×	×	×	×
17	✓	×	✓	×	✓	×	×	✓	×	×	×	×	×	×	×
18	✓	✓	×	×	✓	×	×	×	×	×	✓	×	×	×	×
19	✓	×	✓	×	✓	×	×	×	×	×	✓	×	×	×	×
20	✓	✓	×	×	✓	×	×	×	×	×	×	✓	×	×	×
21	✓	×	✓	×	✓	×	×	×	×	×	×	✓	×	×	×
22	✓	✓	×	×	✓	×	×	×	×	×	×	×	✓	×	×
23	✓	×	✓	×	✓	×	×	×	×	×	×	×	✓	×	×
24	✓	✓	×	×	✓	×	×	×	×	×	×	×	×	×	✓
25	✓	×	✓	×	✓	×	×	×	×	×	×	×	×	×	✓

26	✓	✓	×	×	✓	×	×	×	×	×	×	×	×	×	×
27	✓	×	✓	×	✓	×	×	×	×	×	×	×	×	×	×
28	✓	✓	×	×	✓	×	×	×	×	×	×	×	×	✓	×
29	✓	×	✓	×	✓	×	×	×	×	×	×	×	×	✓	×
30	✓	✓	×	×	×	×	×	×	✓	×	×	×	×	×	×
31	✓	✓	×	×	×	×	×	✓	✓	×	×	×	×	×	×
32	✓	✓	×	×	×	×	×	×	✓	×	✓	×	×	×	×
33	✓	✓	×	×	×	×	×	×	✓	×	×	✓	×	×	×
34	✓	✓	×	×	×	×	×	×	✓	×	×	×	✓	×	×
35	✓	✓	×	×	×	×	×	×	✓	×	×	×	×	✓	×
36	✓	✓	×	×	×	×	×	×	✓	×	×	×	×	×	✓
37	✓	×	✓	×	×	×	×	×	✓	×	×	×	×	×	×
38	✓	×	✓	×	×	×	×	✓	✓	×	×	×	×	×	×
39	✓	×	✓	×	×	×	×	×	✓	×	✓	×	×	×	×
40	✓	×	✓	×	×	×	×	×	✓	×	×	✓	×	×	×
41	✓	×	✓	×	×	×	×	×	✓	×	×	×	✓	×	×
42	✓	×	✓	×	×	×	×	×	✓	×	×	×	×	✓	×
43	✓	×	✓	×	×	×	×	×	✓	×	×	×	×	×	✓
44	✓	✓	×	×	×	×	×	×	×	✓	×	×	×	×	×
45	✓	✓	×	×	×	×	×	✓	×	✓	×	×	×	×	×
46	✓	✓	×	×	×	×	×	×	×	✓	✓	×	×	×	×
47	✓	✓	×	×	×	×	×	×	×	✓	×	✓	×	×	×
48	✓	✓	×	×	×	×	×	×	×	✓	×	×	✓	×	×
50	✓	✓	×	×	×	×	×	×	×	✓	×	×	×	✓	×
51	✓	✓	×	×	×	×	×	×	×	✓	×	×	×	×	✓
52	✓	×	✓	×	×	×	×	×	×	✓	×	×	×	×	×
53	✓	×	✓	×	×	×	×	✓	×	✓	×	×	×	×	×
54	✓	×	✓	×	×	×	×	×	×	✓	✓	×	×	×	×
55	✓	×	✓	×	×	×	×	×	×	✓	×	✓	×	×	×
56	✓	×	✓	×	×	×	×	×	×	✓	×	×	✓	×	×
57	✓	×	✓	×	×	×	×	×	×	✓	×	×	×	✓	×
58	✓	×	✓	×	×	×	×	×	×	✓	×	×	×	×	✓

4.2.2 Preliminary testing of fly ash type geopolymers

When formulating a methodology for pre-screening of material candidates, certain experimental assumptions were required to simplify the investigation. These assumptions, although not necessarily based on fundamentally peer-reviewed principles, might serve to simplify, as well as afford an ideal point of origin for the development of this process. Accordingly, it seemed relatively safe to make a basic assumption that the novel geopolymer cementitious compounds are expected to display similar advantageous physicochemical properties when exposed to comparable similar mixing designs to those noted for the optimal OPC baseline model. Studies by Olivia et al. (2008), Thokchom et al. (2009) and Okoye et al. (2016) have noted promising results for similar geopolymer mixing designs. It is important to note that the optimized OPC sample curing and conditioning methodologies are excluded in these geopolymer pre-screening assumptions, with the reasoning for this described in the following section. As a result, the following initial framework was proposed and maintained throughout preliminary preparation and testing of various geopolymer samples;

- Manufacturing geopolymer pastes with a constant alkaline solution (AS) to binder (B) ratio (AS/B ratio) of 0.33, a metal silicate/alkali hydroxide solution ratio of 3.0 and the concentrations for alkali solutions were fixed at 14 M. These selected parameters were derived from similar studies conducted by Olivia et al. (2008), Thokchom et al. (2009) and Okoye et al. (2016). It can also be noted that the 0.33 AS/B ratio is similar to the 0.33 w/c ratio that was maintianed initially for OPC studies
- Ambient unsealed curing methods were also maintained for all geopolymer samples during initial screening testing. This seems counter-intuitive, as in Chapter 3 it was highlighted that this curing method is less than ideal for envisaged applications, owing to the formation of a more porous and “weak” cementitious structure formation. However, there is reason to the madness and is substantiated by the investigations of (Nath & Sarker, 2015). In their research, a direct correlation between prompt short-term structural linkage formation and long-term durability of a cementitious compound was postulated. In other words, the faster the structural matrix “settles” to start forming the required secondary stabilization bridging interactions required for compound steadiness, the more durable the final product is expected to be. Now, with water and plastic sealed curing, any improvements in this initial settling period was difficult to observe. This is due to the fact that the structural relaxation is assisted by the presence of moisture

(excessive evaporation rates agitates the structure) within the lattice and any improvement in prompt short-term structural linkage formation will not necessarily be as pronounced as curing conditions are ideal and fast. Accordingly, the reasoning behind ambient curing methodologies lies in the fact any improvement in initial structural "settling" will be much more significantly more evident under "worst case conditions" and should be more pronounced under these types of conditions that afford a much slower "settling time". The other curing methods was considered in the full evaluation of the selected geopolymeric samples.

- Sample conditioning of geopolymer samples was also not implemented (in contrast to the ASTM C 1585 (ASTM, 2004) standard) prior to water sorptivity and 10% sulphuric acid resistance testing, in keeping with the "worst case scenario" notion. As for the water sorptivity test set up, the time intervals for recording the change in mass and the equation used to calculate water absorption was still in accordance with the ASTM C 1585 standard (ASTM, 2004).

4.2.3 Preliminary mixing methods and curing for candidate geopolymers

Various mineral clays; Ca-Bentonite, Bentonite-MD, Bentonite-N, Attapulgite, were first placed in crucibles and preheated in an electric furnace at 700℃ for 3 hours (for activation purposes) (Luukkonen et al., 2018), prior to preliminary mixing as shown in Figure 4.1.

Figure 4.1: Candidate mineral clays placed in a furnace at 700℃ for 3 hours.

The mineral clays were allowed to cool down overnight before being used for the manufacture of fly ash type geopolymer samples. Once cooled, various mixtures were formulated as highlighted in Table 4.2.

For this investigation, binder mixes were manipulated by either employing a fully fly ash containing mixture or by varying sample composition by the addition of either 90% fly ash and

either 10 wt. % of a specific mineral clay or 10 wt.% of silica fume. These binder mixtures were then activated with various alkaline solutions as highlighted in Table 4.2. It was observed that the 0.33 AS/B ratio gave highly workable pastes for most fly ash and fly ash/silica fume based geopolymers. However, the 0.33 AS/B ratio formed excessively stiff pastes for fly ash/mineral clay based geopolymers (possibly due to high surface area of mineral clays (Dinakar, 2011)) as well as for samples that were activated with alkali silicate/$Ca(OH)_2$ combinations. This is already indicative of the fact that more moisture is required for these mineral clay samples to hydrate properly, possibly due to more bonds needing to form (which may be advantageous over longer curing periods). As a result, more alkaline solution was added to the binder material (with a AS/B ratio reaching a maximum of 0.50) in an attempt to obtain a similar workability as observed for the fly ash/silica fume samples. This observation is not necessarily ideal as we are no longer working with the defined model in Section 4.2.2 and we are also not comparing our results with the 0.33 w/c ratio baseline model from Chapter 3, but is required to obtain a workable mixture for continuation of study. However, the obtained sorptivity and acid digestion results could still give an indication of prompt short-term linkage formation. The fresh geopolymer pastes were then molded in 50 mm × 50 mm cylindrical moulds for 24 hours and left to cure in an ambient environment for 20 days, before testing for water sorptivity and sulphuric acid resistance.

4.2.4 Preliminary observations

As was noted in Section 4.2.3, an increased AS/B ratio was required to improve the workability of the fly ash/clay geopolymer mixtures. As expected, it was observed that this modification results in excessively porous samples. Additionally, it was observed that samples activated with K_2SiO_3/KOH and K_2SiO_3/NaOH combinations experienced catastrophic degrees of cracking during the first few days of curing, as shown in Figure 4.2, as compared to the Na_2SiO_3/NaOH and Na_2SiO_3/KOH analogues. Consequently, KOH/K_2SiO_3 activated geopolymers could not be tested for water sorptivity and sulphuric acid resistance and were immediately eliminated from consideration. This lead to the suggestion that these samples were more prone to drying shrinkage, caused by excessive loss of moisture during polymerization owing to the ambient curing method. Chemically, this structural failure maybe be ascribed to the larger K^+ ionic radius (*vs.* Na^+). As has been mentioned, positive ions such as Na^+ or K^+ present in alkali solutions compensate for the charge imbalance around the IV-fold coordinated Si and Al-atom in geopolymeric compounds (Davidovits, 1991). Accordingly, it can be postulated that the K^+ ions occupy too much space within these lattices to allow for the timeous

(before the moisture evaporates from mixture) and robust formation of stabilization linkages and affording a very weak structural lattice.

Figure 4.2: Cracking of KOH activated geopolymers during ambient unsealed curing.

4.2.5 Preliminary water sorptivity results

From the sorptivity results observed for the fly ash based geopolymer samples, a similar trend to the non-sensical observations noted for the OPC analogues cured in an ambient environment can be noted (Section 3.2.2). Once again, and as expected, this can be ascribed to excessive evaporation of water from the sample mixture leaving a "dry" and porous structure. This is highlighted by the fact that for most of the samples the preliminary saturation point (end of initial sorptivity) cannot even be defined as the water uptake rate does not decrease within experimental period. However, a notable exception to this is observed for the unmodified fly ash and fly ash/Na silicate samples. For these samples it can be noted that, even though initial sorptivity ends a significant period after where the ASTM standard defines it to be, a clear inflection point can be noted (ASTM, 2004), implying a preliminary saturation point..` Accordingly, it would seem that these candidate samples potentially display a more pronounced prompt short-term structural linkage formation, with the matrix structure allowing fewer available avenues for water uptake. From these sorptivity observations a decision was made to continue the geopolymer investigation with the fly ash and fly ash/Na silicate mixtures but the results may need to be corroborated with the acid digestion results.

Furthermore, from Table 4.3 it can be seen that $NaOH/Na_2SiO_3$ activated geopolymers afford a lower initial sorptivity relative to the KOH/Na_2SiO_3 activated geopolymers. This can be attributed to increased Na^+ and Si ions present in the $NaOH/Na_2SiO_3$ solution, which play an important role in increasing the formation of amorphous Na-rich aluminosilicate structures in the geopolymers samples. In addition, the K^+ ions present in the KOH/Na_2SiO_3 solution, have relatively larger atomic radii as compared to Na^+ ions, making this alkaline solution chemically

less reactive during the dissolution (of Si and Al from source materials) process thus affording poor geopolymer structures.

Table 4.3: Sorptivity results noted for geopolymers made from unmodified fly ash and fly ash/silica fume activated with a NaOH and Na_2SiO_3 mixture.

Mixture	Initial sorptivity (mm/√s)	Secondary sorptivity (mm/√s)
FA + NaOH/Na_2SiO_3	0.0181	0.0027
FA + NaOH/Na_2SiO_3 + SF	0.0322	0.0019
FA + KOH/Na_2SiO_3	0.0875	0.0015
FA + KOH/Na_2SiO_3 + SF	0.0521	0.0032

4.2.6 Preliminary sulphuric acid resistance results

From the results at hand, it can be noted that geopolymer samples, like OPC samples, (Section 3.2.3), also experience high percentage weight (% wt.) gain after prolonged exposure to 10% sulphuric acid. Once again, this can primarily be ascribed to the uptake of the aqueous acid solution into the "dry" and porous lattice of the cementitious compounds and significantly influence the final digestion results. Additional mass gain for the $Ca(OH)_2$ activated samples can also be attributed to the formation of white scale residue, which was observed on the surface of the geopolymer samples as presented in Figure 4.3.

Song (2007) also studied the behaviour of $Ca(OH)_2$ fly ash based geopolymers when exposed to a 10% sulphuric acid solution and reported the presence of white crystals observed on the fly ash based geopolymers to be due to the formation of gypsum ($CaSO_4.2H_2O$). It can thus be additionally suggested that a portion of the weight gain obtained in this study is due to the formation of this gypsum scale, which also lead to the expansion of geopolymer samples. Interestingly, it was found that the formation of gypsum in the study by Song (2007) was only observed after 112 days of being immersed in a 10% sulphuric acid solution, whilst in this study the white residues were only observed within 20 days of acid exposure. This increased rate of formation could be attributed to two main causes; (1) A deficiency in sample conditioning affording very "dry" (specifically on the surface) cementitious samples allowing for easier adhesion and structural proliferation of the formed gypsum and (2) an excess (unreacted) of residual Ca^{2+} ions in solution. This excess is attributed to the fact that the formation of geopolymer species requires the presence of a mono-valent charge balance stabilizer, whereas the Ca^{2+} is and does not adhere to specifications to form required the

stabilization interactions. This may also explain why the $Ca(OH)_2$ activated geopolymers perform so poorly in the sorptivity testing protocols.

Figure 4.3: The formation of white crystals on unconditioned $Ca(OH)_2$ activated fly ash type geopolymers.

4.2.7. Final deductions and critical evaluation of pre-screening method

Owing to the fact that a substantial number of geopolymeric candidate materials, admixtures and alkali-activators needed to be screened in this investigation, a preliminary pre-screening process was required as a time-saving and labour reducing protocol, to eliminate obvious non-ideal constituent formulations. In this methodology, a "worst case scenario" approach (as described above) was undertaken in an attempt to accentuate any significant constituent influences on sample structure. It should however be re-emphasized that this pre-screening method is not a peer-reviewed procedure and the effectivity of its application for this study will be evaluated later in this Section.

Firstly, it should be noted that under ideal circumstances it would be deemed advantageous to evaluate the sorptivity, acid resistance as well as compressive strength of each candidate sample to ensure a more well-rounded preliminary investigation. However, owing to the initial unavailability of a hydraulic press with a press gauge, it was deemed sufficient to only focus on the sorptivity and acid resistance results as time constraints did not allow for any additional delays.

To start, it is imperative that the obvious inadequacy with relation to acid digestion testing of the method be discussed. As can be derived from the above discussions, no significant structural information other than excessive % wt. gain (due to excessive uptake of aqueous acidic solution) and scale formation due to sub-optimal sample conditioning could be observed. A "worst case scenario" approach may sometimes be helpful to reveal substantial

physicochemical effects caused by the variance of constituent materials (to be discussed in the following section) in some studies. However, in this case, the inadequate conditioning of the sample led to a matrix that is so dry, that the rate of moisture (acidic solution) uptake far surpasses the rate of degeneration caused by the acid itself and accordingly "hides" any structural influence effects. Accordingly, it is important to either ensure that samples be properly conditioned prior to testing (more labour intensive) or shift the investigation methodology focus to a different analytical technique for the unconditioned samples.

As it pertains to the investigation of sample water sorptivity, a more advantageous picture can be formulated, with regard to this study. As was noted in the introductory section of the water sorptivity discussion, it was envisaged that this testing methodology would help emphasize prompt short-term structural linkage formation, which in turn should affect the long-term durability of a cementitious compound. In the case of the FA/NaOH/$Na_2Si_2O_3$ and FA/SF/NaOH/$Na_2Si_2O_3$ samples, a clear inflection point can be noted on the sorptivity rate graph. This observation emphasizes a significant reduction in the rate of water uptake, as compared to the other clay, $Ca(OH)_2$ activated, etc. samples. Accordingly, this testing methodology was successful in identifying candidate sample mixtures that potentially display a more pronounced prompt short-term structural linkage formation, with the matrix structure allowing fewer available avenues for water uptake. It is envisaged that the accuracy of this postulation will further be substantiated by density and mercury intrusion porosimetry measurements to be evaluated later in this Chapter. However, from these preliminary sorptivity observations, it would seem wise to continue this geopolymeric investigation with the fly ash (with silica fume) and unmodified fly ash/Na silicate mixtures.

So preliminarily, this pre-screening method was successful in achieving one of its initial aims of eliminating non-ideal candidate mixtures from consideration, while also identifying idealized candidates. It's important to note that these selections could have been further substantiated if the sorptivity results could have been corroborated with compressive strength information. It is envisaged that, in theory and according to literature, these mixtures should also display a high compressive strength but unfortunately, this could not be corroborated in this initial part of study. Accordingly, for the continuation of this study the assumption that reduced porosity implies increased compressive strength has to be accepted.

A second objective was also achieved by the fact that the time and labour required to identify these candidate materials was also significantly reduced. If all the samples noted in Table 4.2

were prepared to required ASTM specifications and considering the fact that only one drying oven was available in the lab facilities, it would have taken an average of 35+ days to prepare and test each sample. This is a conservative estimation as only two sample set mixtures can be dried and cured at the same time (and subsequently tested). Not to mention the increased amount of labour required for sample conditioning. In this case, all 58 samples were screened within a single ±115-day period, some initial hands-on experience with the materials was obtained and two main candidate mixtures were successfully identified. Accordingly, this method was hugely successful as a time-saving protocol.

Unfortunately, this approach only limits the study to one AS/B ratio and a specified wt.% admixture at a time. It has to be documented that varying AS/B ratio will obviously have different effects on the various sample types and optimizing the parameters for each sample individually but would be deemed an exhaustive and inefficient approach. This is especially evident when considering the initial observations for the clay mixtures (Section 4.2.4). It was highlighted that these samples required a higher AS/B ratio to obtain a workable mixture consistency. As noted in Chapter 2, moisture is the driving force behind the secondary stabilization reactions that afford geopolymers their well-publicized durability. So, even though more acidic solution initially over diluted the mixture to afford negative results for the sorptivity testing, the possibility remains that these mixtures could be more durable after prolonged periods of curing. This argument also holds true if the wt.% admixture is also manipulated but once again, all possible combinations cannot realistically be optimized and tested in the specific time-frame.

The actual success of this screening methodology may finally be highlighted when the final candidate mixtures are fully compared to the OPC baseline model and improved durability is noted for the fly ash and fly ash/silica fume based geopolymeric samples. This comparison will be undertaken in the following sections with the various consideration noted in Section 4.4 incorporated into the research methodology.

4.2.8 Post-screening considerations

This preliminary screening work was important in identifying parameters that can be improved in order to achieve high durability geopolymers. In this section, the following considerations were put in place to modify further improve the geopolymer studies;

- Due to cracking of KOH/K_2SiO_3 and K_2SiO_3/NaOH based geopolymers and the less workable paste from $Ca(OH)_2$ activated geopolymers, the use of K_2SiO_3 and $Ca(OH)_2$ as activating liquids were not employed in further geopolymer studies.

- Fly ash/ mineral clay based geopolymers and KOH/Na_2SiO_3 activated geopolymers were not used in further geopolymer studies due to the high initial sorptivity values high porosity obtained by these geopolymers. As a result, fly ash and fly ash/silica fume based geopolymers, activated with Na_2SiO_3/NaOH are deemed to be better suited for obtaining durable geopolymers. This also allows for timeous completion of this study as mentioned previously.

- The metal silicate/alkali hydroxide solutions need to be prepared a day prior to fly ash or fly ash/silica fume activation to allow the solution to cool down. The ratio of silicate/alkali hydroxide were also modified to 2.5 instead of 3.0 for this section of investigation. This was based on newly sourced literature obtained from studies by Hardjito & Rangan (2005) and Yahya et al. (2015) who concluded that the 2.5 ratio resulted in higher compressive strength as opposed to 0.5, 1.0, 1.5, 2.0 and 3.0.

- The AS/B ratio were also varied (0.31, 0.33, 0.36 and 0.40) to optimize the manufacture of geopolymers (Hardjito & Rangan, 2005). Sample conditioning as according to the ASTM C 1585 mentioned in Chapter 3 was implemented in geopolymer studies prior to water absorptivity, compressive strength and sulphuric acid resistance tests.

4.3 Methodology of fly ash and fly ash/ silica fume based geopoplymers synthesis

4.3.1 Alkaline solution preparation

For this investigation the alkaline solution was defined as the combination of NaOH and Na_2SiO_3. Accordingly, NaOH pellets were dissolved in distilled water to obtain a 14 M solution and then left to cool down for 5-6 hrs. The Na_2SiO_3 solution was then added to the NaOH solution, maintaining a Na_2SiO_3/NaOH ratio of 2.5 (m/m) and was allowed to cool down overnight before being used to manufacture fly ash and fly ash/silica fume based geopolymers.

4.3.2 Preparation of fly ash based and fly ash/silica fume based geopolymers.

Fly ash based geopolymers were made by mixing fly ash source material with the Na_2SiO_3/ and NaOH alkaline solutions. Similarly, the fly ash/silica fume based geopolymers were prepared by replacing various fly ash quantities with 10% (m/m) silica fume as according to four mixes shown in Table 4.4. The alkaline solution-to-binder ratios (AS/B ratios) for both fly

ash and fly ash/silica fume based geopolymers varied from 0.31. 0.33, 0.36 to 0.40 similar to the w/c ratios of OPC samples prepared in Chapter 3. The dry materials (fly ash, fly ash/silica fume) were thoroughly mixed with the alkaline solution to obtain a glossy homogenous mixture and were cast in 50 mm × 50 mm cylindrical plastic moulds. 36 samples were cast for each fly ash and fly ash/silica fume based geopolymers. From the 36, 12 samples were tested for water absorptivity, 12 for sulphuric acid resistance and 12 for compressive strength. Of the 12 triplicates of 4 had AS/B ratios of 0.31, 0.33, 0.36 and 0.40 respectively. All fly ash based geopolymers are referred to as F-GlP and all the fly ash/silica fume based geopolymers are referred to as FS-GlP. In order to differentiate between the 4 AS/B ratios, the letters A, B, C and D are attached to the type of geopolymers made, were mix A, B, C and D corresponds to the mix with the AS/B ratios of 0.31, 0.33, 0.36 and 0.40 respectively as shown in Table 4.4.

Table 4.4: Different fly ash and fly ash/silica fume based geopolymer mixes, with various AS/B ratios.

	Fly ash based geopolymers (F-GlP)				**Fly ash/silica fume based geopolymers (FS-GlP)**			
Mix sample name	F-GlP A	F-GlP B	F-GlP C	F-GlP D	FS-GlP A	FS-GlP B	FS-GlP C	FS-GlP D
Fly ash (g)	325	300	275	250	292.5	270	247.5	225
Silica fume (g)	-	-	-	-	32.5	30	27.5	25
AS/B ratios	0.31	0.33	0.36	0.40	0.31	0.33	0.36	0.40

4.3.3 Curing of fly ash and fly ash/silica fume geopolymers

As stated previously, sealed curing was chosen as the optimum curing method for geopolymers studies (as seen in Figure 4.4), based on the suggestions from OPC compressive strength testing results and discussions, and obtained in Chapter 3 of this study. Therefore, for sample curing of both fly ash and fly ash/silica fume based geopolymers, the cementitious compounds were subjected to sealed curing in plastic for 28 days to prevent excessive water evaporation, before sample conditioning and to also adhere to ASTM standards.

Figure 4.4: Geopolymer candidate samples cured in sealed plastic bags.

4.3.4 Conditioning of fly ash and fly ash/silica fume geopolymers

Sample conditioning of geopolymers was also carried out in accordance with the ASTM C1585-04 (ASTM, 2004). After 28 days of sealed curing, both fly ash and fly ash/silica fume based geopolymers were placed in an environmental chamber created from a desiccator containing a KBr solution (identical to the one described in chapter 3). The desiccator containing the samples was placed in the oven at 50℃ for 3 days, to maintain a constant relative humidity (85%). After 3 days of conditioning, the samples were removed from the oven and placed in plastic containers for 15 days prior to water absorptivity, compressive strength and acid resistance testing.

4.3.5 Water absorptivity for geopolymers

Post sample conditioning, the average diameters (mm) and average thicknesses (mm) were measured using a Vernier caliper and were recorded prior to water absorptivity testing. Both fly ash and fly ash/silica fume based geopolymers were also coated with petroleum jelly on the sides of the cylindrical samples to ensure a unidirectional flow of water and was loosely covered with plastic on the surface that was not exposed to water. After coating the geopolymers with petroleum jelly, their masses were measured and recorded as the initial mass (g) of the samples, before testing. It should be noted that the same water absorptivity setup used for OPC samples in Chapter 3 was also used for geopolymers studies. Once the geopolymer samples were immersed in distilled water, the changes in their masses due to water uptake were recorded at the time intervals similar to that which was specified in Chapter 3 for OPC studies.

The average diameters, calculated surface areas and initial masses for fly ash and fly ash/silica fume based geopolymers prior to water absorptivity tests are given in Table 4.5.

Table 4.5: A summary of the average diameters, calculated surface area and initial masses recorded for geopolymer samples prior to water sorptivity testing.

Sample I.D	**Average diameter (mm)**	**Surface area (mm^2)**	**Initial mass (g)**
F-GlPA-1	49.50	1925.20	139.12
F-GlPA-2	49.03	1888.81	142.87
F-GlPA-3	49.05	1890.31	141.23
FS-GlPA-1	48.93	1881.11	135.71
FS-GlPA-2	51.00	2067.76	151.22
FS-GlPA-3	49.45	1921.27	137.56
F-GlPB-1	49.37	1915.10	138.18
F-GlPB-2	49.33	1912.00	139.84
F-GlPB-3	49.50	1925.20	141.56
FS-GlPB-1	49.34	1912.77	119.58
FS-GlPB-2	50.83	2030.04	124.47
FS-GlPB-3	48.88	1877.24	121.26
F-GlPC-1	49.44	1920.53	114.85
F-GlPC-2	49.03	1888.97	115.06
F-GlPC-3	49.46	1922.05	114.95
FS-GlPC-1	49.21	1902.40	120.26
FS-GlPC-2	48.76	1868.07	121.81
FS-GlPC-3	50.01	1965.04	122.04
F-GlPD-1	49.07	1891.12	103.79
F-GlPD-2	49.01	1886.96	112.03
F-GlPD-3	49.25	1905.76	111.61
FS-GlPD-1	48.78	1869.60	110.04
FS-GlPD-2	49.63	1935.56	117.15
FS-GlPD-3	49.27	1907.31	124.98

The absorptivity of the fly ash and fly ash/silica fume geopolymer samples was also determined using equation (1) in this experiment.

$$I = \frac{\triangle M}{a/d}, \quad \textbf{(1)}$$

4.3.6 Sulphuric acid resistance test

For testing the resistance of geopolymeric samples to acid attack, the conditioned geopolymer samples were placed in plastic containers containing 10% sulphuric acid for 20 days. After every 2 days of sample immersion, the samples were taken out of the H_2SO_4 solution, rinsed with distilled water and their change in masses (g) were measured. Equation (2) as according to the ASTM C267 (ASTM, 2001) was used to calculate the % weight change.

$$\%\ \text{weight change} = \left[{}^{(w-c)}/_{c}\right] \times 100 \quad (2)$$

where, c is conditioned weight of specimen (g), and

w is weight of specimen after immersion (g).

The H_2SO_4 solution was replaced every 3 days of immersion, to maintain the concentration/pH of the solution.

4.3.7 Compressive strength testing

The 50 mm × 50 mm cylindrical geopolymer samples with 4 mixes of varying AS/B ratios were tested for compressive strength after 28 days of sealed curing and 15 days of sample conditioning. Prior to testing for compression, the diameters (mm) and thicknesses (mm) of the geopolymer samples were measured using a Vernier caliper. Both fly ash and fly ash/silica fume based geopolymer samples were tested on 10t bench press bench press with a pressure gauge, where the maximum load applied to each sample was recorded when the samples were completely destroyed.

4.4 Results and discussion for geopolymers durability evaluations

This section of the study attempts to report and evaluate the obtained results pertaining to the durability of fly ash (F-GlP) and fly ash silica fume based (FS-GlP) geopolymers. Water absorptivity, sulphuric acid resistance and compressive strength results will be analysed and compared to the sealed cured baseline OPC samples (from Chapter 3), throughout this discussion. Comparison of geopolymer results were made specifically in comparison to results obtained from the sealed cured OPC samples and not to OPC samples that were cured in air and water. This is because sealed curing was chosen as the optimum curing condition for geopolymer samples according to the conclusions noted in Chapter 3. Additionally, the

conclusions from the baseline OPC investigation also led to the focus of results being based on the effect of the various AS/B ratios on; water absorptivity, sulphuric acid resistance and compressive strength of the geopolymer samples.

4.4.1 Initial observations

In the early stages of the sealed curing preparation methodology, minor cracking was observed on the fly ash based geopolymer (F-GlP) materials with a AS/B ratio of 0.31 and 0.33 (mix A and B), prior to testing. As suggested previously, the fly ash based geopolymers may have either experienced drying shrinkage during curing (Kuenzel, et al., 2012) or the shortage of moisture in the lattice may lead to an insignificant degree of surface cracking. Shrinkage in these specimens could also have occurred due to the loss of water (contained in the alkaline solutions) during the polycondensation reaction of geopolymerization or through evaporation of water during curing (Kuenzel, et al., 2012). However, this cracking may only be superficial with minimal effect noted on the inherent structural stability.

4.4.2 Water sorptivity testing for fly ash and fly ash/silica fume based geopolymers

Figure 4.5 illustrates a typical water absorptivity (mm) versus the square root of time ($s^{1/2}$) plot for geopolymer samples. This Figure was plotted for each geopolymer sample, in order to define the initial and secondary slopes of the absorption curve, which is noted as the initial and secondary sorptivity of each sample. In this illustration, the blue line represents initial sorptivity and the red line is indicative of the secondary sorptivity (ASTM, 2004).

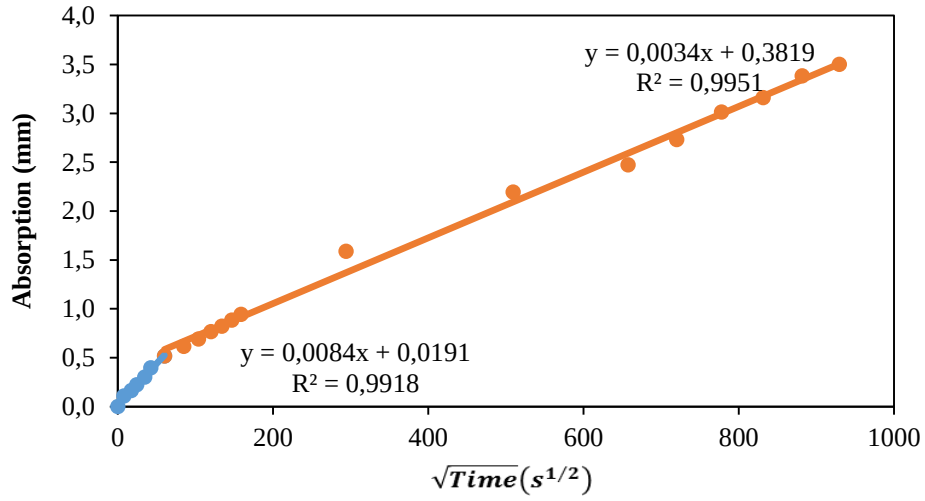

Figure 4.5: An illustrative example of the initial and secondary sorptivity for an F-GlPB-2 sample with an AS/B ratio = 0.33.

The data for the triplicate specimens (of the same mixture) were averaged and presented as absorption vs. $s^{1/2}$ traces, as shown in Figures 4.6 - 4.7. Figures 4.6 and 4.7 present the water absorptivity for fly ash based geopolymers (F-GlP) and fly ash silica fume based geopolymers (FS-GlP) respectively, with varying AS/B ratios (0.31-0.40).

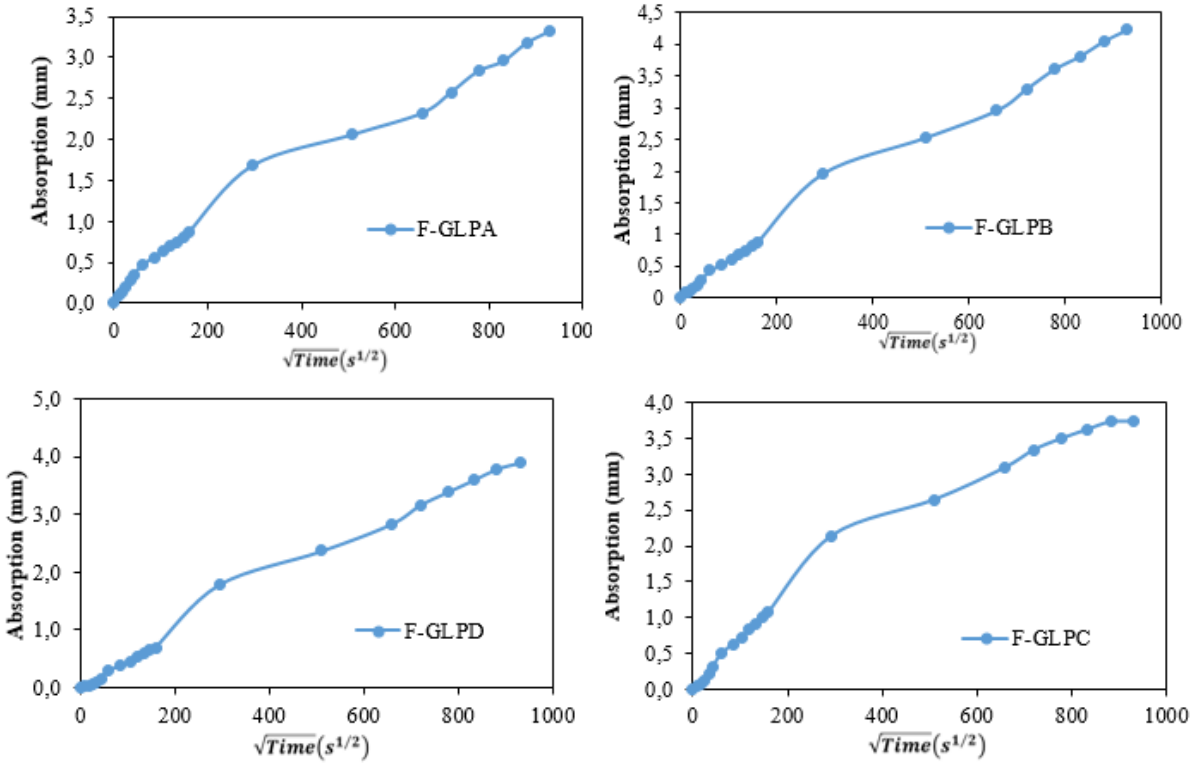

Figure 4.6: Averaged water absorptivity plot for fly ash based geopolymers (F-GlP) with an AS/B ratio = 0.31, 0.33, 0.36, 0.40.

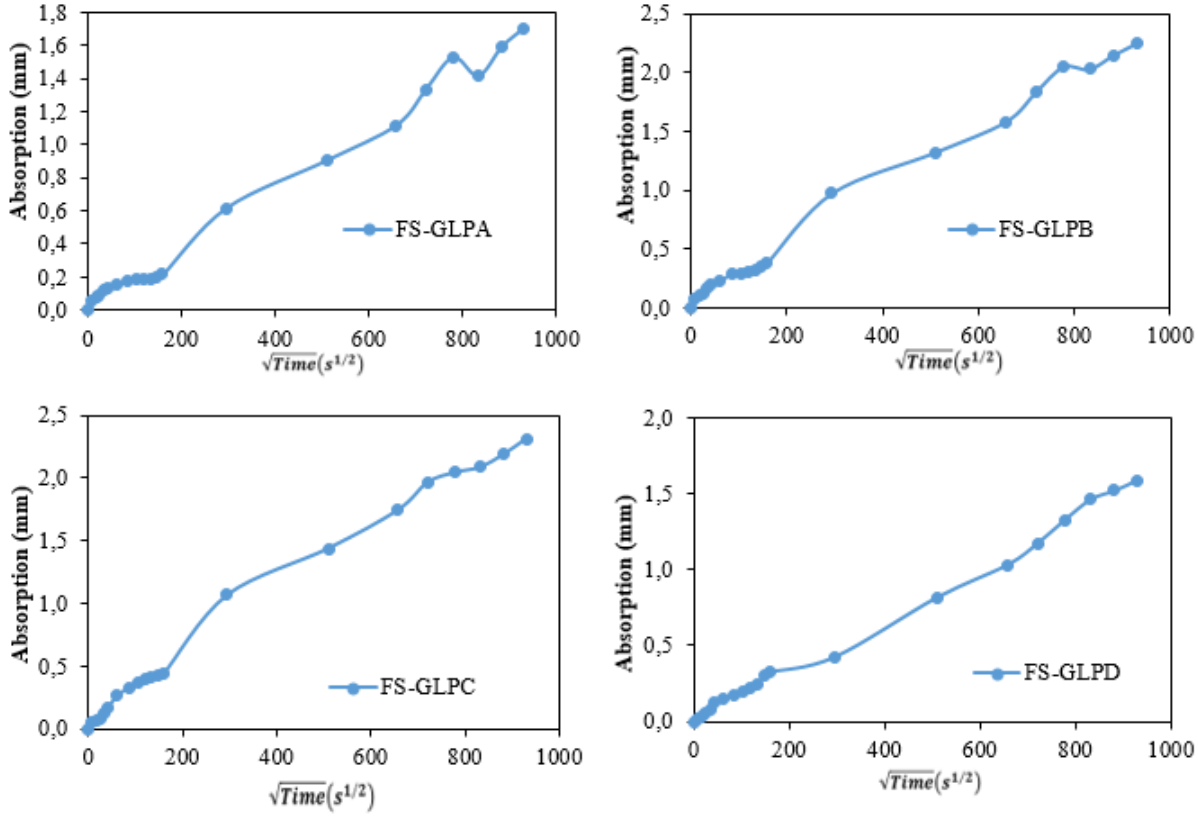

Figure 4.7: Averaged water absorptivity plot for fly ash/silica fume based geopolymers (FS-GlP) with an AS/B ratio = 0.31, 0.33, 0.36, 0.40.

It can be noted that the fly ash and fly ash silica fume based geopolymers (as seen in Figures 4.6 - 4.7), display an initial increasing linear trend in their water absorptivity graphs. A brief inflection point (at ± 3600 s) is also observed, where the samples seem to reach moisture saturation but slow additional absorption is noted until the completion of experiment, presenting an almost increasing near-linear trend again (in most cases). From this, it is evident that the F-GlP and FS-GlP do not reach saturation but rather continually absorb moisture, but at much lower rates during the secondary part of the experiment.

The initial and secondary sorptivity values obtained from Figures 4.6 - 4.7, for the triplicate of each mixture were averaged and reported in Table 4.6. The Table reveals that the secondary sorptivity values for both F-GlPs and FS-GlPs are significantly lower than the initial sorptivity values. This substantiates the obvious suggestion that the rate of water ingress in the secondary part of the experiment is decelerating due to a substantial initial uptake of moisture. However, the secondary sorptivity values for geopolymer samples are comparatively higher than the secondary sorptivity rates observed for the OPC analogous samples. This indicates that the

geopolymer capillary pores are still taking up water as compared to the OPC samples which reached full saturation in a much shorter amount of time.

It can accordingly be postulated that this continuous uptake of moisture may possibly be ascribed to the formation of additional bonding structure within the geopolymer lattice. As has been mentioned on several occasions during the course of this investigation, moisture is the life-blood of the reactions required to form the intricate aluminosilicate structures that afford these types of compounds their renowned structural durability (Davidovits, 1991). These secondary stabilization interactions may take longer to form, owing to the complexity of the inherent structural lattice, which in turn requires higher formation energies to form the complex bonds.

This continuous uptake of moisture also implies that the shape (slope) of the saturation curves (secondary sorptivity) would differ substantially for those noted for OPC types samples and cannot be compared in a logical manner. It was also noted in Chapter 3, that owing to the fact that there is not much change in the mass of the samples during the secondary absorption (OPC samples), these values are not necessarily indicative of the specific sample physicochemical characteristics. It can therefore be concluded that initial sorptivities better describe the sample's overall sorptivity and/or the sample porosity (ASTM, 2004) and will be the main focal point for this comparative study.

With this in mind, Table 4.6 reveals that the geopolymer samples display a significantly lower rate of initial absorption *vs*. the OPC analogues. This, in turn, implies a reduced porosity and a more densely packed matrix structure for these new candidate mixes. It is envisaged that this observation will be further quantitatively substantiated by mercury intrusion porosimetry (MIP) and qualitative bulk density measurements (helium pycnometry), later in this Chapter.

Chapters 1 and 2 emphasized the fact that the presence of a disproportionate number of pores will be very detrimental to the inherent strength and durability of cementitious materials. These pores tend to weaken the internal structure of cement and make it susceptible to the ingression of water, sulphates or acids (Fernando & Said, 2011). This noticeable flaw is not ideal for a core-catching material candidate and it is deemed that the less porous and more structurally sound the geopolymeric structures are, the more applicable these mixtures will be for the envisaged application.

Table 4.6 also shows that FS-GlPs exhibited lower average sorptivity values than those observed for F-GlPs, in all geopolymer mixes. This suggests that the inclusion of silica fume

in fly ash based geopolymers resulted in the filling of little voids between fly ash particles, leading to a more densely packed and less permeable structure.

Table 4.6: Average initial water sorptivity rates for fly ash (F-GlP) and fly ash/silica fume (FS-GlP) based geopolymers relative to the initial water sorptivity rates for plastic sealed OPC type samples.

AS/Binder Ratio	**Fly ash based (mm/√s)**		**Fly ash/silica fume (mm/√s)**		**Plastic sealed cured (mm/√s)**	
	Initial sorptivity	Secondary sorptivity	Initial sorptivity	Secondary sorptivity	Initial sorptivity	Secondary sorptivity
0.31	0.0052 (8)	0.0027 (15)	0.0047 (9)	0.0017 (9)	0.0122 (11)	0.0020 (10)
0.33	0.0050 (9)	0.0036 (8)	0.0021 (10)	0.0021 (9)	0.0049 (9)	0.0016 (11)
0.36	0.0048 (8)	0.0027 (10)	0.0028 (7)	0.0020 (10)	0.0055 (9)	0.0012 (10)
0.40	0.0044 (6)	0.0035 (11)	0.0019 (10)	0.0019 (11)	0.0059 (12)	0.0031 (18)

4.4.1.2 Effect of AS/B ratio on sorptivity plots for fly ash based (F-GlP) and fly ash/silica fume (FS-GlP) based geopolymers

From the results noted in Table 4.6, Figure 4.8 can clearly be plotted to illustrate the effect of the alkaline solution to binder ratio (AS/B ratio) on initial sorptivity of fly ash based geopolymers. It can be deduced that as the AS/B ratio increases, the rate of water absorption slightly decreases. This is a somewhat surprising observation, as one would expect that dilution effects on the binder material would afford a more porous structural matrix (similar to the OPC observations). However, it has been noted in past investigations that increased AS/B ratio may escalate the formation of geopolymer hydration products, thus yielding more compact geopolymer matrices that are less permeable to moisture intrusion (Al Bakri Abdullah et al., 2012).

It should also be noted that a relatively small variance in results (mm/√s) is observed, when noting the sorptivity values for the various AS/B ratio mixes. Accordingly, when considering the errors on each of these values, it could be possible that these values do not differ at all. It is thus imperative that the additional testing protocols be undertaken to clarify ambiguity.

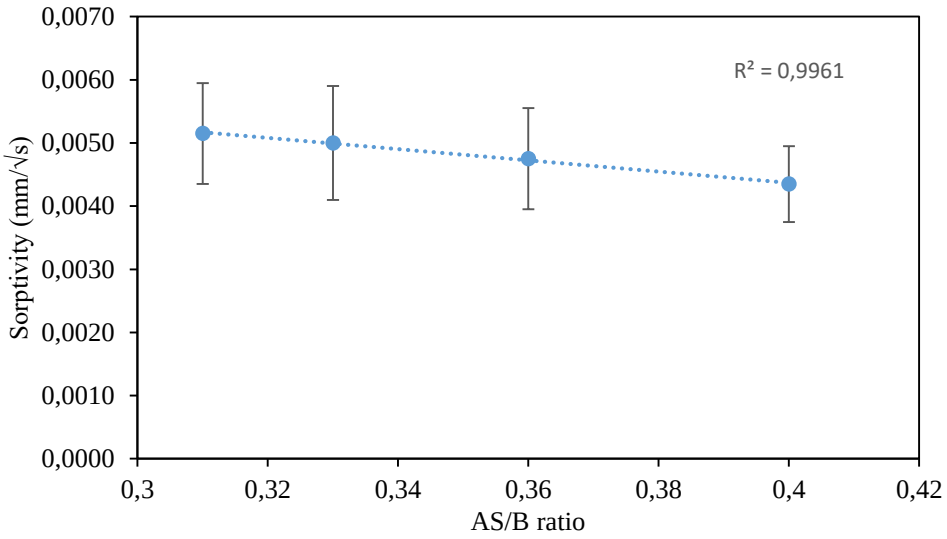

Figure 4.8: Effect of AS/B ratio on initial sorptivity rates for fly ash based geopolymers (F-GlP).

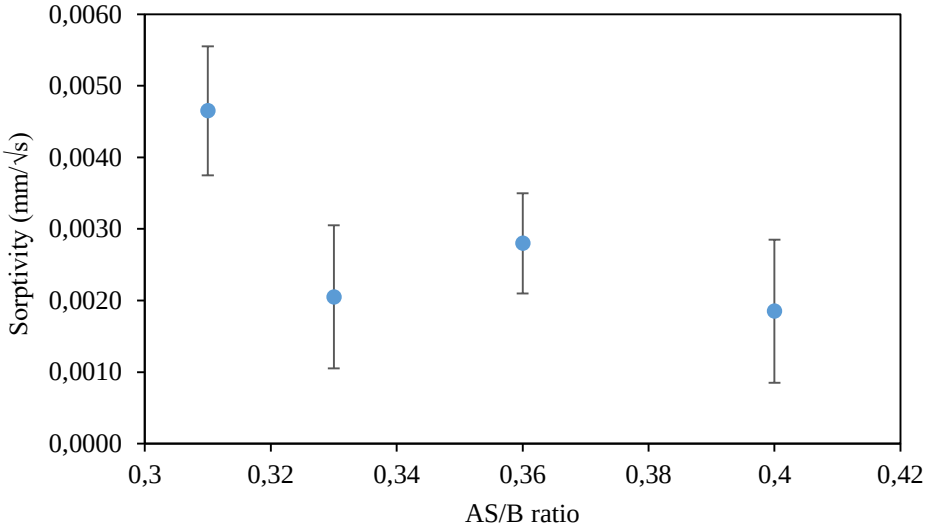

Figure 4.9: Effect of AS/B ratio on initial sorptivity rates for fly ash/silica fume based geopolymers (FS-GlP).

Figure 4.9 also presents the surprising decrease in the initial sorptivity as the AS/B ratio increases from 0.31-0.33 and after the 0.36 ratio for FS-GlP samples. A slight increase in sorptivity is observed at the 0.36 AS/B ratio, which substantiates the requirement for these sorptivity values to be reaffirmed with additional testing methodologies. This increase in sorptivity as a function of increased AS/B ratio may be ascribed to the increase in the concentration of OH^- ions. Memom et al. (2013) reported that an excess of OH^- ions tend to

hinder with the dissolution process of geopolymerization affording an incomplete geopolymerization process. This gives rise to the presence unreacted fly ash in the matrix, and essentially to an increase in sorptivity.

Even though there is some uncertainty on the precision of the sorptivity (mm/√s) values for the aforementioned experiments, it would seem that these candidate geopolymer materials and specifically the FS-GlP mix, significantly out-performed the OPC baseline model with relation to water sorptivity.

4.4.3 Sulphuric acid resistance testing for candidate geopolymer samples

During a nuclear incident, boron carbide B_4C, which is a material that is mixed with stainless steel for the production of control rods, could possibly be oxidized. The oxidation reaction of B_4C results from the interaction of B_4C with water (that is used as a moderator or a coolant) in the reactor. This reaction leads to the release of CO_2 gases, boric acids and boron oxide (Steinbrück, 2005). It is therefore imperative that the core catcher must be able to withstand acidic conditions (boric acid) in the case of a molten corium spill.

As indicated by many tests, geopolymer concrete theoretically displays an improved ability to resist acidic chemical damage. This property can be ascribed to the lack of dependency on lime in the cementitious mixture that makes it less prone to acid attack, as compared to OPC which is easily degraded in acid. Although boric acid resistance was not tested in this study, another commonly used acid, sulphuric acid, will be reviewed. Research on the sulphuric acid resistance of fly ash based geopolymer matrices is relevant to this study in obtaining recommendations for optimum geopolymer materials that could enhance containment structures of the reactor core.

The performance and durability of F-GlP and FS-GlP samples when immersed in 10% sulphuric acid (H_2SO_4) were analyzed in terms of visual changes and mass loss as a function of time. The % weight change was again determined by equation (2) based on the ASTM C267**.**

$$\%\ \text{weight change} = \left[{}^{(w-c)}/_{c}\right] \times 100 \qquad (2)$$

(a) Visual observations from acid digestion testing

Figure 4.10 illustrates the appearance of F-GlP and FS-GlP samples when exposed to a 10% sulphuric acid solution for 2 days. From this, it can be seen that unlike OPC samples, observed

in Chapter 3, the geopolymer samples did not undergo a significant structural degradation and remain intact even after 2 days of being immersed in acid.

Figure 4.10: A visual illustration of fly ash (F-GlP) and fly ash/silica fume (FS-GlP) geopolymers immersed in 10% sulphuric acid solution after 2 days of exposure.

This structural stability is additionally emphasized when considering Figure 4.10. In this depiction, it was impressively noted that the geopolymeric samples still remained structurally intact even after 20 days of immersion in acid, with just minor erosions observed on the FS-GlP samples. Additionally, the geopolymer samples did not undergo significant rates of acid digestion, which tends to lead to excessive mass loss and thus the change in their initial sizes or volume is almost negligible. This durability is very advantageous when considering the harsh environments these materials are envisaged to be exposed to. Furthermore, the F-GlPs had a slight change in color, from a slightly darker shade of grey to a lighter shade of grey (maybe due to a significant degree of SO_4^{2-} interactions). The FS-GlPs showed no color change after 20 days of immersion in 10% sulphuric acid.

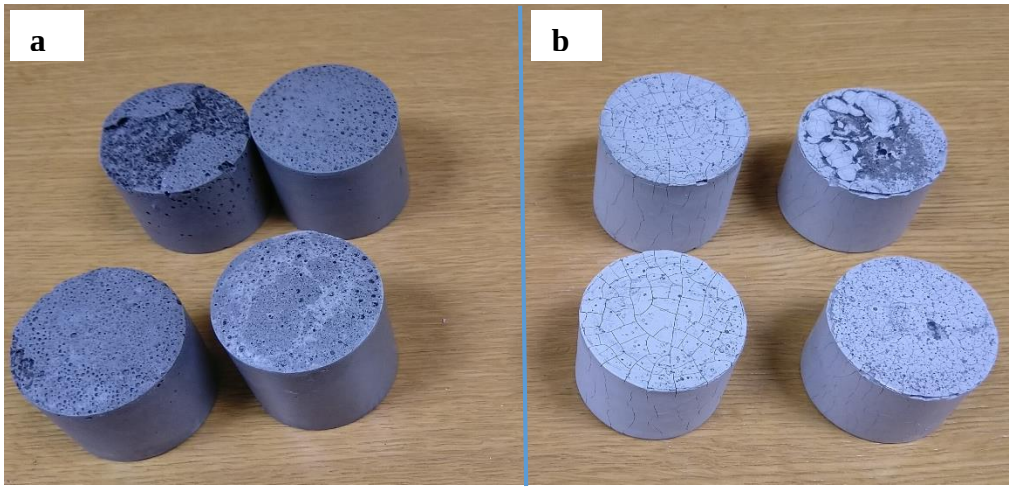

Figure 4.11: Geopolymers showing (a) fly ash/silica fume based geopolymers (FS-GlP) with minor erosions on the surface (b) fly ash based geopolymers (F-GlP) with slightly more pronounced cracking and color changes 20 after days of immersion in 10% sulphuric acid.

As mentioned previously in Section 4.4.1, a slight degree of post-conditioning cracking was observed on fly ash based geopolymers for mix A, B and C, prior to sulphuric acid immersion. The cracking on the F-GlPs became more pronounced or defined during sulfuric acid testing. The definition of cracks on F-GlPs could be attributed to the more abundant infiltration avenues for the acid solution into the geopolymer lattice thus affording a larger surface are for SO_4^{2-} interactions and accordingly catalyzing increased digestion rates.

When comparing the depictions of the OPC samples (Figure 3.17) *vs*. the geopolymeric samples (Figure 4.11) after 20 days of 10% H_2SO_4 exposure, it becomes obvious that the geopolymeric samples are much more robust to these harsh conditions. It has been well defined that the dependency on lime in the OPC cementitious mixture is the main reason for its susceptibility to acid digestion. As was noted in Chapter 2, geopolymeric samples have a much lower $Ca(OH)_2$ content as compared to the OPC analogues and contributes to its superiority as a possible candidate mixture. Additionally, this envisaged acid resistance could also be ascribed to the famous geopolymeric stabilization interactions. These interactions do not only reduce the amount of pores (defined from sorptivity testing), limiting the area of sample exposed to the acidic solution, but these compounds also afford a more complex and robust structural matrix. This conclusion will hopefully be further substantiated by density and MIP investigations to be highlighted later in this Chapter.

When considering only the visual observations for all sample sets, post-acid digestion, it is very obvious that the geopolymeric samples significantly outperformed the OPC baseline

analogues in terms of durability. As has been mentioned in Chapter 1, it is envisaged that a more durable core-catching material be identified for the specific application. It is not necessarily envisaged that a core-catcher will be continually exposed to a significant quantity of H_2SO_4 solutions but this improved resistance is a definite indicator of geopolymer structural superiority over OPC mixtures durability in overly harsh conditions.

(b) Gravimetric observations for fly ash (F-GlP) and fly ash/silica fume based geopolymers (FS-GlP) exposed to 10% H_2SO_4

4.4.3.1 (A) Fly-ash geopolymer (F-GlP) analogue

Figure 4.12 illustrates the % weight loss (% wt.) of fly ash based geopolymers in 10% sulphuric acid solution for 20 days. It can be noted in the comparative illustration that the F-GlP with an AS/B ratio of 0.31 undergoes the highest degree of % wt. loss (3.14 %), whilst, as the AS/B ratio is increased, the fly ash based geopolymers experienced less % wt. loss, in the range 0.58 % - 1.28 %. The higher % wt. loss for 0.31 AS/B ratio (mix A) is attributed to the surface cracking that was observed on the samples prior to water and sulphuric acid testing (a greater surface is exposed to the acidic solution). This observation along with the higher water absorptivity rates noted for mix A (0.31), leads to the suggestion that this specific sample matrix is more susceptible to acid intrusion versus samples with AS/B ratios between 0.33-0.40. This may not be an expected observation, when considering that it is expected that the degree of porosity is envisaged to increase with higher AS/B ratio. This anomaly may be unique to fly ash type samples, but further investigations are required to substantiate this.

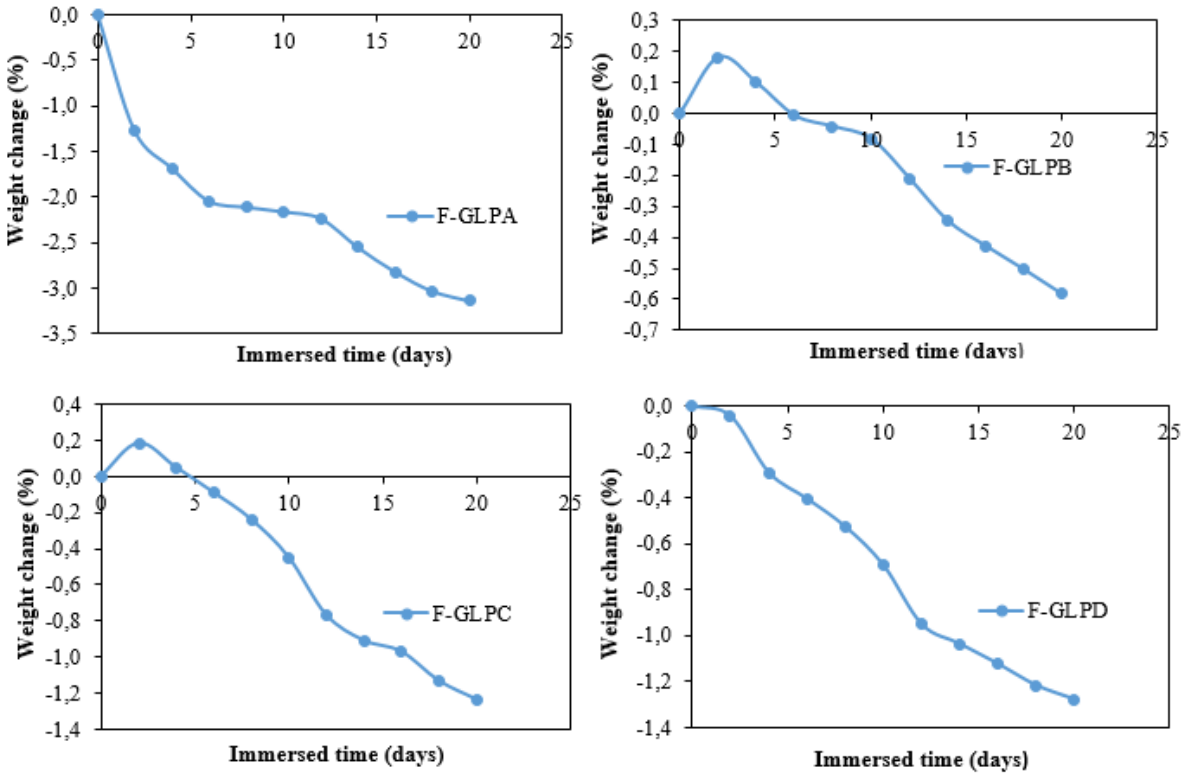

Figure 4.12: Percentage weight (% wt.) change of fly ash based geopolymers (F-GlP) with an AS/B ratio = 0.31, 0.33, 0.36 and 0.40, exposed to 10% H_2SO_4 solution over a 20 day period.

An initial mass gain can also be noted for the B and C samples, with minimal initial (first 2 days) digestion noted for the D mixture. This is an obvious contradiction to expected results. As noted in the pre-screening testing in Section 4.3.7, some geopolymeric samples require a higher moisture content, to fully "wet" the cementitious candidates. Accordingly, this initial uptake of moisture can be ascribed to a "thirsty" lattice structure. In other words, the rate of moisture uptake is greater than the tempo of matrix digestion. This noted uptake is less pronounced with an increase in AS/B ratio because the lattice is more already more saturated with moisture. Albitar et al. (2017) also reported on this sudden initial increase and subsequent % wt. decrease trend for geopolymer concretes, immersed in 3% sulphuric acid.

When ignoring the outlier trace for mix A and only considering trace B-D, it becomes evident that the rate of digestion increases slightly with an increased AS/B ratio mix, reaching a maximum for mix D (1.28 %) after 20 days of immersion. This observation is expected as a theoretically more porous structure (envisaged for higher AS/B ratio) allows for easier proliferation of the acid solution throughout the matrix. However, this variance is so small, no definitive conclusion could be reached.

4.4.3.2 (B) Fly-ash/Silica fume geopolymer analogue

The % wt. loss digestion trace for fly ash/silica fume (FS-GlP) based geopolymers in a 10 % sulphuric acid solution, is presented in Figure 4.13. Once again, an initial increase in the % wt., followed by a sudden decrease can be noted for the 0.31 and 0.33 analogue samples and can again ascribed to a preliminary uptake of moisture by a "thirsty" lattice. It is very noticeable that these trends bear a striking resemblance to the results noted for the F-GlPs, but a critical comparison is undertaken later in this Section.

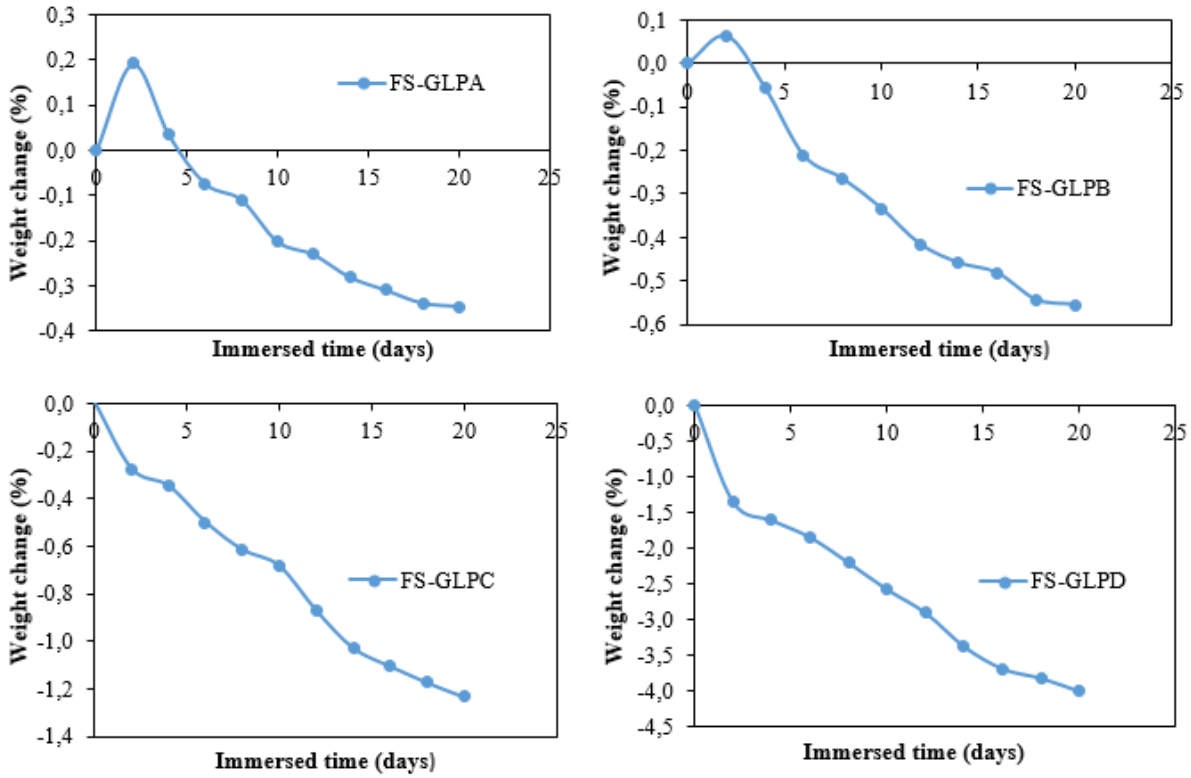

Figure 4.13: Percentage weight (% wt.) change of fly ash/silica fume based geopolymers (FS-GlP) with an AS/B ratio = 0.31, 0.33, 0.36 and 0.40, exposed to 10% H_2SO_4 solution over a 20 day period.

Once again, it is also quite evident that the rate of digestion increases with an increased AS/B ratio mix, reaching a maximum for mix D (4.00%). As has been described, this observation is expected as a more porous structure (owing to a more dilute binder mixture) allows for easier proliferation of the acid solution throughout the matrix and affording a larger surface are for potential digestion. In the next section, the obtained results for the geopolymeric acid digestion

experiments will be compared with the OPC baseline results and the durability of the aluminosilicate compounds will be evaluated as a function of % wt. loss in acidic conditions.

4.4.3.3 Comparison of acid resistance of fly ash and fly ash/silica fume samples with OPC baseline model

Table 4.7 is a summary of the final acid digestion % wt. losses noted for the, OPC, fly ash (F-GlP) and fly ash/silicate fume (FS-GlP) samples, that were examined during the course of this investigation. This comparative table serves to highlight the obvious durability of the geopolymer compounds in a 10% sulphuric acid solution.

Table 4.7: A comparative table of % weight (% wt.) loss noted for the various samples that were investigated during this study.

AS/B ratios (w/c ratio)	OPC % wt. loss	Fly ash % wt. loss	Fly ash/silica fume % wt. loss
0.31	83.95 (33)	3.14 (21)	0.34 (9)
0.33	77.10 (27)	0.58 (10)	0.56 (10)
0.36	68.07 (29)	1.24 (10)	1.23 (9)
0.40	76.78 (34)	1.28 (11)	4.00 (10)

From first glance, it is very obvious that a substantial decrease of the degree of digestion damage can be noted for the geopolymer samples *vs.* results obtained for the OPC analogues. This is not an unexpected observation when considering the literature noted in Chapter 2. As indicated by various referenced investigations, geopolymer concrete displays an improved ability to resist acidic chemical damage (Shankar & Khadiranaikar, 2012 and Bakharev, 2005). This property can be ascribed to the lack of dependency on lime in the cementitious mixture that makes it less prone to acid attack, as compared to OPC which is easily degraded in acid (Shankar & Khadiranaikar, 2012)**.** Another study by Okoye et al. (2016) also confirmed that the presence of silica fume in fly ash based geopolymers lead to a more acid resistant geopolymer as compared to OPC samples, when immersed in of NaCl (5%) and H_2SO_4 (2%) solutions. The impermeability of fly ash-silica fume based geopolymers was deemed to be partly responsible for the resistance against acid attack, as opposed to porous OPC samples (Khater, 2013).

As has been mentioned, research on the sulphuric acid resistance of fly ash based geopolymer matrices is relevant to this study in obtaining recommendations for optimum geopolymer materials that could enhance containment structures of the reactor core. The results noted in Table 4.7 substantiate this postulation of improved geopolymer durability in acidic solutions. A catastrophic percentage weight loss (> 69 wt %) was noted for all the OPC analogue samples. It is obvious that such a degree of degradation will results in a cataclysmic structural failure. This is obviously not ideal for core-catching applications and it is deemed that the geopolymeric candidates will be much more effective for desired application purposes.

When comparing the F-GlP and FS-GlP samples, no significant difference can be noted other than for the 0.40 AS/B ratio analogues. In this case the dilution effects are more pronounced in the fly ash silica fume samples, affording a more porous structure and a greater susceptibility to acid digestion. The 0.31 AS/B ratio of fly ash sample is not included in this comparison as the aforementioned cracking on the surface may have influenced results.

4.4.4 Compressive strength results for fly ash and fly ash/silica fume based geopolymers

The quality and durability of a cementitious material in any structural application is of primary importance to the successful use of the candidate compound. In this study, the compressive strength testing of geopolymeric candidate materials was conducted as a useful indicative parameter of the cementitious material, especially in resisting external stresses that may exist in core catching applications. It is also envisaged that the results from this testing protocol would clarify some potential discrepancies with relation to results observed for water sorptivity and acid digestion experiments.

As mentioned previously, it is crucial that the concrete used in core catcher systems are able to withstand and entrap, not only the melted corium, but also contain as much of the residual heat and radiation flux from the corium material as possible, in case of a nuclear reactor accident. As has previously been mentioned in Chapter 3, this testing protocol is deemed the most pivotal test of this study, according to required application. With the aforementioned in mind, the average compressive strength results for F-GlP and FS-GlPs with varying AS/B ratios are tabulated in Table 4.8. P-OPM baseline results are also denoted in this table for easy comparison with geopolymer samples. It is important to note that both F-GlP and FS-GlP samples were tested on 10t bench press bench press with a pressure gauge, where the maximum load applied to each sample was recorded when the samples were completely destroyed.

Table 4.8: Compressive strength results for fly ash- (F-GlP), fly ash/silica fume based (FS-GlP) geopolymers and OPC cementitious mixtures with varying AS/B ratios.

AS/B (w/c) ratios	F-GLP	FS-GLP	P-OPM
0.31	27.33 (36)	9.01 (27)	30.94 (33)
0.33	28.30 (33)	10.04 (36)	23.39 (36)
0.36	29.04 (33)	10.19 (33)	9.01 (66)
0.40	35.10 (30)	10.60 (33)	22.44 (30)

4.4.4.1 Effect of AS/B ratios on the compressive strengths of fly ash (F-GlP) and fly ash/silica fume based (FS-GlP) geopolymers and comparison thereof with OPC baseline samples

Figure 4.14 illustrates the trends for the compression of F-GlP and FS-GlP based geopolymers with response to the increase in AS/B ratios. From this graph, the OPC and fly ash geopolymer candidates display a similar compressive strength at a lower moisture content, with the fly ash sample completely outperforming the OPC analogues at higher AS/B ratio (w/c). Interestingly, even though the FS-GlP analogues outperformed the OPC and F-GlP candidate mixtures in relation to water sorptivity observations, but is less structurally durable. This anomaly is clarified by results from a similar investigation by Ramezanianpour & Moeini (2018). It was found in their study that an increased additional content of silica fume in geopolymer pastes does not always lead to improved physicochemical performances. The reason being ascribed to the fact that even though the finer particles (silica fume) act as pore filler in concrete structures increasing density (reducing sorptivity), it might have an overall degenerative effect on cementitious structure. They noted that in some instances, the finer particles are more readily accessed or taken up by the alkaline reaction solutions very promptly (due to increased surface area), leaving the larger particles with less alkaline liquid to react with and subsequently crippling the aluminosilicate macro structure (Wong & Razak, 2005).

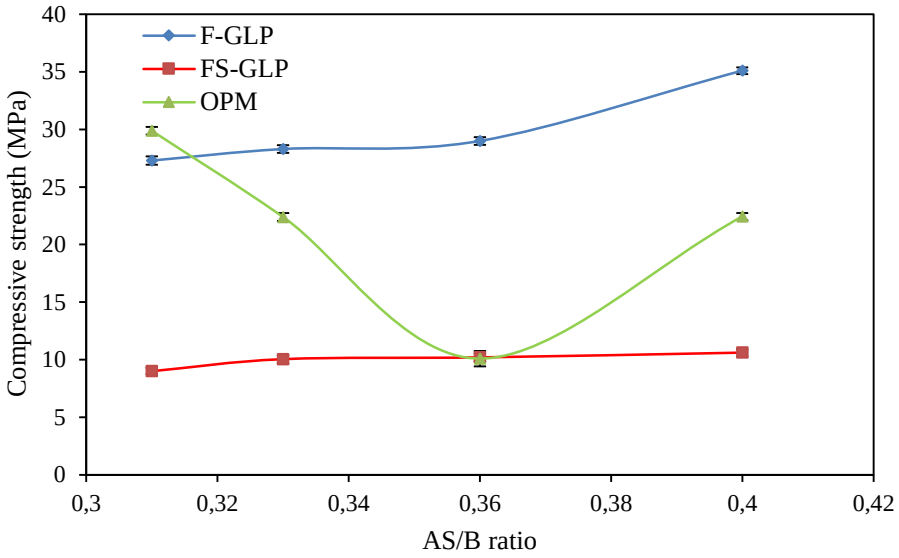

Figure 4.14: Effect of AS/B ratio on compressive strength of fly ash (F-GlP) and fly ash/silica fume based (FS-GlP) geopolymers and comparison thereof with OPC baseline samples.

As was noted in Chapter 3, the overall decreasing compressive strength trend for the OPC baseline analogue (green trace) can be ascribed to binder dilution effects, which affords a more porous structural lattice. When considering the fly ash geopolymer candidate, a contradictory steady increase in compressive strength with increased AS/B ratio is observed. Interestingly, this result is in accordance with the trends noted for the water sorptivity experiments and subsequently quells some of the uncertainty around the obtained results in section. In Section 4.4.1, it was postulated that a secondary, slow continuous uptake of moisture can possibly be ascribed to the formation of additional bonding structure within the geopolymer lattice. This was observed by the fact that the fly ash lattices never reached saturation during sorptivity testing. In other words, the moisture within the lattice kept on being employed for secondary stabilization interactions affording a denser and apparently stronger structural lattice.

As has been mentioned on several occasions during the course of this investigation, moisture is the life-blood of the reactions required to form the intricate aluminosilicate structures that afford these types of geopolymer compounds their renowned structural durability (Davidovits, 1991). These secondary stabilization interactions may take longer and obviously require more moisture to form, owing to the complexity of the inherent structural lattice, which in turn requires higher formation energies to form the complex bonds.

4.4.4.1 Preliminary identification of idealized mixture for core-catching applications and verification of pre-screening method

A preliminarily postulation of ideal candidate mixture can now be identified when considering the water sorptivity, acid resistance and compressive strength testing methodologies from Chapters 3 and 4.

It was observed that both types of fly ash based candidate mixtures significantly outperformed the OPC idealized baseline model and we can immediately eliminate the OPC mixtures from consideration. This deduction was already deemed a successful outcome with relation to this study. It was mentioned in Chapter 1, that candidate mixture that physicochemically outperforms the established OPC cementitious materials for core-catching applications be identified.

When consider both the F-GlP and FS-GlPs, the selection of idealized mixture is slightly more complicated. Comparable results were observed for both sample sets with relation to acid resistance and this requires selection to be made on compressive strength and water sorptivity observations.

As discussed in the previous section, it would seem that FS-GlP have superior resistance to moisture ingress into the structural lattice, implying a more dense (optimal) structural formation. However, compressive strength results contradict this observation. This anomaly was ascribed to the finer particles (silica fume) that were more readily accessed by the alkaline reaction solutions (due to increased surface area), leaving the larger particles with less alkaline liquid to react with (un-activated) to form required stabilization bonding interactions and subsequently crippling the aluminosilicate macro structure (Wong & Razak, 2005).

In contrast, the F-GlP analogue did not perform as well with relation to sorptivity testing but significantly outperformed the FS-GlP candidate mixtures with relation to structural integrity. It has been defined that structural integrity is the most essential property required by a core-catching cementitious material. Therefore, the F-GlP mixtures are optimal for the envisaged use.

Now that that optimal mixture has been identified, an idealized AS/B ratio (within set parameters of this investigation) can be postulated. It can be safely assumed that from the results obtained in this chapter that F-GlP samples with a higher AS/B ratio (0.40) are deemed ideal for the proposed application of this study. This is selection is ascribed to the lowest initial

sorptivity rate, pronounced acid resistance and highest compressive strength as compared to the other AS/B mixtures. From the obtained results, it is envisaged that increasing the (AS/B ratio) above 0.40 will further improve the physicochemical properties and structural durability of the cementitious matrix. However, this falls beyond the scope of the initial parameters set in Section 3.9.

4.5 Quantitative evaluation of candidate material structural lattice

From the ASTM approved material evaluations in the previous sections, a preliminary, optimal geopolymeric formulation could be identified in Section 4.4.4.1. However, for the sake of scientific completeness, some additional quantitative analytical datasets will also be useful to substantiate the postulated optimized characteristics in the previous sections. The analytical techniques identified to corroborate the physical material assessments are; helium displacement pycnometry (for quantitative skeletal density determinations) as well as mercury intrusion porosimetry (MIP) (for pore size distribution and % porosity evaluations).

An AccuPyc II 1340 helium displacement pycnometry system was used for density determinations. Enough sample to nearly fill two thirds of the sample chamber volume of the pycnometer (approximately 2 to 3 g) was weighed and placed inside the sample vessel of the instrument. Determinations were performed in triplicate at an equilibration rate of 0.05 psig/min. The results from the investigation are presented in Table 4.9

The AutoPore IV 9500 Mercury Intrusion Porosimeter (MIP) located at Necsa was used for porosity determinations, with the following applicable parameters: Contact angle: ~130°; Pressure range: 0.1 - 60000 psia; Surface tension of the liquid: 485 dynes/cm. Pore size distribution is determined from the volume of Hg intruded at each pressure increment, while the total porosity is based on the total intruded Hg-volume.

Table 4.9: A summary of cementitious candidate material skeletal density.

Sample	AS/B (w/c) ratio	Density (g/cm^{-3})
A-OPM	0.40	1.9785 (18)
P-OPM	0.40	2.1879 (9)
F-GlPB	0.33	2.2361 (7)
F-GlPD	0.40	2.2392 (11)
FS-GlPB	0.33	2.2423 (11)
FS-GlPD	0.40	2.2464 (8)

Table 4.10: A summary of cementitious candidate material median pore diameter and relative porosity.

Sample	AS/BR (w/c) Ratio	Median pore diameter (µm)	Porosity (%)
A-OPM	0.40	0.0186	47.6869
P-OPM	0.40	0.0133	32.4657
F-GlPB	0.33	0.0079	24.9462
F-GlPD	0.40	0.0068	23.8741
FS-GlPB	0.33	0.0085	23.1488
FS-GlPD	0.40	0.0079	22.6294

4.5.1 Analytical assessments of various cementitious core-catching material candidates (Density determinations and porosity evaluations)

From Table 4.9 and 4.10 some very applicable conclusions can be made with regard to this over-arching comparative investigation. These results substantiate the selection of most applicable curing method selection, geopolymeric mixture superiority and also the optimized moisture content determinations. It should be noted that owing to time constraints, particular samples had to be selected to highlight the most relevant information.

It was concluded in Chapter 3 that ambient cured samples afford a less densely packed and porous structural lattice. This observation was ascribed to excessive evaporation of moisture from the cementitious mixture, affording a more porous compound. When considering the results from Tables 4.9 and 4.10 it is obvious that the ambient cured OPC sample (0.40) is definitively less dense (1.9785 (11) $g.cm^{-3}$) and more porous (47.6869 %) than the plastic sealed cured analogue (2.1879 (9) $g.cm^{-3}$, 32.4657 %). This porous internal structural lattice affords more avenues for the uptake of destructive acidic solutions as well as causing a higher rate of water absorption, which is not ideal for envisaged core-catching applications. In the case of OPC type samples, a direct correlation between compound density and compressive strength has been well-documented (Al Bakri Abdullah et al., 2012). Accordingly, these results also satisfactorily substantiate the compressive strength results from Chapter 3. This evaluation thus adequately clarifies why the sealed cured OPC samples significantly outperformed the ambient sample in terms of water sorptivity and compressive strength.

The second point of confirmation was focussed on geopolymeric matrix superiority *vs*. the OPC analogue mixtures. From the obtained results in Table 4.9 and 4.10, it is clearly noted that

the geopolymeric samples are considerably denser and less porous as compared to the corresponding OPC samples. As noted in the previous section, the reduced porosity (lower sorptivity) was postulated to imply a denser structural lattice and these analytical results reaffirm this theory. Once again, a more dense and robust structure is ideal for envisaged application and when considering the incomparable superior acid resistance of the geopolymeric analogues, the elimination of the OPC samples is a mere formality.

Finally, when comparing the four F-GlP and FS-GlP samples, two principal points of comparison was identified. It was noted that the water sorptivity and to a lesser extent the compressive strength of the geopolymeric samples improved as a function of increased AS/B ratios. In other words, there was improved structural durability observed for the geopolymeric samples with increased AS/B ratios.

These results also quantitatively clarified why the FS-GlP samples displayed the lowest rate of initial sorptivity. These samples were noted to be noticeably less porous than the F-GlP analogues and this reduction subsequently hinders the uptake of moisture into the structural lattice. This minimized porosity was ascribed to silica fume filling the open “areas” within the structural lattice, in previous sections. Additionally, the compressive strength superiority of FS-GlP was also validated by these results. From Table 4.9 and 4.10, the F-GlP median pore diameters were smaller than the values observed for the FS-GlP samples, implying that the “holes” within the lattice are not as pronounced for the F-GlP compounds, affording a more robust structure. Although, it might be argued that this was partially negated by the increased overall porosity observed for the F-GlP analogues, when considering the clarification that silica fume may not necessarily be advantageous the structural formation (even though it decreases porosity), this observation makes sense. It is thus deemed that these qualitative observations not only substantiate the results observed from the materials testing protocols but also motivate the selection of the 0.40 F-GlP samples as optimal formulation for core catching application (according to prescribed parameters).

Chapter 5: Conclusions from study and recommendations for future investigations

Enhancing safety systems in nuclear power plants should be a continuous process, for the purpose of preventing and mitigation of possible nuclear accidents. In this regard, a well-developed nuclear fuel core catcher system is an essential compartment within the reactor, which should be able to cope with the extreme conditions afforded by a complete core melt, while also displaying a lower degree of concrete ablation. In the following sections, the methodology (and success) of development of such a cementitious system will be discussed and evaluated, according to the prescribed requirements set out in Chapter 1. If these requirements are sufficiently met, this study will be deemed successful and useful for further development of novel cementitious core catching compounds.

5.1 Overview of investigative requirements

In this study, the use of geopolymer material over currently established OPC mixtures in nuclear fuel 'core catching' application was proposed. This postulation stems from the well-documented geopolymeric superiority with regard to; a low unbound water and lower calcium content within the structural compound lattice, making geopolymer materials less prone to acid attack, pore water evaporation and concrete ablation relative to OPC materials. The over-arching aim of this study was to develop the OPC and novel geopolymer matrices and to use OPC results as baseline for comparison with envisaged geopolymer species to attempt to supersede current OPC core catching applications. After completion of these comparative testing protocols, it was envisioned that the selection of an optimized geopolymeric formulation could be suggested for required application. It was proposed that the durability of OPC and geopolymer samples be evaluated by subjecting these cementitious materials to water absorptivity measurements, sulphuric acid resistance analysis and finally to compressive strength testing protocols, as mentioned in Chapters 1 and 2.

5.2 Theoretical considerations of cementitious geopolymer sample evaluations

In Chapter 2, an in-depth literature review was undertaken in an attempt to theoretically evaluate potential geopolymeric candidate mixtures and also to identify which structural characteristics need to be optimized for idealized application. In this regard, several aluminosilicate source materials, various alkaline activators and some admixtures were identified and possible applicability discussed for possible continuation of this study. These candidate materials were summarized in this Chapter (also see Table 4.2). These selections were limited due to compound availability and cost but the overall amount of possible

candidate formulations were deemed sufficient for this investigation (in Chapter 4). Chapter 2 also highlighted previous investigations, where the superiority of geopolymer matrices (and specifically fly ash based compounds) over OPC type compounds were noted. Accordingly, this investigation primarily served to theoretically prove fly ash geopolymer applicability for core catching applications. It was concluded that by systematic evaluation of the obtained literature, the applicability of fly ash based geopolymers was deemed plausible for continuation of study.

Additionally, this literature review afforded greater clarity on the required testing methodology for cementitious compounds. In-depth background of the ASTM testing protocols was also included in the aforementioned chapter and possible pitfalls identified. It was thus concluded that compressive strength testing, acid resistance testing and sorptivity measurements would serve as ideal testing protocols to evaluate the candidate cementitious samples (ASTM, 2004).

5.3 Preliminary synthetic considerations and OPC baseline development

In the next part of the study, preliminary synthetic work was done on OPC-type samples to obtain familiarity with the manufacturing of OPC samples and to optimize these structures to serve as a baseline for comparison with envisaged geopolymers. In this regard, various water to cement (w/c) ratios (0.31, 0.33, 0.36, and 0.40) and three different curing methods (ambient air curing, water curing and enclosed sealed curing) were employed during the exploratory manufacturing of OPC samples. This was done for the optimization of w/c ratio and to determine the best curing method for OPC as baseline for geopolymer synthesis.

From these initial results, it was observed that increasing the w/c ratio results in a more porous structural lattice for OPC samples due to increased dilution effects. As such, the 0.31 w/c ratio was considered the optimum w/c ratio for OPC samples when compared to 0.33, 0.36 and 0.40 w/c ratios. This w/c ratio resulted in low initial sorptivity rates of 0.0349 $mm/s^{1/2}$ as opposed to 0.33, 0.36 and 0.40 w/c ratios which resulted in 0.0419 $mm/s^{1/2}$, 0.0687 $mm/s^{1/2}$, and 0.0765 $mm/s^{1/2}$ initial sorptivity rates respectively. This observation implied a denser (and more robust) compound structure. In addition, the 0.31 w/c ratio had the highest overall compressive strength observed for all curing methods and substantially outperformed the other analogue formulations.

When considering the investigated curing methods, it was noted that air cured samples displayed the lowest degree of sulphuric acid attack, but it was suggested that these “dry” samples favored the initial ingress of the watery acid solution over the rate of potential

structural damage caused by acid digestion. These ambient cured samples also exhibited significantly higher initial sorptivity rates and much lower compressive strength values, implying a less durable structure. This is obviously not deemed ideal for required application and immediate eliminates this curing methodology from consideration. From the results for the water and plastic sealed cured samples, similar acid digestion and water sorptivity measurements were noted for both methods, but with the water curing methodology affording improved compressive strength. Accordingly, when all the results were collated and evaluated, it was found that plastic cured samples (compressive strength of 30.94 MPa) were chosen as the optimum baseline curing method for geopolymers samples in the next section of investigation. It is important to note that the water-cured samples were not excluded from comparative discussions, as their durability was found to be similar to the sealed cured analogues.

From the aforementioned, it can be confirmed that this initial OPC synthetic testing methodology was not only successful in affording the required familiarity with the synthetic procedure required for cementitious compounds but also assisted in the identification of idealized curing methodologies. In addition, an optimal OPC baseline formulation could identified for geopolymeric parameter comparison, in Chapter 4.

It should be noted that the pre-scribed synthetic parameters (in Chapter 3) were defined according to a combination of known literature and preliminary synthesis observations. Accordingly, it should be emphasized that these so-called “optimal formulations” are a best guess estimate, as time limitations did not allow for an exorbitant study of OPC type cements. However, as noted in Chapter 3, the obtained physicochemical results are quite comparable with optimized formulations noted in literature and are accordingly deemed useful for comparative purposes.

5.4 Candidate material pre-screening methodologies

From the literature discussion in Chapter 2, several aluminosilicate source materials, various alkaline activators and some admixtures were identified and possible applicability discussed for possible continuation of this study. However, individual practical screening of each possible formulation, with the defined AS/B ratios (derived from Chapter 3), would be a futile and laborious process. This led to the requirement for the development of a pre-screening methodology to quickly identify the most applicable candidate formulations.

A preliminarily prescreening was employed by analyzing various selected geopolymer samples manufactured from fly ash mixed with either silica fume or mineral clay additives and activated with various alkaline solutions in ambient conditions, with no sample curing procedures, to afford as "worst case scenario". It was postulated that this approach would emphasize or highlight certain candidate material's superiority over others.

During this study, it was observed that the fly ash mineral clay based geopolymers performed poorly and were immediately eliminated as possible candidates for core catcher applications. It should again be stressed that these compounds were mixed under "worst case conditions" and these circumstances may not necessarily be advantageous for mineral clay type geopolymer production. This is further substantiated by that fact that these samples required a higher AS/B ratio to obtain a workable consistency as compared to the other samples. In other words, under the synthetic assumptions set out in the beginning of Chapter 4, clay type geopolymers are not ideal for application in this study but under another pre-set group of synthetic conditions (possibly higher AS/B ratio than 0.40), may still afford superior physicochemical results. This requires further investigation is subsequent studies.

However, when considering the pre-set "worst case" conditions, fly ash (F-GlP) and fly ash silica fume (FS-GlP) based geopolymers showed the most promising results during pre-screening and were selected to be further analyzed for the aforementioned durability tests and optimized for the consideration of core-catching applications. Even though the pre-screening methodology only focused on a very small window (AS/B ratio 0.31 – 0.40) of possible mixtures, two superior candidate formulations could still be pin-pointed. It can accordingly be deemed that this methodology was useful in saving a substantial amount of time and labour to individually cure and condition each sample set.

So, in summary, this pre-screening methodology is still not completely refined and doesn't incorporate all possible variable factors within the evaluation structure. However, when considering the lack of required infrastructure at the beginning of this investigation, this pre-screening method was successful in identifying potential superior candidate mixtures in a timeous manner. If these identified formulations were to out-perform the baseline OPC analogues, it would be considered that this pre-screening methodology extremely successful.

5.5 Evaluation of selected geopolymer formulations

Even though, plastic curing was chosen as the optimum curing method for fly ash and fly ash silica fume based geopolymers (noted from conclusions in Chapter 3), the optimum w/c ratio

obtained for OPC studies (w/c 0.31) could not necessarily be superimposed to this part of the investigation. It is possible that for fly ash and fly ash/silica fume based geopolymer studies, this ratio will afford different physicochemical results for geopolymer studies (as seen for the clay type geopolymers). Therefore, altered alkaline solution to binder (AS/B) ratios (0.31, 0.33, 0.36, 0.40) were also employed in the manufacturing process of both fly ash and fly ash/silica fume based geopolymers. This expanded investigation was made possible by the time saved during the elimination of a substantial amount of other formulations by pre-screening, allowing for a more refined investigation in this section.

From such a highly in-depth investigation, it was concluded that as the AS/B ratio increases, the durability of both geopolymer type samples also improves, which is in contrast to OPC observations. This lead to the suggestion that a secondary, slow continuous uptake of moisture forms additional bonding structures within the geopolymer lattice. As a result, the 0.40 AS/B ratio exhibited in the lowest water sorptivity rates, lower degrees of sulphuric attack damage and in the highest compressive strength for the fly ash based geopolymers (F-GlP).

It was also found that the addition of silica fume to fly ash based geopolymers reduced the overall structural permeability/porosity but did not improve the overall compressive strength potential of the geopolymer structure. This observation was ascribed to the silica fume that readily absorbs alkaline solution due to its increased surface area, leaving fly ash particles with less alkaline liquid to react with affording in incomplete geopolymerization (Wong & Razak, 2005). Owing to this observation, the F-GlP source material with a AS/B ratio of 0.40 was deemed to be the ideal candidate for required application, under the pre-scribed assumptions of this study. This satisfies the aim prescribed aim of investigation noted in Chapter 1.

5.6 Geopolymer durability comparison with OPC baseline analogues

When considering the comparative outcomes highlighted in Table 4.6, as well as Tables 4.7 and 4.8, for the sorptivity, acid digestions and compressive strength observations, some useful deductions could be made. From this, it was obvious that the fly ash based geopolymers completely out-performed the OPC samples when considering these testing methodologies and accordingly implied that these matrices were significantly more robust. Throughout this study it has been continually highlighted that a superior, more robust, cementitious formulation is required for the envisaged core-catching application. Currently, OPC type structures are entrenched in this application but according to the results from this investigation, geopolymeric analogues are better fortified for this application.

In addition, these results also substantiated the success of the pre-screening methodology described in Chapter 3 and Section 5.4. It can now be unequivocally stated that not only was this method effective in identifying potential candidate materials, but it was proven that these selections afforded superior formulations.

5.7 Recommendations for future investigations

Although it may be difficult to dispute the overall success of this study in successfully defining a geopolymeric cementitious formulation that outperforms the entrenched OPC matrices for potential core-catching application, it is admitted that some additional recommendations be addressed for an improved screening process. These recommendations might have been known prior to the onset of this investigation but could not be addressed due to various constraints. However, the importance of these considerations should not be understated. A list of possible recommendations for future investigations is listed below;

- An expanded pool of geopolymeric candidate materials may afford an even better formulation for envisaged application
    - This also implies the re-evaluation of fly ash mineral clay type geopolymers, as differing mixing protocols may lead to improved physicochemical properties for these samples.
- The use of other, less readily available or more expensive aggregates and additional reinforcement can be incorporated to reduce cracking on geopolymer samples
- For higher performance geopolymer materials, heat curing could be implemented or used to improve on dissolution process, thus improving the induced compressive strength of these materials
- If a pre-screening methodology is required, an expanded “window” of study would be deemed ideal. This entails a larger screening area with relation to w/c ratios, curing times and sample conditioning methodologies.
- SEM, XRD and Raman/IR analysis and could also be investigated to clearly define the physical characterization of the cementitious materials and help to identify the factors that afford advantageous durability properties.
- The addition of neutron moderators as well as radiation shielding components could be employed and analysed in geopolymer samples for better deductions on the use of geopolymer materials in nuclear core cater applications.

References

ACAA, 2003. Fly ash facts for highway engineers. 74th ed. Aurora, USA: American Coal Ash Association.

Adam, A. & Horianto, X., 2014. The effect of temperature and duration of curing on the strength of fly ash based geopolymer mortar. *Procedia Engineering,* 95, pp. 410-414.

Al Bakri Abdullah, M.M., Kamarudin, H., Abdulkareem O.A.K.A., Ghazali, C.M.R., Rafiza, A.R. & Norazian, M.N., 2012. Optimization of alkaline activator/fly ash ratio on the compressive strength of manufacturing fly ash-based geopolymer. *In Applied Mechanics and Materials* , 110-116, pp. 734-739.

Al Bakri A.M., Kamarudin, H., BinHussain, M., Khairul Nizar, I., Zarina, Y. & Rafiza, A.R., 2011. The effect of curing temperature on physical and chemical properties of geopolymers. *Physics Procedia,* 22, pp. 286-291.

Al Bakri A.M., Kamarudin, H., BinHussain, M., Khairul Nizar, I., Rafiza, A.R. & Zarina, Y., 2015. Comparison of geopolymer fly ash and opc to the strength of concrete. *Journal of Computational and Theoretical Nanoscience,* 19(12), pp. 3592-3595.

Albitar, M., Ali, M., Visintin, P. & Drechsler, M., 2017. Durability evaluation of geopolymer and conventional concretes. *Construction and Building Materials,* 136, pp. 374-385.

Allelein, H., Neu, K. & Van Dorsselaere, J., 2005. Assessment and development of molten corium concrete interaction models for the integral code ASTEC. *Nuclear Engineering and Design,* pp. 285-308.

Al-Shathr, B. & Al-Attar, T., 2016. Effect of curing system on metakaolin based geopolymer concrete. *Journal of University of Babylon,* 24(3), pp. 569-576.

Andini, S. . Cioffi, R., Colangelo, F., Grieco, T., Montagnaro, F. & Santoro, L., 2008. Coal fly ash as raw material for the manufacture of geopolymer-based products. *Waste Management,* 28(2), pp. 416-423.

ASTM C1585, 2004. *Standard Test Method for Measurement of Rate of Absorption of Water by Hydraulic-Cement Concretes,* West Conshohocken, PA: ASTM International.

ASTM C267, 2001. *Standard test methods for chemical resistance of mortars, grouts, monolithic surfacings, and polymer concretes.* West Conshohocken, PA, USA: ASTM International.

Autef, A., Joussein, E., Poulesquen, A., Gasgnier, G., Pronier, S., Sobrados, I., Sanz, J. & Rossignol, S., 2013. Influence of metakaolin purities on potassium geopolymer formulation: the existence of several networks. *Journal of Colloid and Interface Science,* 408, pp. 43-45.

Azeez, A., Mohammed, K., Abdullah, M., Hussin, K., Sandu, A. & Razak, R., 2013. The effect of various waste materials' contents on the attenuation level of anti-radiation shielding concrete. *Materials,* 6(10), pp. 4836-4846.

Bakharev, T., 2005. Resistance of geopolymer materials to acid attack. *Cement and Concrete Research,* 35(4), pp. 658-670.

Barbhuiya, S. & Kumala, D., 2017. Behaviour of a sustainable concrete in acidic environment. *Sustainability,* 9(9), pp. 1556.

Bernal, S.A., Provis, J.L., Brice, D.G., Kilcullen, A., Duxson, P. & van Deventer, J.S., 2012. Accelerated carbonation testing of alkali-activated binders significantly underestimates service life: the role of pore solution chemistry. *Cement and Concrete Research,* 42(10), pp. 1317-1326.

Bozkurt, N. & Yazicioglu, S., 2010. Strength and capillary water absorption of lightweight concrete under different curing conditions. *Indian Journal of Engineering and Materials Science,* 17(2), pp. 145-151.

Carroll, H., 1970. Clay minerals:a guide to their x-ray identification, Colorado: *The Geological Society.*

Castro, J., Bentz, D. & Weiss, J., 2011. Effect of sample conditioning on the water absorption of concrete. *Cement and Concrete Composites,* 33(8), pp. 805-813.

Chang, C. & Chen, J., 2006. The experimental investigation of concrete carbonation depth. *Cement and Concrete Research,* 36(9), pp. 1760-1767.

Chen, L., Wang, Z., Wang, Y. & Feng, J., 2016. Preparation and properties of alkali activated metakaolin-based geopolymer. *Materials,* 9(9), pp. 767.

Claisse, P. A., 1997. Absorption and sorptivity of cover concrete. *Journal of Materials in Civil Engineering*, 9(3), pp. 105-110.

Conant, E., 2012. To catch a falling core: Lessons of Chernobyl for Russian Nuclear Industry, Moscow: Scientic American.

Criado, M., Palomo, A. & Fernández-Jiménez, A., 2005. Alkali activation of fly ashes. Part 1: Effect of curing conditions on the carbonation of the reaction products. *Fuel*, 84(16), pp. 2048-2054.

Darraugh, N., 2009. Air void characterization in fresh cement paste through ultrasonic attenuation using an immersion procedure (Doctoral dissertation). Georgia Institute of Technology.

Davidovits, J., 1991. Geopolymers: Inorganic polymeric new materails. *Thermal Anaylsis*, 37, pp. 1633-1656.

Davidovits, J., 1994. Properties of geopolymer cements. *Alkaline Cemements and Concretes*, pp. 131-149.

Davidovits, J., 2002. Years of successes and failures in geopolymer applications. Market trends and potential breakthroughs. *In Geopolymer 2002 Conference* 28, pp. 29. Melbourne (Australia), Geopolymer Institute Saint-quentin (France).

Davraz, M., 2015. The effect of boron compound to cement hydration and controllability of this effect. *Acta Physica Polonica A*, 128, pp. B26-B33.

Deb, P., Nath, P. & Sarker, P., 2013. Properties of fly ash and slag blended geopolymer concrete cured at ambient temperature. *New Developments in Structural Engineering and Construction*, pp. 571-576.

Deb, P., Nath, P. & Sarker, P., 2015. Drying shrinkage of slag blended fly ash geopolymer concrete cured at room temperature. *Procedia Engineering*, 125, pp. 594-600.

Dhir, R., Hewlett, P. & Chan, Y., 1987. Near surface characteristics of concrete: assessment and development of in-situ test methods. *Magazine of Concrete*, 39(141), pp. 183-195..

Diaz, E., Allouche, E. & Eklund, S., 2010. Factors affecting the suitability of fly ash as source material for geopolymers. *Fuel*, 89, pp. 992–996.

Dinakar, P., 2011. High reactive metakaolin for high strength and high performance concrete. *Indian Concrete Journal,* 85(4), pp. 32-34.

Diyora, S., Solanki, G., Anuj, K. & Anuj, C., 2015. A review on compressive strength of plain opc cement concrete with flyash using different water cement ratio. *International Journal of Advance Engineering and Research Development* , 12(1), pp. 129-134.

Donne, M., Dorner, S. & Schumacher, G., 1976. Preliminary design of a borax internal core-catcher for a gas cooled fast reactor *(No. KFK--2352).* Karlsruhe (Germany): Kernforschungszentrum Karlsruhe (Germany).

Duan, P., Yan, C., Zhou, W., Luo, W. & Shen, C., 2015. An investigation of the microstructure and durability of a fluidized bed fly ash–metakaolin geopolymer after heat and acid exposure. *Materials & Design*, 74, pp. 125-137.

Duxson, P., Fernández-Jiménez, A., Provis, J.L., Lukey, G.C., Palomo, A. & van Deventer, J.S., 2007. Geopolymer technology: the current state of the art. *Journal of Materials Science,* 42(9), pp. 2917–2933.

Fernando, P. & Said, J., 2011. Resistance to acid attack, abrasion and leaching behavior of alkali-activated mine waste binders. *Materials and Structures*, 44(2), pp. 487-498.

Fillmor, D., 2004. Literature review of the effects of radiation and temperature on the aging of concrete. Idaho Falls: Idaho National Engineering and Environmental Laboratory.

Giannopoulou, I. & Panias, D., 2007. Structure, design and applications of geopolymeric materials. In proceedings of the 3rd international conference on deformation processing and structure of matreials. Athens, National Technical University of Athens.

Haji-Esmaelii, H., 2012. Admixtures for use in geopolymers (Doctoral dissertation). Thunder Bay: Lakehead University.

Hall, C., 1989. Water sorptivity of mortars and concretes: a review. *Magazine of Concrete Research,* 41(147), pp. 51-61.

Hardjito, D. & Rangan, B., 2005. Development and properties of low-calcium fly ash-based geopolymer concrete. Perth: Curtin University of Technology.

Hosan, A., Haque, S. & Shaikh, F., 2016. Compressive behaviour of sodium and potassium activators synthetized fly ash geopolymer at elevated temperatures: a comparative study. *Journal of Building Engineering,* 8, pp. 123-130.

Hu, M., Zhu, X. & and Long, F., 2009. Alkali-activated fly ash-based geopolymers with zeolite or bentonite as additive. *Cement and Concrete Composites,* 31(10), pp. 762-768.

IAEA, 2006. Environmental consequences of the chernobyl accident and their remediation: twenty years of experience, Vienna, Austria: IAEA.

IAEA, 2006. IAEA safety standards for protecting the people and the environment, safety series no. Sf-1. Vienna, IAEA.

Indu, D. & Elangovan, R., 2016. Optimum mix proportioning of high strength self compacting concrete. *International Journal of Engineering Trends and Technology,* 37, pp. 342-349.

IRSN, 2013. *IRSN France.* [Online] Available at: https://www.irsn.fr/en/publications/thematic/documents/irsn_booklet_radioactive_waste.pdf
[Accessed 20 March 2017].

Izzat, A.M., Al Bakri, A.M.M., Kamarudin, H., Sandu, A.V., Ruzaidi, G.C.M., Faheem, M.T.M. and Moga, L.M., 2013. Sulfuric acid attack on ordinary Portland cement and geopolymer material. *Revista de Chimie,* 64(9), pp. 1011-1014.

Jennings, H.M., Bullard, J.W., Thomas, J.J., Andrade, J.E., Chen, J.J. & Scherer, G.W., 2008. Characterization and modeling of pores and surfaces in cement paste. *Journal of Advanced Concrete Technology,* 6(1), pp. 5-29.

Jennings, H., Thomas, J., Rothstein, D. & Chen, J., 2002. Cements as porous materials. In: *Handbook of Porous Solid.* pp. 2971-302.

Johannesson, B. & Utgenannt, P., 2001. Microstructural changes caused by carbonation of cement mortar. *Cement and concrete Research,* 31(6), pp. 925-931.

Khairallah, R., 2009. Analysis of autogenous and drying shrinkage of concrete (doctoral dissertation): McMaster University.

Khan, M., Castel, A. & Noushini, A., 2016. Carbonation of a low-calcium low-calcium fly ash geopolymer concrete. *Magazine of Concrete Research* 69(1) pp. 24-34

Khater, H., 2013. Effect of silica fume on the characterization of the geopolymer materials. *International Journal of Advanced Structural Engineering,* 5(1), pp. 12.

Kim, Y., Lee, K., Bang, J. & Kwon, S., 2014. Effect of W/C ratio on durability and porosity in cement mortar with constant cement amount. *Advances in Materials Science and Engineering*, 2014.

Krupskaya, V., Zakusin, S., Tyupina, E., Dorzhieva, O., Zhukhlistov, A., Belousov, P. & Timofeeva, M., 2017 Experimental Study of Montmorillonite Structure and Transformation of Its Properties under Treatment with Inorganic Acid Solutions. *Minerals*, 7(4), pp. 49.

Kuenzel, C., Vandeperre, L.J., Donatello, S., Boccaccini, A.R. & Cheeseman, C., 2012. Ambient temperature drying shrinkage and cracking in metakaolin-based geopolymers. *Journal of the American Ceramic Society,* 95(10), pp. 3270-3277.

Kutlić, A., Bedeković, G. & Sobota, I., 2012. Bentonite processing. *Rudarsko-geološko-naftni zbornik*, 24(1), pp. 61-65.

Lee, S., van Riessen, R. & Chon, C., 2016. Benefits of Sealed-Curing on Compressive Strength of Fly Ash-Based Geopolymers. *Materials*, 9(7), pp. 598.

Levitt, M., 1969. Non-destructive testing of concrete by the initial surface absorption method. In: *Non-destructive Testing of Concrete and Timber.* London: Thomas Telford Publishing, pp. 23-26.

Li, X., Zheng, E. & Ma, C., 2011. Factors affecting the compressive strength of class C fly ash geopolymer. *Applied Mechanics and Materials.* Trans Tech Publications, 99, pp. 960-964.

Luukkonen, T., Abdollahnejad, Z., Yliniemi, J., Kinnunen, P. & Illikainen, M., 2018. One-part alkali-activated materials: A review. *Cement and Concrete Research,*103, pp. 21-34.

Mallisa, H. & Turuallo, G., 2017. The maximum percentage of fly ash to replace part of original portland cement (OPC) in producing high strength concrete. Palu , AIP Publishing, 1903(1) pp. 030012.

Mane, S. & Jadhav, H., 2012. Investigation of geopolymer mortar and concrete under high temperature. *International Journal of Emerging Technology and Advanced Engineering*, 2(12), pp. 384-390.

Memon, F.A., Nuruddin, M.F., Khan, S., Shafiq, N.A.S.I.R. & Ayub, T., 2013. Effect of sodium hydroxide concentration on fresh properties and compressive strength of self-compacting geopolymer concrete. *Journal of Engineering Science and Technology,* 8(1), pp. 44 - 56.

Memon, F., Nuruddin, M. & Shafiq, N., 2013. Effect of silica fume on the fresh and hardened properties of fly ash-based self-compacting geopolymer concrete. *International Journal of Minerals, Metallurgy and Materials,* 20(2), pp. 205-213.

Mettler, F., Johnson, J. & Thaul, S., 1997. An evaluation of radiation exposure guidance for military operations*: Interim Report*, Washington DC: National Academies Press.

Mikheykin, S., 2017. Aluminosilicate and glass for incorporation of problematic liquid radioactive waste , Moscow : IAEA .

Muñiz-Villarreal, M.S., Manzano-Ramírez, A., Sampieri-Bulbarela, S., Gasca-Tirado, J.R., Reyes-Araiza, J.L., Rubio-Ávalos, J.C., Pérez-Bueno, J.J., Apatiga, L.M., Zaldivar-Cadena, A. & Amigó-Borrás, V., 2011. The effects of temperature on the geopolymerization process of a metakaolin-based geopolymer. *MLBLUE Materails Letters,* 65, pp. 995-998.

Mustafa Al Bakri, A.M., Kamarudin, H., Bnhussain, M., Rafiza, A.R. & Zarina, Y., 2012. Effect of Na_2SiO_3/NaOH ratios and NaOH Molarities on compressive strength of fly-ash-based geopolymer. *ACI Materials Journal,* 109(5), pp. 503-508.

Nadirshah, E., 1959. Indian standard methods of test for strength of concerete. Bombay: Bureau of Indian Standards.

Nahata, Y., Kholia, N. & Tank, T., 2014. Effect of curing methods on efficiency of curing of cement mortar. *APCBEE Procedia,* 9, pp. 222-229.

Nanavati, S.C., Lulla, S.J., Singh, A.R., Mehta, D.B., Patel, A.M. & Lade, A.D., 2017. A review on fly ash based geopolymer concrete. *Journal of Mechanical and Civil Engineering*, 14(4), pp. 12-16.

Nath, P. & Sarker, P., 2015. Use of OPC to improve setting and early strength properties of low calcium fly ash geopolymer concrete cured at room temperature. *Cement and Concrete Composites,* 55, pp. 205-214.

Nazari, A., Maghsoudpou, A. & Sanjayan, J., 2014. Characteristics of boroaluminosilicate geopolymers. *Construction and Building Materials,* 70, pp. 262-268.

NEI, 2008. *nei.org.* [Online] Available at: https://cna.ca/wp-content/uploads/2014/05/Chernobyl-accident-and-its-Consequences.pdf [Accessed 24 March 2017].

Okoye, F., Durgaprasad, J. & Singh, N., 2016. Effect of silica fume on the mechanical properties of fly ash based-geopolymer concrete. *Ceramics International,* 42(2), pp. 3000-3006.

Olivia, M., Nikraz, H. & Sarker, P., 2008. Improvements in the strength and water penetrability of low calcium fly ash based geopolymer concrete. *The 3rd ACF International Conference-ACF/VCA.* Perth, Australia, Curtin University of Technology.

Pacheco-Torgal, F., Castro-Gomes, J. & Jalali, S., 2008. Alkali-activated binders: A review: Part 1. Historical background, terminology, reaction mechanisms and hydration products.. *Construction and Building Materials,* 22(7), pp. 1305-1314.

Palomo, A. & dela Fuente, J., 2003. Alkali-activated cementitous materials: Alternative matrices for the immobilisation of hazardous wastes Part I. Stabilisation of boron. *Cement and Concrete Research,* 33(2), pp. 281-288.

Palomo, A., Grutzeck, M. & Blanco, M., 1999. Alkali-Activated Fly Ashes, Cement for the Future. *Cement and Concrete Research,* 29(8), pp. 1323-1329.

Patel, V., 2009. Sorptivity testing to assess durability of concrete against freeze-thaw cycling. *Masters Abstracts International,* 48(5), pp. 49.

Petermann, J., Saeed, A. & Hammons, M., 2010. Alkali-activated geopolymers: a literature review, Applied Research Associates Inc Panama City Fl.

Phoo-ngernkham, T., Maegawa, A., Mishima, N., Hatanaka, S. & Chindaprasirt, P., 2015. Effects of sodium hydroxide and sodium silicate solutions on compressive and shear

bond strengths of FA–GBFS geopolymer. *Construction and Building Materials,* 91, pp. 1-8.

Puertas, F., Martínez-Ramírez, S., Alonso, S. & Vazquez, T., 2000. Alkali-activated fly ash/slag cements: strength behaviour and hydration products. *Cement and Concrete Research,* 30(10), pp. 1625-1632.

Ramezanianpour, A. & Moeini, M., 2018. Mechanical and durability properties of alkali activated slag coatingmortars containing nanosilica and silica fume. *Construction and Building Materials,* 163, pp. 611-621.

Rostami, V., 2012. Development of early carbonation curing to replace steam curing for precast dry-mix concrete. Montreal: McGill University.

Ryu, G., Lee, Y., Koh, K. & Chung, Y., 2013. The mechanical properties of fly ash-based geopolymer concrete with alkaline activators. *Construction and Building Materials,* 47, pp. 409-418.

Sabir, B., Wild, S. & O'farrell, M., 1998. A water sorptivity test for martar and concrete. *Materials and Structures,* 31(8), pp. 568.

Šahinagić-Isović, M., Markovski, G. & Ćećez, M., 2012. Shrinkage strain of concrete - Causes and types. *Gradevinar,* 64(9), pp. 727-734 .

Salman, A., 2016. Production and properties of geopolymer attapulgite bricks, Iraq: Building and Construction Engineering Department, University of Technology.

Satpute, S., Shirasath, M. & Hake, S., 2016. Investigation of alkaline activators for fly-ash based geopolymer concrete. *Ijarrie,* 2(5), pp. 22-27.

Schmidt, M. & Slowik, V., 2013. Capillary pressure controlled concrete curing in pavement construction. *Airfield and Highway Pavement : Sustainable and Efficient Pavements,* pp. 295-306.

Schulze, D., 2005. Clay minerals. West lafayette: Elsevier Ltd. pp. 246-254

Sevón, T., 2005. Molten core concrete interactions in nuclear accidents, Finland: Julkaisija Utgivare.

Shamsai, A., Rahmani, K., Peroti, S. & Rahemi, L., 2012. The effect of water-cement ratio in compressive and abrasion strength of the nano silica concretes. *World Applied Sciences Journal,* 17(4), pp. 540-545.

Shang, H. & Yi, T., 2013. Freeze-thaw durability of air-entrained concrete. *The Scientific World Journal.*

Shankar, H. & Khadiranaikar, R. B., 2012. Performance of geopolymer concrete under severe environmental conditions. *International Journal of Civil and Structural Engineering,* 3(2), pp. 396-407.

Siddique, R. & Khan, M., 2011. Silica fume: *In Supplementary Cementing Materials.* Berlin, Heidelberg: Springer, pp. 67-119.

Song, X., 2007. Development and performance of class F fly ash based geopolymer concrete against sulphuric acid attack. Sydney: The University of New South Wales.

Song, X., Marosszeky, M., Brungs, M. & Munn, R., 2005. Durability of fly ash based geopolymer concrete against sulphuric acid attack. Lyon, UNSW, Syndney, pp. 17-20.

Srinivasan, K. & Sivakumar, A., 2012 . Strength properties of geopolymer mortar containing binary and ternary blends of bentonite. *ARPN Journal of Engineering and Applied Sciences* , 7(11), pp. 1436-1445.

Steinbrück, M., 2005. Oxidation of boron carbide at high temperatures. *Journal of Nuclear Materials,* 336(2-3), pp. 185-193.

Steins, P., Poulesquen, A., Diat, O. & Frizon, F., 2012. Structural evolution during geopolymerization from an early age to consolidated material. *Langmuir,* 28(22), pp. 8502-8510.

Talaber, J., 1981. Factors influencing the qaulity of cement, Budapest: Department of Building Materials, Technical University.

Tasdemir, C., 2003. Combined effects of mineral admixtures and curing conditions on the sorptivity coefficient of concrete. *Cement and Concrete Research,* 33(10), pp. 1637-1642.

Taveri, G., Tousek, J., Bernardo, E., Toniolo, N., Boccaccini, A.R. and Dlouhy, I., 2017. Proving the role of boron in the structure of fly-ash/borosilicate glass based geopolymers. *Materials Letters,* 200, pp. 105-108.

Temuujin, J., van Riessen, A. & Williams, R., 2009. Influence of calcium compounds on the mechanical properties of fly ash geopolymer pastes. *Journal of Hazardous Materials,* 167, pp. 82–88.

Thokchom, S., Ghosh, P. & Ghosh, S., 2009. Effect of water absorption, porosity and sorptivity on durability of geopolymer mortars. *ARPN Journal of Engineering and Applied Sciences,* 4(7), pp. 28-32.

Tippayasam, C., Balyore, P., Thavorniti, P., Kamseu, E., Leonelli, C., Chindaprasirt, P. & Chaysuwan, D., 2016. Potassium alkali concentration and heat treatment affected metakaolin-based geopolymer. *Construction and Building Materials,* 104, pp. 293–297.

Van Jaarsveld, J. Van Deventer, J., & Lorenzen, L., 1996. The potential use of geopolymeric materials to immobilise toxic metals: Part I. Theory and applications. *Minerlas Engineering,* 10(7), pp. 659-669.

Vijayakumar, R., 2013. Evaluating shrinkage of fly ash - slag geopolymers, Urbana: University of Illinois at Urbana-Champaign.

Waltar, A., 2003. The medical, agricultural, and industrial applications of nuclear technology, Global New Orleans, LA: Pacific Northwest National Laboratory.

Wong, H. & Razak, H., 2005. Efficiency of calcined kaolin and silica fume as cement replacement material for strength performance. *Cement and Concrete Research,* 35(4), pp. 696-702.

Xu, H. & Van Deventer, J., 2000. The geopolymerisation of alumino-silicate minerals. *International Journal of Mineral Processing,* 59(3), pp. 247-266.

Xu, H. & Van Deventer, J., 2003. Effect of source materials on geopolymerization. *Industrial & Engineering Chemistry Research,* 42(8), pp. 1698–1706.

Yahya, Z., Abdullah, M., Hussin, K., Ismail, K., Razak, R. & Sandu, A., 2015. Effect of solids-to-liquids, Na_2SiO_3-to-NaOH and curing temperature on the palm oil boiler ash (Si^+ Ca) geopolymerisation system. *Materials,* 8(5), pp. 2227-2242.

Yao, X., Zhang, Z., Zhu, H. & Chen, Y., 2009. Geopolymerization process of alkali–metakaolinite characterized by isothermal calorimetry. *Thermochimica Act,* 493, pp. 49–54.

Yip, C., Lukey, G. & Van Deventer, J., 2005. The coexistence of geopolymeric gel and calcium silicate hydrate at the early stage of alkaline activation.. *Cement and Concrete Research,* 35(9), pp. 1688-1697.

Zhang, M., Zhao, M., Zhang, G., Mann, D., Lumsden, K. & Tao, M., 2016. Durability of red mud-fly ash based geopolymer and leaching behavior of heavy metals in sulfuric acid solutions and deionized water. *Construction and Building Materials,* 124, pp. 373–382.

Zhang, Q. & Guang, Y., 2012. Dehydration kinetics of Portland cement paste at high temperature. *Journal of Thermal Analysis and Calorimetry,* 110(1), pp. 153-158.

Appendix A

Table A1: Database of the chemical analysis of clay samples

Mineral clays	**Mass composition of clay samples (%)**			
	Bentonite–Ca	**Bentonite- MD**	**Bentonite MX80**	**Attapulgite**
SiO_2	58.2	59.10	55.0	62.0
Al_2O_2	17.7	18.60	20.0	7.00
Fe_2O_3	6.25	4.40	3.67	3.00
FeO	1.60		0.30	
CaO	3.30	1.90	0.50	1.50
MgO	0.59	4.00	2.50	9.00
K_2O	0.20	0.30	0.60	0.30
Na_2O		2.50	2.75	0.10
MnO				
TiO_2	0.33		0.10	
P_2O_2				
L.O.I	11.40	8.90		

Alkaline solutions

Sodium silicate

Sodium silicate solution (Na_2O = 7%, SiO_2 = 26.5% and 65.5% water) was supplied by Monitoring and Control Laboratories MCL (PTY) LTD.

Sodium hydroxide (NaOH) and potassium hydroxide (KOH)

ACS reagents, sodium hydroxide and potassium hydroxide were both supplied by sigma-aldrich. The sodium hydroxide (≥85% percent purity) and potassium hydroxide (≥85%) in pellet form were used to make 14 M solutions.

$Ca(OH)_2$

An ACS reagent calcium hydroxide (≥95% percent purity) from sigma-aldrich was used in this study to make a 5M $Ca(OH)_2$ solution